Cracow University of Technology

Faculty of Environmental Engineering and Energy

Doctoral Dissertation

Modelowanie układów trigeneracji energii elektrycznej, ciepła i chłodu z wykorzystaniem układów PV/T i pompy ciepła.

Modelling of PV/T and heat pump trigeneration systems for electricity, heat and cooling.

Mgr. inż. Filip Bartyzel

Supervisor: Prof. dr hab. inż. Paweł Ocłoń

Assistant Supervisor: Dr hab. inż. Piotr Cisek, prof. PK

Kraków, 2025

Streszczenie

Wykorzystanie odnawialnych źródeł energii staje się koniecznością, ponieważ źródła nieodnawialne mają niezaprzeczalny negatywny wpływ na środowisko. Dlatego wiele krajów i instytucji kładzie coraz większy nacisk na alternatywne źródła energii. Szczególną uwagę przyciągają alternatywne źródła ciepła, takie jak sprężarkowe pompy ciepła zasilane energią elektryczną. Wraz ze wzrostem zainteresowania zieloną energią, zintegrowane systemy grzewcze stają się niezbędne. Systemy te są często wyposażone w zbiorniki magazynujące ciepło i alternatywne, przyjazne dla środowiska źródła ciepła, co zmniejsza zależność od energii elektrycznej z sieci, gdzie energia jest często wytwarzana w sposób nieprzyjazny dla środowiska. Problemem związanym z systemami zintegrowanymi jest sposób współdziałania poszczególnych elementów oraz dobór odpowiedniego wyposażenia. Ponieważ wydajność tych urządzeń zależy od wielu czynników, stanowi to poważne wyzwanie projektowe.

Jednym z przykładów systemu energii odnawialnej jest RESHeat, dla którego opracowano symulacje przy użyciu programu TRNSYS. Symulacje te są jednym z głównych aspektów niniejszej pracy doktorskiej. System RESHeat składa się z sprężarkowej pompy ciepła, paneli fotowoltaicznych, paneli słonecznych, gruntowego wymiennika ciepła i, co najważniejsze, podziemnego zasobnika ciepła. Ze względu na wiele niezależnych elementów systemu opracowano odpowiedni model symulacyjny w celu przewidzenia zachowania poszczególnych elementów i oszacowania ich rocznej wydajności oraz przebiegu parametrów w czasie. Inną ważną częścią pracy było porównanie wyników symulacji z pomiarami uzyskanymi z rzeczywistego systemu.

Porównując wyniki symulacji z rzeczywistym systemem, zauważono, że największe różnice wynikały z wykorzystanych danych klimatycznych – Meteonorm – opartych na statystycznych danych klimatycznych dla danego regionu, tj. najbardziej prawdopodobnych warunkach atmosferycznych, które wystąpią w danym momencie. Jednak ze względu na zmiany klimatyczne dane pogodowe wykorzystane w symulacji różniły się od rzeczywistych parametrów pogodowych w 2024 r. – dane w symulacji były mniej optymistyczne, zakładając wyższą liczbę HDD, co można wyjaśnić ociepleniem klimatu.

Kolejnym aspektem, w którym odnotowano znaczące różnice, była wydajność samej sprężarkowej pompy ciepła, co tłumaczono niedoskonałościami danych laboratoryjnych otrzymanych od producenta pompy – dane te są uzyskiwane w warunkach laboratoryjnych –

idealnych warunkach – które później znacznie różnią się od rzeczywistych parametrów pracy pompy ciepła w systemie, w którym została zainstalowana.

Abstract

The use of renewable energy sources is becoming a necessity as non-renewable sources have an undeniably negative environmental impact. This is why many countries and institutions are placing increasing emphasis on alternative energy sources. Alternative heat sources, such as compressor heat pumps powered by electricity, are attracting particular attention. As the focus shifts towards green energy, integrated heating systems are becoming essential. These systems are often equipped with heat storage tanks and alternative, eco-friendly heat sources, reducing reliance on electricity from the grid, where energy is often generated in an environmentally unfriendly manner. The problem with integrated systems is how the components interact with each other and how to select the appropriate equipment. As the efficiency of these devices depends on many factors, this presents a significant design challenge.

One example of a renewable energy system is RESHeat, for which simulations were developed using the TRNSYS programme. These simulations are one of the most important aspects of this doctoral thesis. The RESHeat system comprises a compressor heat pump, photovoltaic panels, solar panels, a ground heat exchanger and, most importantly, a ground-buried heat storage tank. Due to the system's many independent components, an appropriate simulation model was developed to predict the behaviour of the components individually and estimate their annual efficiency and the course of the parameters over time. Another important part of the thesis involved comparing the simulation results with measurements obtained from the actual system.

When comparing the simulation results with the actual system, it was noticed that the biggest differences were caused by the climate data used – Meteonorm – which is based on statistical climate data for a given region, i.e. the most likely atmospheric conditions that will occur at a given moment. However, due to climate change, the weather data used in the simulation differed from the actual weather parameters in 2024 – the data in the simulation was less optimistic, assuming a higher number of HDD, which can be explained by climate warming.

Another aspect where significant differences were noted was the efficiency of the compressor heat pump itself, which was explained by the shortcomings of the laboratory data received from the pump manufacturer – this data is obtained under laboratory conditions - ideal conditions - which later differ significantly from the actual operating parameters of the heat pump in the system where it was installed.

Acknowledgment

We often like to imagine that our success is solely the result of our hard work and that we owe it exclusively to ourselves, but if we look at a person's life as a whole, the path to a given moment in life or career has intersected at various stages with other people whose presence has allowed us to be where we are today.

Special thanks go to my beloved wife, Beata. If our paths had not crossed some time ago, I would not be where I am today, and this thesis would most likely not have been completed, thank you for your patience and constant support during its creation.

Thanks are also due to other people who have made me who I am today and who have contributed to the creation of this work, I would like to thank to my parents.

I would also like to thank my supervisors, Professor Paweł Ocłoń and Assistant Supervisor Dr. Piotr Cisek, for their support, thanks to which I was able to complete this doctoral thesis.

The majority of the research activities for this thesis were conducted for RESHeat, and the results were utilised for a variety of publication activities related to the project.

Table of Contents

1. Introduction

The motivation for undertaking this dissertation derives from the necessity to address the requirements for present-day construction, with a particular emphasis on nZEB buildings. “Nearly zero-energy building’ means a building that has a very high energy performance, as determined in accordance with Annex I. The nearly zero or very low amount of energy required should be covered to a very significant extent by energy from renewable sources, including energy from renewable sources produced on-site or nearby”[1].

The main goal of an nZEB building is to have zero energy requirements from external sources, including energy from the grid. To meet this requirement, nZEB buildings need to integrate renewable energy sources such as solar collectors, photovoltaic (PV) panels, and geothermal heat exchangers. This is particularly important in times of turbulent energy markets and mounting pressure from the European Union and environmental institutions to reduce carbon emissions. Modern buildings should have as little environmental impact as possible while still providing optimum comfort, hot water and access to electricity. Currently, energy used for building requirements constitutes 40% of energy usage in the European Union. For this reason, they have been identified as the main target for energy reduction [2]. To this purpose, it is necessary to develop a system that meets the above requirements. Such a system needs to be equipped with solar energy devices (solar collectors, photovoltaic panels), highly efficient heat and cooling generation systems (heat pumps with ground heat exchangers) and energy storage systems (underground heat storage) to compensate for fluctuations in the supply and demand of energy in the system. The above system can be difficult to control, as its overall performance depends on the performance of the individual components. Therefore, the need arises to simulate the whole of such a complex system. In the work published so far, there are many studies of the individual components of a system such as RESHeat, but there are not many studies dealing with the simulation of the integrated system and the interactions between the individual system components. In the following dissertation, the simulation of the entire system is addressed, alongside the estimation of the efficiency of said system as a whole, and the performance of each individual component.

The RESHeat system (Renewable Energy System for Residential Building Heating and Electricity Production) is an example of a typical application for the use of waste heat from installed tracking (sun-tracked) PVT panels. The dissertation presents the integration of PVTs with an underground thermal energy storage (UTES) system, which consists of an insulated tank for domestic hot water (DHW) production. Waste heat from the PVT panels and excess

heat from the solar collectors is used to charge the underground heat storage tanks and regenerate the ground. A numerical model of the UTES with PVTs and solar collectors has been created to account for the effect of heat exchange in the ground.

The RESHeat pilot project was implemented in the ZBK buildings. The ZBK buildings are located in the eastern part of Krakow on Działkowa Street. The estate at Działkowa Street consists of four municipal buildings managed by the City of Krakow. The pilot installation was installed in a building consisting of 24 apartments, storage cells and garages.

2. Analysis of the status quo

In recent years, there has been an observable increase in the use of renewable energy sources as the primary means of heating and cooling residential properties. This trend is evident throughout the European Union; however, the most pronounced increase in recent years has been observed in Poland.

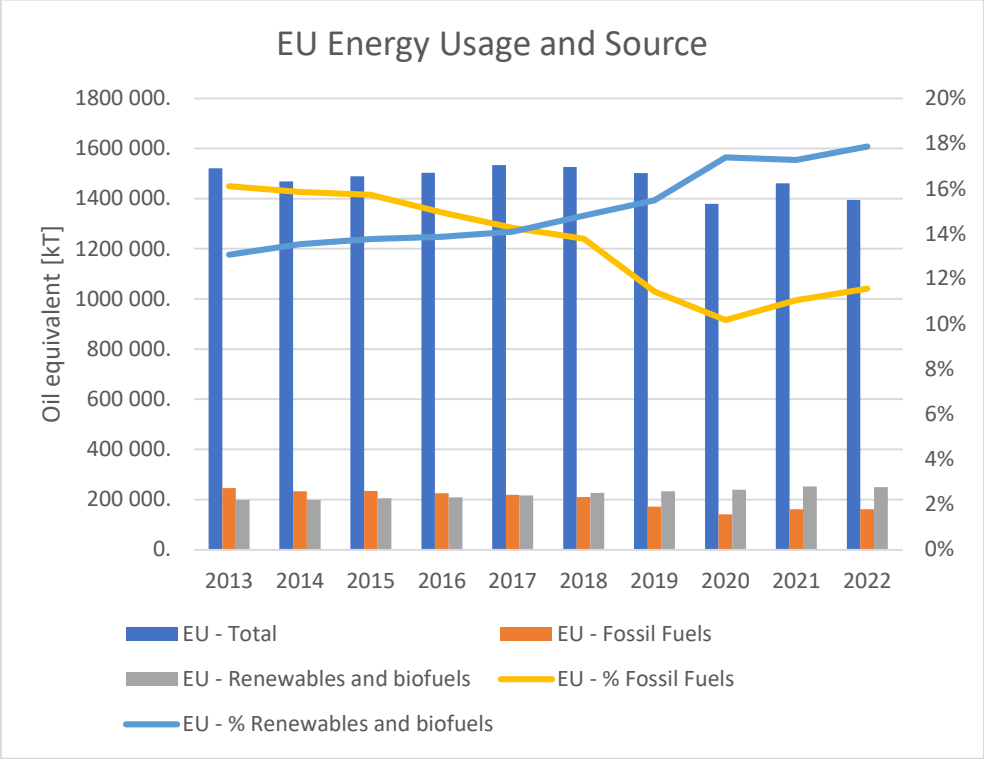

Figure 1 - Energy usage, source and share used for domestic heating in EU countries [3].

As can be seen from the graph above, there is a trend towards reducing the use of non-renewable energy sources (including fossil fuels) in favour of renewable sources. In EU countries, the share of renewables exceeded that of fossil fuels in 2017.

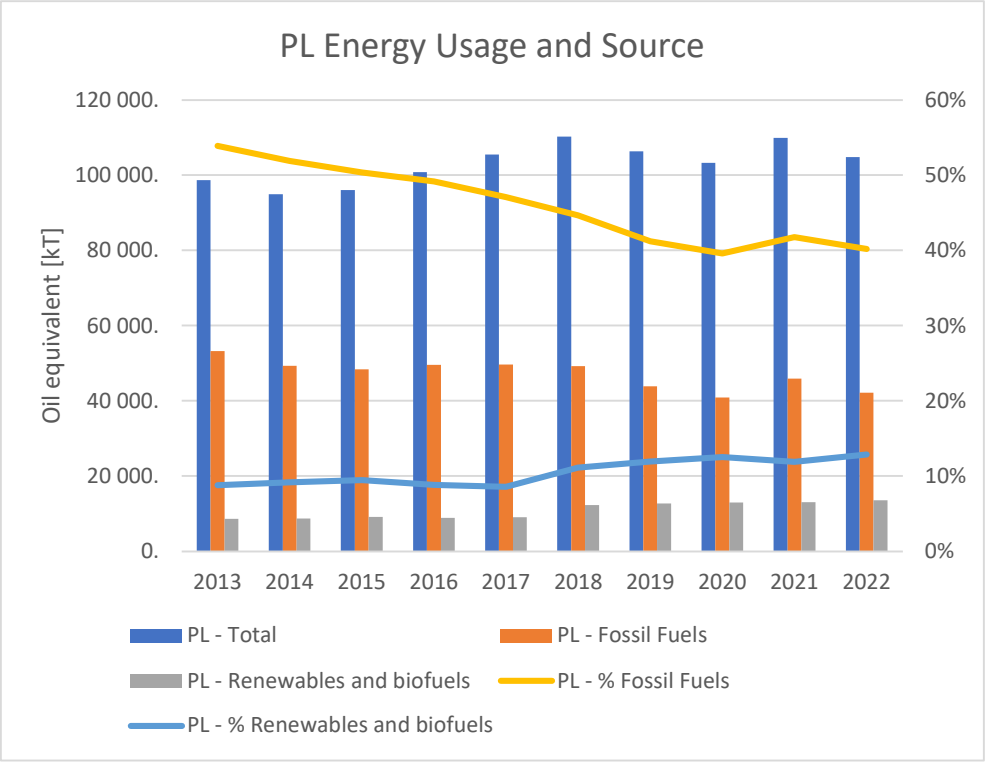

Figure 2 - Energy usage, source and share used for domestic heating in Poland [3].

Poland still relies heavily on fossil fuels for heating. However, this proportion is decreasing rapidly. Poland is one of the countries where renewable energy sources have been adopted more widely in recent years, with fossil fuels (including coal) being used much less.

2.1. Renewables on growth path in Poland

In the EU, heat pumps have been identified as a key tool for the decarbonisation of residential heating, and have been included in the 'European Green Deal', namely the EU Energy Sector Integration Strategy (July 2020) and the Building Sector Strategy, the so-called 'Renewal Wave'. Both strategies coherently outline a model for the energy transition in the European Union. It consists of electricity generation mainly from renewable energy sources and the integration of energy sectors according to the principle of 'energy efficiency first', i.e. primarily the efficient electrification of transport, individual heating and district heating.

According to information from the think tank Ember, compiled on the basis of updated National Energy and Climate Plans (NECPs) prepared by EU Member States, the share of so-called clean electricity could reach an average of 83% in 2030 and the average share of RES in electricity production in the energy mix could reach 63%. The vast majority of EU countries have already announced the complete decarbonisation of electricity in their energy mix between

2035 and 2040. This means, among other things, that the full decarbonisation of heat produced by electric heat pumps or electric transport could be achieved rapidly.

The International Energy Agency's (IEA) document of 18 May 2021, the so-called 'Net Zero by 2050' roadmap, and the cross-cutting analysis 'The Future of Heat Pumps', published on 28 November 2022, are crucial to the outlook for the heat pump market in Europe in the coming years. This is also confirmed by the document published in October 2022, the so-called "World Energy Outlook 2022". (WEO). According to these studies, electric heat pumps are expected to meet half of the world's heat demand by 2045 and provide almost two-thirds of the heat in developed (OECD) countries by 2050. The total number of installed heat pumps is therefore expected to increase from 180 million units in 2020. to 600 million units in 2030 (almost a fourfold increase) and tenfold to 1.8 billion units in 2050. At the same time, the International Energy Agency (IEA) is calling on all developed countries to phase out the sale of stand-alone gas, oil and coal-fired boilers by 2025. According to the European Commission's REPowerEU package, such a plan is to be implemented in all European Union countries by 2029 through the revision of eco-design regulations for heating appliances. Without waiting for changes in EU regulations, a dozen EU countries have already announced bans on the use of fossil fuel boilers in new or existing residential buildings in the coming years [4].

Compared to 2021, sales of heat pumps in Poland increased by 120% in 2022. For central water heating units, the increase was 130%. Even more impressive was the 137% increase in the number of air-to-water heat pumps sold. Notably, the Polish air-to-water heat pump market has grown over 100-fold in the last 10 years. This is the fifth consecutive year that the Polish market for air-to-water heat pumps has recorded year-on-year sales growth of around 100%, and the last two years have seen the highest sales growth for heat pumps in Europe.

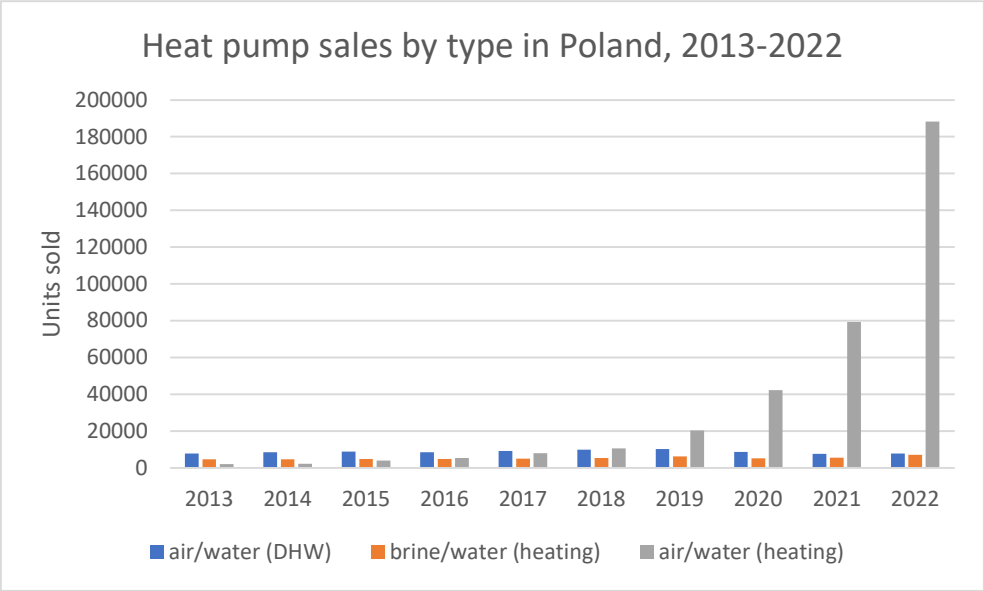

Figure 3 - Sales of heat pumps in Poland by type [4]

Sales of ground source heat pumps also increased significantly, with brine/water units seeing a 28% rise. In contrast, sales of air-to-water heat pumps for domestic hot water increased by only around 2%. This amounts to more than 200,000 units sold in 2022, including 188,200 air-to-water units, around 7,200 ground source heat pumps, and 7,900 water-to-water heat pumps.

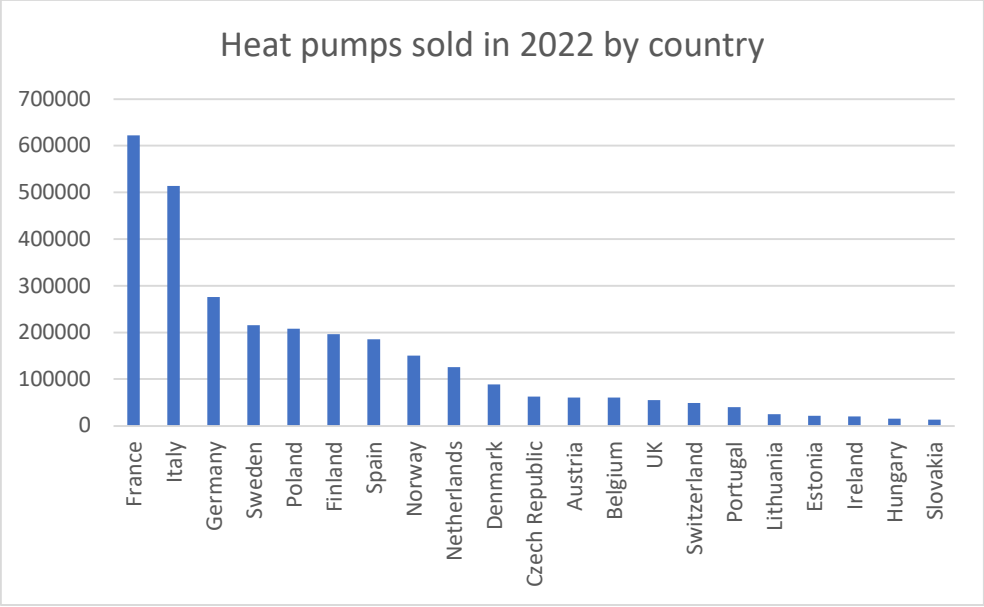

Figure 4 - Heat pumps sold in 2022 by country [5]

Based on the data shared by EHPA total number of heat pumps sold in 21 countries in Europe was 3 millions.

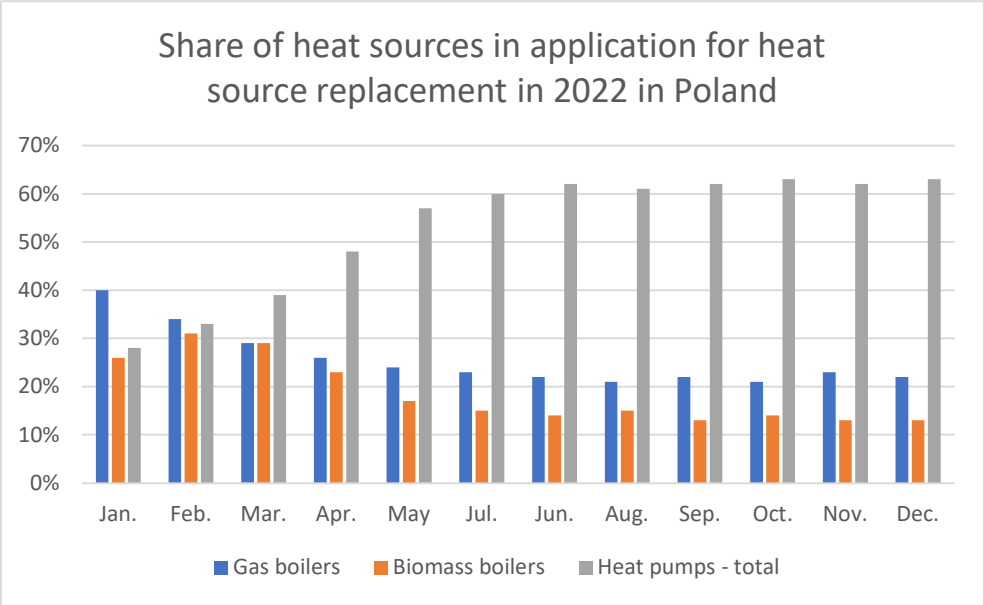

Figure 5 - Share of heat sources in heat source replacement applications [4]

This means that the share of heat pumps in the total number of heating units sold on the Polish market in 2022 (taking into account their 10% decrease compared to 2021) could have been close to 30%, and taking into account the air conditioners with heating function sold, this was already almost every second heating unit sold [4].

As can be seen from the data above, heat pumps have become a key tool for the energy transition in Poland and may well enable Poland to meet its targets for reducing CO2 emissions and limiting the consumption of non-renewable energy sources. The majority of heat pumps sold in 2022 were installed in existing buildings with different heating system parameters and different heat and hot water production requirements. Therefore, it is important to pay more attention to the performance of a device such as a heat pump, especially in retrofit installations, which pose additional challenges to the efficiency and effectiveness of such a system.

2.2. Current state of research

On the basis of the literature survey, it can be seen that current scientific output lacks simulation models for advanced RES systems simultaneously equipped with heat storage. The solutions to date have had PV panels or solar collectors, but no seasonal heat storage and no ground regeneration option in a ground heat exchanger. At the same time, most of the existing solutions and their simulations did not validate their components based on measured data. Another shortcoming is the lack of optimisation of the systems to increase the COP above 4,

which ensures low energy consumption of the system and an increase in the coverage of energy demand by renewable energy without significantly increasing the amount of energy sources.

There are a number of publications dealing with the integration of a system such as a ground source heat pump in a residential building. One of them is the publication by Girard et al [6]. In their publication they consider the possibility of integrating a ground source heat pump in a residential buildings in Europe. This paper investigates the possibility of increasing the efficiency of ground source heat pumps (GSHPs) in space heating mode by using solar collectors. A new simulation tool for solar-assisted ground source heat pumps (SGSHPs) is presented along with an analysis of the effect of solar collectors on improving heat pump performance. Solar radiation and climate temperature data from 19 European cities were used to simulate SGSHP and GSHP systems for a typical residential house. The overall coefficients of performance (COP) varied between 4.4 and 5.8 for SGSHP and between 4.3 and 5.1 for GSHP, depending on the location from north to south. The results show that the coupling of solar collectors has a greater impact on improving efficiency in regions that benefit from higher irradiance. However, greater savings in operating costs are achieved in milder climatic conditions. The publication does not address the subject of energy storage and its potential impact on system efficiency, and the possibility of reducing the demand for electricity drawn from the grid. Nouri G. et. Al [7] discusses solar-assisted ground source heat pump (SAGSHP) systems, which have recently been the focus of attention for many researchers due to their potential to increase the share of renewable energy. The aim of their paper is to provide a comprehensive overview of the research that has been carried out on SAGSHP heat pumps in order to facilitate their comparison in terms of characteristics. The authors' literature review showed that solar energy influences the efficiency of GSHPs. It is noteworthy that advanced configurations of SAGSHPs performed better than traditional ones and recorded higher COPs, which calls for further research. The economic evaluation of the SAGSHP using the new tri-generation systems showed a minimum payback period of five years due to the large savings in operating costs. Finally, the authors highlight future research needs due to the overall research gap in improving SAGSHPs to achieve higher efficiencies. Sheng Z. et. al [8] present the latest developments in renewable energy systems for heating, cooling and electricity generation in buildings using thermal energy storage. With the need for a transition to clean energy in many countries and regions, and the goal of achieving zero energy consumption in buildings, it is crucial to provide efficient heating/cooling systems for buildings based on renewable energy. Buildings account for around 40% of total energy consumption and offer significant potential

for primary energy savings. The authors discuss the use of different systems based on renewable energy sources, including: the presentation of hybrid systems based on renewable energy sources, methodologies for their design and methods for optimising the use of renewable energy sources in buildings. Currently, the main systems used in buildings are based on heat pumps and photovoltaics. However, the sources of these energy systems are unstable and influenced by the climatic environment. This requires a combination of thermal and electrical energy storage to achieve high efficiency. Recent developments in thermal and chemical energy storage include battery energy storage systems and hydrogen energy systems, due to the urgent need to overcome the difficulties of high cost, relatively low efficiency and challenging storage environment, etc. For thermal energy storage, phase change materials (PCMs) show great potential - they can be used to store thermal energy during periods of low energy demand or availability and recover it during periods of high consumption. This review also presents the latest developments in PCMs for use in buildings, both for heating and cooling.

Qiu and Thomas [9] address the issue of heat pump operation in unfavourable weather conditions. A common problem with heat pumps in unfavourable conditions, such as low outdoor temperatures or high heat load temperatures, is that they achieve low COP values. In the case of low temperatures, it is necessary to develop devices that use a two-stage compression cycle. Such devices demonstrate greater efficiency over a wider range of heat source and heat load temperatures. In this article, the authors describe a model of a two-stage heat pump equipped with an economiser and inter-stage refrigerant injection. This article specifies the optimal operating parameters of the device, which translate into maximising the COP. It was shown that the two-stage heat pump was able to achieve a COP of 2.85 and 2.7 at an outdoor temperature of -30 °C for the following refrigerants: R290 and R410A.

The widespread adoption of heat pumps is a cornerstone of strategies to decarbonize the residential heating sector. However, accurately predicting their real-world performance remains a significant challenge. Existing models are frequently either overly complex, necessitating extensive and frequently inaccessible building data, or overly simplistic, resulting in the failure to capture the dynamic factors that significantly influence efficiency. In order to address this gap, Rogeau et al. [10] developed a novel, generic heat pump model to provide technologically accurate performance estimates using minimal inputs, namely local weather data and standard full-load Coefficient of Performance (COP) curves. The model's primary innovation lies in its capacity to simulate three distinct operating modes: full-load, inverter-controlled partial load, and on/off cycling. The system under discussion integrates two effects. Firstly, it incorporates

the performance-degrading effects of defrosting cycles in cold, humid conditions. Secondly, it incorporates the efficiency benefits of weather compensation, which adjusts the heat sink temperature based on outdoor conditions.

This robust methodology was applied to map the performance of heat pumps across Europe, using data from over 4,100 locations to generate high-resolution maps via a spatial kriging interpolation method. The results, which are made openly available, reveal significant geographical variations in the Seasonal Coefficient of Performance (SCOP), with values as high as 4.25 in milder southern and western coastal regions. The maps provide a clear illustration of the significant impact of latitude, climate (oceanic vs. continental), and altitude on operational efficiency. Furthermore, the study emphasises the critical importance of modelling part-load behaviour, as neglecting it can lead to SCOP estimation errors ranging from an 18% underestimation for modern inverter-driven heat pumps to a 37% overestimation for older on/off models.

This has profound implications for building retrofits. The research provides a clear quantitative analysis of the consequences of improper retrofit sequencing. In the event of the installation of a heat pump prior to the enhancement of a building's thermal envelope, the subsequent reduction in heating demand results in the unit being oversized. This results in the heat pump operating frequently in inefficient partial-load ranges, which can degrade its SCOP by up to 50%. This approach, known as the "wrong order" method, has been shown to result in significant financial losses for homeowners. These losses can be attributed to higher initial equipment costs and inflated long-term energy bills. The most effective and economical strategy is to perform the thermal retrofit first and then install a heat pump of the correct size.

Although system-level modelling provides a comprehensive overview of the performance of heat pumps, the efficiency of the entire system is contingent on its core components, particularly the compressor. A significant gap has existed in the ability to perform consistent, like-to-like technoeconomic comparisons of different compressor technologies for small-scale applications (<30 kWth). As demonstrated by A. V. Olympios et al. [11], a data-driven framework was established by the compilation of a database of published information on 120 commercially available compressors, including 40 units each of the rotary-vane, scroll, and reciprocating-piston types. Consequently, two novel sets of tools were developed from this database. Initially, performance maps were developed to predict the isentropic efficiency of each compressor type as a function of the operating pressure ratio and the inlet volumetric flowrate. Secondly, cost correlations were established in order to predict the price of a compressor based on its size. The

analysis yielded insights into the distinct operational niches of each technology. Scroll compressors have been shown to exhibit optimal efficiency levels of approximately 75%, however, this is only at low pressure ratios (below 5.5). This characteristic renders them particularly well-suited for mild climates. It has been demonstrated that the performance of the system is subject to a significant decline when operated in colder conditions, which necessitate higher pressure ratios. Conversely, reciprocating-piston compressors demonstrate optimal functionality at elevated pressure ratios (5.5–7.5), exhibiting an efficiency level that exceeds 70%, a characteristic that renders them particularly well-suited for colder climates. Rotary-vane compressors have been demonstrated to offer a versatile and economical solution, providing consistently high efficiency (~70%) across a wide range of pressure ratios. However, it should be noted that their use is limited to smaller-scale applications. These tools were subsequently integrated into a heat pump model in order to conduct a technoeconomic analysis across a range of locations (UK, Finland, and Greece) and building types. For typical residential households, heat pumps equipped with rotary-vane compressors consistently yielded the lowest Levelised Cost of Heat (LCOH) and shortest Payback Time (PBT), primarily due to their significantly lower capital cost. In the case of larger commercial applications where rotary-vane compressors are not an option, the optimal choice is climate-dependent. The findings of this study indicated that scroll compressors were more cost-effective in the milder climates of the UK and Greece. Conversely, reciprocating-piston compressors exhibited a slight performance and cost advantage in the colder winters of Finland. The research concludes that optimal compressor selection is not universal but must be tailored to the specific climate, heating demand, and scale of the application in order to ensure both technical efficiency and economic viability.

C Vering et al. [12] created the open-source Vapor Compression Library (VCLib) in the Modelica programming language. This development resulted in the creation of a comprehensive and accessible platform for modelling vapor compression cycles. The library has been created to facilitate the needs of students and researchers by offering a modular, scalable, and thoroughly documented framework for simulating heat pump systems. VCLib has been developed on the basis of a modular and scalable architectural approach, the distinguishing feature of which is the separation of a complete heat pump model into distinct layers: an application layer, an interconnection layer, and a component layer. This structure caters to users with varying levels of expertise; students can use pre-built models at the application level, while researchers can develop and interchange detailed component models at the component layer. The library contains a comprehensive set of component models, including compressors, heat

exchangers, expansion valves, and sensors. These models are available at different levels of detail, ranging from simple map-based representations to complex physical models. The inherent modularity of the system facilitates the straightforward construction and modification of diverse heat pump configurations, while its scalability permits the investigation of various system sizes and designs.

A fundamental innovation of VCLib is its emphasis on usability and clear documentation, particularly for educational purposes. The library employs Unified Modeling Language (UML) class diagrams to visually represent the complex, object-oriented structure of the Modelica models. The generation of these diagrams is initiated automatically by a parser known as ADOCSM, which translates the Modelica code into a clear graphical format. This approach enables new users to swiftly comprehend the relationships between different submodels, such as inheritance and composition, thereby significantly reducing the learning curve and enhancing the quality of documentation.

The practical application of VCLib is demonstrated through a dynamic, closed-loop simulation of a heat pump cycle. The simulation demonstrates the library's capacity to accurately replicate the interdependencies inherent in the system, including the response of the expansion valve to variations in compressor speed, thereby maintaining a constant level of superheat. This capability renders VCLib a potent instrument for the study of system dynamics and the development of sophisticated control strategies. The library is freely available on GitHub with the intention of fostering a collaborative community of developers and users to continually improve its quality and expand its capabilities. Subsequent endeavours will concentrate on incorporating more sophisticated component models, including detailed scroll compressors, and enhancing the numerical robustness of closed-loop simulations.

Cheng et al. [13] conducted a series of experiments on an R32 refrigeration system in order to systematically investigate how electrical efficiency is affected by compressor frequency, pressure ratio, evaporation temperature, and the suction state of the refrigerant. The results of the study revealed several key relationships. The findings of the study demonstrated a direct correlation between electrical efficiency and the transition from a superheated vapor to a two-phase mixture (wet compression) in suction conditions. The rate of decline in electrical efficiency was found to be more pronounced during wet compression. Furthermore, an inverse relationship between efficiency and both the pressure ratio and the evaporation temperature was identified. This suggests that higher pressure ratios and higher evaporation temperatures result in lower electrical efficiency. Moreover, an increase in the compressor's operating frequency

has been demonstrated to result in a reduction in electrical efficiency. This phenomenon has been attributed to elevated levels of flow resistance and heat losses that occur at higher speeds.

It is evident that, in consideration of the empirical findings, a comprehensive semi-empirical model for electrical efficiency was formulated. The model integrates functions that account for the linear effects of superheat and vapor quality with a standardising function for variable frequency. In order to verify the model's accuracy, it was subjected to a series of validation experiments conducted under diverse operating conditions. The comparison demonstrated a highly significant correlation between the predicted and measured values, with a maximum relative error of 1.81% and a minimum of 0.035%. This level of precision is superior to that of previously published models and is notable for its inclusion of wet compression effects. The authors conclude that the model is highly reliable, though its application is best suited for operating conditions where the compressor frequency is near or above its rated speed and the suction vapor quality remains above 0.9 to ensure the safe and stable operation of the compressor.

In order to address the inherent limitations of standalone solar water heaters and air source heat pumps, namely inconsistent hot water supply and poor winter performance respectively, Y. Ma et al. [14] in their study modelled and simulated a hybrid solar-coupled air source heat pump system. The present study employs the TRNSYS software to investigate the year-round performance of an integrated system designed to provide domestic hot water for a student residence. The primary objective of the study was to ascertain whether the coupled system could overcome the individual drawbacks of each technology to deliver a reliable and energy-efficient hot water supply throughout the year. Key parameters such as solar collector area and storage tank volume were analysed to provide optimisation guidance.

The simulation results conclusively demonstrate the viability and effectiveness of the hybrid system. The primary conclusion of this study is that the system is capable of reliably meeting the daily hot water demand, achieving the target temperature of 50°C during the supply time in every month of the year. The analysis revealed a distinct seasonal pattern in energy consumption, thus confirming the system's intended synergistic operation. During summer months, the utilisation of solar energy is optimised, thereby significantly reducing the operational load on the heat pump, which exhibits the lowest energy consumption during this period. The total annual energy consumption for the system was calculated to be 9100.47 kWh, with the heat pump component accounting for 6252.01 kWh of that total.

In conclusion, the study validates the solar-coupled air source heat pump as a robust and efficient solution for year-round domestic hot water production. The findings demonstrate that by strategically integrating solar thermal energy with an air source heat pump, the system ensures a reliable hot water supply while effectively addressing the challenges posed by winter frosting and low efficiency, which are prevalent in standalone air source heat pumps. The results of the study provide a valuable reference for the optimal design and management of such hybrid systems, offering a clear pathway to improving the performance and energy savings of solar hot water systems.

In their study, A. Saleem and C.E. Ugalde-Loo [15] set out to address the critical need for decarbonising the building sector. They presented a detailed dynamic analysis of an energy system based on a reversible heat pump with thermal storage. This system has been designed to meet the year-round heating, cooling, and domestic hot water (DHW) demands of a residential building in the UK. The TRNSYS software was utilised to develop a multi-zone model of a typical terraced house in Cardiff, Wales. This model incorporated real 2022 weather data and realistic internal heat gains from occupancy, lighting, and appliances to ensure the model's accuracy. The thermal performance of the reversible heat pump system was then compared against a conventional gas boiler configuration in order to evaluate its effectiveness as a low-carbon alternative.

The study's primary conclusion is that the heat pump system exhibits a substantial energy efficiency advantage. Over the course of a year, the heat pump configuration consumed approximately 1.6 times less energy than the gas boiler in order to meet the building's thermal needs. The research also highlighted the critical importance of including internal heat gains in thermal models, as their presence altered the heat pump's annual energy consumption by 15.5%. It is evident that these gains have the effect of reducing the heating load during the winter months, yet simultaneously increasing the cooling load that is required during the summer months.

Despite its superior energy efficiency, the analysis revealed that the heat pump system's annual operational cost is roughly 1.7 times higher than that of the gas boiler. This economic disparity is attributed solely to the current UK energy tariff structure, where the price of electricity per kWh is substantially higher than that of natural gas. In conclusion, the study demonstrates that reversible heat pumps are a technically robust and highly efficient technology capable of addressing both heating and cooling demands. Nevertheless, the economic viability and widespread adoption of these technologies are currently constrained by prevailing energy

pricing policies. The findings suggest that for the UK to successfully decarbonize its residential heating and cooling sector, a supportive policy framework is necessary to align the economic incentives with the clear environmental and energy-efficiency benefits of heat pump technology.

In their study, Q. Wang et al. [16] propose and model an optimised, multi-stage, solar-assisted groundwater heat pump (MU-SAGWHPS) system. In cold climates, standard GWHP systems frequently extract more heat than they replenish. This results in a gradual decrease in groundwater temperature, which, in turn, reduces the system's performance coefficient over time. This research introduces a novel system design and control strategy that utilises solar energy more efficiently to both supplement the heat pump's operation and actively recharge heat into the groundwater, thereby mitigating thermal imbalance.

A significant innovation of this work is the creation of a new dual-interface software module, designated Type299, for the TRNSYS simulation platform. The development of this custom module was driven by the necessity to accurately model the dynamic thermal balance of groundwater. This was achieved by the simultaneous accounting for heat exchange with the heat pump and heat replenishment from the solar collectors. The TRNSYS model, including the newly developed module, was subjected to a validation process that entailed a comparison with a full year of experimental data from a case study system in Shenyang, China. The simulation results demonstrated a maximum relative error of 9.37% in groundwater temperature predictions.

The simulation results for the optimised system demonstrate significant performance improvements over the original configuration. The recently implemented multi-stage utilisation strategy has resulted in an estimated annual increase of approximately 32.9% in solar energy utilisation. This objective is realised through the utilisation of solar energy, which is employed not only for direct heating, but also for pre-heating water for the heat pump's evaporator and for storing excess heat in the groundwater during transitional seasons. This approach enhances the system's maximum comprehensive performance coefficient to 4.54, representing an improvement of 23.8% over the original system. A 10-year operational forecast demonstrates that the optimised system effectively counteracts the annual drop in groundwater temperature; after a decade, the groundwater temperature is projected to be 3.1°C higher than it would be with the original system. In conclusion, the study successfully demonstrates that the proposed MU-SAGWHPS and its associated control strategy can significantly enhance solar energy

utilisation, improve the long-term operational efficiency of the heat pump, and ensure the thermal sustainability of the groundwater source.

In next analysed research article, R. Buyukzeren and A. Kahraman [17] present a novel investigation into the optimal combination of photovoltaic (PV) and solar thermal collectors used to assist an air source heat pump (ASHP) for the provision of domestic hot water (DHW). The research addresses a gap in the existing literature by comparatively analysing hybrid solar configurations and validating the simulation models against experimental data. Initially, an ASHP system was tested in a climatic room to validate a simulation model developed in TRNSYS. The results showed a high degree of accuracy, with a maximum deviation of only 4.5% between experimental and simulated performance parameters.

Following the validation process, the model was employed to simulate and compare various scenarios for a DHW system in Konya, Turkey. This was achieved by adding one, two, or three solar components in different combinations of PV and thermal collectors. The objective of this study was to ascertain the most energy-efficient and economically viable configuration for each scenario, with this being based on the available roof space. The analysis revealed that for systems assisted by one or two solar components, the superior choice from an energetic and economic perspective was the use of only thermal collectors, with payback periods of 3.9 and 4.3 years, respectively.

In the case of the three solar components scenario, the results were more nuanced. The configuration that exhibited the greatest energy efficiency was determined to be a combination of one thermal collector and two PV panels, which generated more electricity than the system consumed annually. However, the most economical option, due to the lower installation and auxiliary costs of PV systems, was the configuration using three PV collectors, which had the shortest payback period of 4.6 years. In conclusion, the study successfully demonstrates that combining solar thermal and photovoltaic collectors with an air source heat pump can significantly improve system performance and reduce energy consumption. The findings provide clear guidance on selecting the optimal type and number of solar collectors based on both energy efficiency and economic profitability, highlighting that the most energetically efficient system is not always the most financially advantageous one.

In their study, P. Liu et al. [18] proposed a novel heating system that integrates phase-change material (PCM) into the thermal storage water tank. A simulation model of the enhanced system was developed on the TRNSYS platform, and its performance was analysed for the heating

period in Xi'an City. The novel design entails the implementation of a layer of myristic acid/expanded graphite composite PCM encircling the water tank, thereby enabling the storage of surplus solar heat during daylight hours and its subsequent release during nocturnal periods. This facilitates the stabilisation of water temperature and the reduction in the operational load on the ASHP.

The simulation results demonstrate significant performance enhancements compared to a conventional solar air-source heat pump (ASHP) system without PCM. A salient finding of the present study is that the incorporation of phase-change thermal storage into solar collectors enhances the overall efficiency of the system by 5.9%. The underlying principle behind this phenomenon is that the PCM absorbs excess heat from the water tank. This, in turn, enables the solar collector to operate at a lower inlet temperature, thereby enhancing its efficiency. In addition, the PCM functions as a thermal buffer, thereby effectively reducing the rate of temperature decline in the water tank during periods of non-heating and nocturnal hours. The consequence of this is a water supply temperature that is more stable, with fluctuations that are significantly reduced in comparison with the conventional system.

In conclusion, the study validates that incorporating phase-change heat storage is an effective strategy for optimizing solar ASHP heating systems. The enhanced system has been demonstrated to achieve two principal benefits. Firstly, it has been shown to make more efficient use of available solar energy. Secondly, it has been demonstrated to enhance operational stability. As a primary finding, it was determined that the phase-change system exhibited a total energy saving of 484.91 kWh during the heating period when compared with the traditional system. This was primarily due to a reduction in the necessity for the ASHP and auxiliary electric heaters to compensate for heat loss in the storage tank. This finding indicates a discernible energy-saving benefit, thus paving the way for the development of more efficient and stable solar-based heating solutions.

J. F. Belmonte et al. [19] conducted a study in which they examined the performance of two solar-assisted heat pump (SAHP) systems. These systems were designed to provide space heating for a single-family house in Madrid, Spain. The study investigated the use of short-term diurnal storage as an alternative to costly seasonal storage. The majority of extant research on SAHPs concentrates on large-scale applications in cold climates; however, this study explores the viability of such systems for smaller residential buildings in milder regions. The present study employs the TRNSYS simulation program to conduct a comparative analysis of a standard SAHP system, which utilises water tanks for thermal storage, and an innovative system

that incorporates an intermediate latent heat storage tank containing a phase-change material (PCM).

The simulation results revealed an unexpected degradation in system performance when the PCM tank was integrated using conventional thermostatic controls. The principal finding was that the incorporation of the PCM tank had a substantial detrimental effect on the system's capacity to effectively transfer solar energy to the heat pump. In comparison with the reference system comprising solely water tanks, the PCM-integrated system exhibited a reduction in the useful solar energy collected and transferred to the heat pump's evaporator of almost 30%. This inefficiency resulted in a significant reduction in the system's heating availability, with the system meeting only 72.8% of the heating demand, compared to 98.9% for the reference system.

In conclusion, the study demonstrates that the addition of a PCM tank to an SAHP system does not guarantee improved performance and can, in fact, be detrimental if not properly controlled. The observed degradation in performance is attributed to two factors. Firstly, the slow thermal response of the PCM, known as the "rate problem", and secondly, the limitations of simple thermostatic controls in managing the complex charging and discharging cycles of a latent heat store. The authors conclude that for PCM storage to be effective in such dynamic applications, the development of more advanced, predictive control strategies is essential. In order to achieve this, it is essential that these strategies take into account forecasts of heating demand and accurately estimate the PCM's state of charge. This will optimise the timing of energy storage and release, thereby overcoming the inherent delays in the material's thermal response.

In their paper, W. Wang and A. Zare [20] presented and simulated a hybrid multifunctional solar-assisted heat pump (SAHP) system capable of providing space heating, space cooling, domestic hot water (DHW), and onsite electricity generation for residential buildings. The system's innovative design employs unglazed photovoltaic-thermal (PVT) collectors, which serve three distinct purposes: the generation of electricity, the collection of solar heat for domestic hot water (DHW) heating, and the dissipation of heat via radiative cooling at night for space cooling applications. The system's intricate operation, incorporating fourteen distinct modes, was modelled and simulated utilising TRNSYS software for two distinct U.S. climates: a cold, mixed climate (Baltimore) and a milder, dry climate (Las Vegas).

The simulation results demonstrate the system's high efficiency and significant potential for energy self-sufficiency. A salient finding is the system's high seasonal performance factor (SPF), which quantifies the ratio of useful thermal energy delivered to the total electricity consumed. For a configuration comprising 30 m² of PVT collectors and a 2 m³ storage tank, the multifunctional SAHP system achieved an annual SPF of 2.7 in Baltimore and 3.7 in Las Vegas. These values represent a substantial improvement over a conventional reference system, with the SAHP being approximately 70% more efficient in Baltimore and nearly twice as efficient in Las Vegas.

In conclusion, the study validates the proposed multifunctional SAHP as a highly effective and versatile solution for residential energy needs. The onsite electricity generation from the PVT collectors was found to be capable of covering a significant portion of the building's total electricity demand, with a 53% offset in Baltimore and an 83% offset in Las Vegas. The research also highlighted the importance of a unique operational mode where the heat pump actively charges the thermal storage tank during the coldest months, a strategy that was shown to reduce system energy consumption by up to 34%. The findings indicate that climate has a significant impact on performance and that the integration of PVT collectors for heating, cooling, and power generation offers a promising pathway toward decarbonising residential buildings.

In their study, Dannemand et al. [21] analysed the performance of a novel solar-assisted heat pump system that had been designed for residential domestic hot water (DHW). The system, which was installed at the Technical University of Denmark, uniquely combines an unglazed photovoltaic-thermal (PVT) collector with a heat pump and two separate storage tanks: a domestic hot water (DHW) tank and a buffer tank. The buffer tank functions as a low-temperature heat source for the heat pump, which is charged either by solar thermal energy from the PVT collector or by ambient air when solar radiation is unavailable. A detailed simulation model of this complex system was created in the TRNSYS software and meticulously validated against experimental data, with deviations between measured and simulated energy quantities found to be less than 6%.

Utilising the validated model, a parametric analysis was conducted to ascertain the optimal component sizes and system configurations for year-round operation. The primary conclusion derived from this analysis was that the initial demonstration system was excessively large for its designated DHW-only load, and that substantial performance enhancements could be attained through optimisation. The enhanced system design comprised a larger 7 m² PVT

collector, a smaller 0.2 m^3 buffer tank, a smaller 0.1 m^3 DHW tank, and reduced pipe lengths with enhanced insulation.

In conclusion, the study demonstrates that the principle of using a PVT-charged buffer tank as a heat source for a liquid-to-liquid heat pump is a viable and high-performing concept. The optimised system demonstrated significant enhancements in comparison with the initial configuration, generating 55% more electricity and utilising 23% less annually. This resulted in a solar electrical fraction of 1.51 and a renewable energy fraction of 0.75. The findings suggest that this system has the potential to demonstrate superior performance in comparison to conventional air-to-liquid heat pumps, while concurrently being more cost-effective than systems that necessitate ground-sourced heat exchangers. However, for the system to be economically viable, it must be appropriately sized to accommodate a broader thermal load, encompassing both space heating and domestic hot water (DHW), as opposed to solely addressing DHW requirements.

In their study, Nouri et al. [22] evaluated different configurations of a solar-assisted ground source heat pump (SAGSHP) system for supplying heating, cooling and domestic hot water to a house in Tabriz, Iran, which has a cold climate. Using the TRNSYS simulation tool, they compared a stand-alone GSHP with three solar-assisted configurations: direct expansion (DX), indirect expansion in series (IDX-Series) and indirect expansion in parallel (IDX-Parallel). The system was modelled with a 9 m^2 evacuated tubular solar collector and three 75-metre-deep boreholes.

The IDX-Parallel configuration was found to be the optimal system, exhibiting the lowest annual power consumption (7,948.94 kWh) and a high overall coefficient of performance (COP) of 3.96. Although the DX system achieved a slightly higher COP of 4.00, its energy consumption was greater than that of the parallel system. The study also highlighted the significant advantage of solar assistance: recharging the ground with solar energy maintains a more stable soil temperature over time, which is crucial for long-term efficiency in heating-dominated regions such as Tabriz.

From environmental and economic standpoints, the research concluded that the IDX-Parallel system is a feasible and beneficial alternative to conventional systems. It produces significantly lower CO_2 emissions than a conventional natural gas and electricity-based system. While the initial investment is high, resulting in a payback period of around 13 years, this is reduced to six years when societal benefits such as environmental savings and potential income from

natural gas exports are considered. This demonstrates the system's viability and potential for promoting energy-efficient housing in northern Iran.

Pinamonti and Baggio [23] in their paper analysed and optimised various solar-assisted heat pump (SAHP) systems with energy storage to find the most energy-efficient and cost-effective solutions for residential buildings. The study used TRNSYS software to simulate heating and cooling systems for three building types representing new (high insulation), renovated (medium insulation) and old (low insulation) constructions. The performance of photovoltaic (PV) and solar thermal (ST) systems combined with battery and thermal storage was evaluated based on primary energy demand and annualised global cost over a 20-year period. The key findings revealed that the optimal system configuration depended heavily on the building's insulation level. For a highly insulated building, a PV system with a battery achieved the greatest energy reduction (30%), but a solar thermal (ST) panel system was more financially advantageous in the long term. For a building with medium insulation, a PV installation was the most profitable choice in terms of both energy (a 25% reduction) and economics. Conversely, for a building with low insulation, ST panel integration was the optimal solution, providing a 26% energy reduction and being the most cost-effective option. The study also found that battery storage is most effective in cases of high and medium insulation, with an optimal capacity of around 9.6 kWh. In conclusion, the research demonstrates that there is no one-size-fits-all solution for SAHP systems. The optimal choice involves balancing energy savings with investment cost, depending on the building's energy load. Although PV systems can offer higher energy savings in certain situations, ST systems are often a more financially viable solution, particularly for buildings with very low or very high energy demands. This highlights the necessity of tailoring SAHP system design to the specific characteristics of individual buildings to achieve the best balance of performance and cost.

In their research, Pilou et al. [24] examine an integrated energy system designed to provide office buildings with 100% renewable heating and cooling by combining solar and geothermal energy. The core components of the system are photovoltaic-thermal (PVT) collectors, a borehole thermal energy storage (BTES) field and a multi-source heat pump which can flexibly draw heat from the ambient air, solar-heated water or the ground. The study used a numerical tool developed in Python to simulate the system's performance for a typical office building in two distinct climates: Athens, Greece (warm) and Copenhagen, Denmark (cold).

The key findings demonstrate the system's high efficiency and environmental benefits. The heat pump consistently achieved a high coefficient of performance (COP), with annual winter

values exceeding 4.0 in Athens and reaching approximately 3.8 in Copenhagen. This high system performance is due to its ability to select the most favourable heat source, thereby minimising the heat pump's workload. Although direct self-consumption of the PVT-generated electricity was moderate — exceeding 30% in Athens and 11% in Copenhagen — the potential for a high renewable energy share is substantial. Supplementing the PVT collectors with standard PV panels could meet up to 82% of the net electricity demand in Athens and 61% in Copenhagen, despite limitations in rooftop space.

In conclusion, this study validates the solar-geothermal integrated concept as a promising solution for decarbonising office buildings in various European climates. The system significantly outperforms standard solutions such as gas boilers or air-source heat pumps in terms of primary energy demand and greenhouse gas emissions. For the reference case in Athens, the system produced more electricity than it consumed over the course of a year, resulting in negative primary energy demand. The research highlights that a building's energy efficiency level is a more decisive factor in optimising performance than simply increasing the number of PVT collectors.

Based on the literature review, it can be seen that the current scientific output lacks simulation models for advanced RES systems with simultaneous heat storage. The existing solutions have PV panels or solar collectors, but no seasonal heat storage and no ground regeneration option in a ground heat exchanger. At the same time, most of the existing solutions and their simulations have not validated their components with measured data. Another shortcoming is the lack of optimisation of the systems to increase the COP above 4, which ensures low energy consumption of the system and an increase in the coverage of energy demand by renewable energy without significantly increasing the amount of energy sources. In addition, my work addresses the difficulties that arose because the system was implemented in an existing building, which places different demands on the system and compromises its efficiency. Simulations and optimisation of the system's operating parameters were carried out during construction with the aim of achieving a COP of at least 4, which could not be found in the existing literature. At the time of the initial literature and research review in 2020, the availability of whole system simulation was extremely limited. However, as demonstrated in recent research, particularly from 2022 to 2024, there is an increased focus on the performance of the entire system. Consequently, simulations of the system in TRNSYS, Modellica, Matlab, or comparable software were conducted.

3. Purpose, thesis and innovation of the dissertation topic

The aim of the dissertation is:

- Development of a mathematical model of the compressor heat pump and RESHeat installation in the ZBK building, which allows the year-round simulation of the system and all its components.
- Experimental validation of the developed model on the basis of measured data obtained in the demonstration plant for the ZBK building.
- Optimisation of the RESHeat system to ensure an annual average heat pump COP of at least 4.0.

The thesis: It is possible to develop a heating system for an existing building, based on a heat pump, photovoltaic cells, underground storage, ground heat exchanger and PV/T and solar collectors with a solar tracking system, that will provide 100% of the building's thermal energy needs from RES with an average annual heat pump COP above 4.

The main innovations of my thesis compared to the existing state of knowledge are:

- Development of a mathematical model of a compressor heat pump operating within a complex system.
- Development of simulation tools to model all parameters of the RESHeat system throughout the year.
- Optimisation of the system to achieve an annual average COP of over 4.0 and cover 100% of the building's energy requirements using renewable resources.
- Experimental validation of the developed model based on the constructed system.

Working in parallel with the development of the system allowed me to observe its strengths and weaknesses prior to construction and verify hypotheses on its operation as observed during simulations.

4. Simulation of heat pump cycle

One of the key components of the RESHeat project, and the focus of this dissertation, is the compressor heat pump and its operation within a heating system. As the compressor heat pump is the main source of heat for the RESHeat system all year round, it is crucial that it operates at

its best, as this will enable the RESHeat project to achieve its main objectives. Python code was written for this dissertation to simulate a ground source heat pump cycle using a vapour compression heat pump model. The code's primary objective was to determine the evaporating and condensing temperatures, as well as the refrigerant mass flow, that would satisfy the desired outlet water temperature on the condenser side while adhering to a UA-LMTD model for both the evaporator and condenser water loops.

4.1. Assumptions of the heat pump mathematical model

The compressor heat pump model created in the Python programming language is based on a specific assumption:

- The model represented in the code is steady-state, meaning that it does not consider transient or dynamic effects.
- The model consists of a single-stage vapour compression cycle containing an evaporator, a single-stage compressor, a condenser and an expansion valve. It does not contain multi-stage compressors, economisers, etc.
- The model is based on idealised components with simple efficiency models. The compressor uses an isentropic efficiency to relate the actual enthalpy rise to the ideal isentropic enthalpy rise.
- The expansion valve assumes isenthalpic expansion, meaning that no work is done and there is no heat exchange.
- The evaporator and condenser are modelled using the UA-LMTD method on the water side of the heat exchanger, with no explicit pressure drop on the refrigerant side.
- The model considers a pure refrigerant, for which the thermodynamic properties are obtained from the CoolProp REPROP-based fluid properties library for the selected refrigerant (R410A). The enthalpies of the refrigerant in its single phase (liquid or vapour) are obtained at saturation points that are increased or decreased by subcooling/superheating offsets.
- The subcooling and superheating offsets are constant values.
- The water part of the model, which contains the ground source and heat load loops, is described by the liquid's mass flow and the loop inlet temperatures. Pressure drops in

these loops are neglected; the code simply uses the water mass flow rate and specific heat capacity for each loop.

- No external heat losses to the environment, such as those from the compressor or pipes, are considered in this model.
- There are no advanced control strategies implemented in the software other than adjusting the liquid's mass flow, evaporation and condensation temperatures to meet the outlet setpoint of the load.

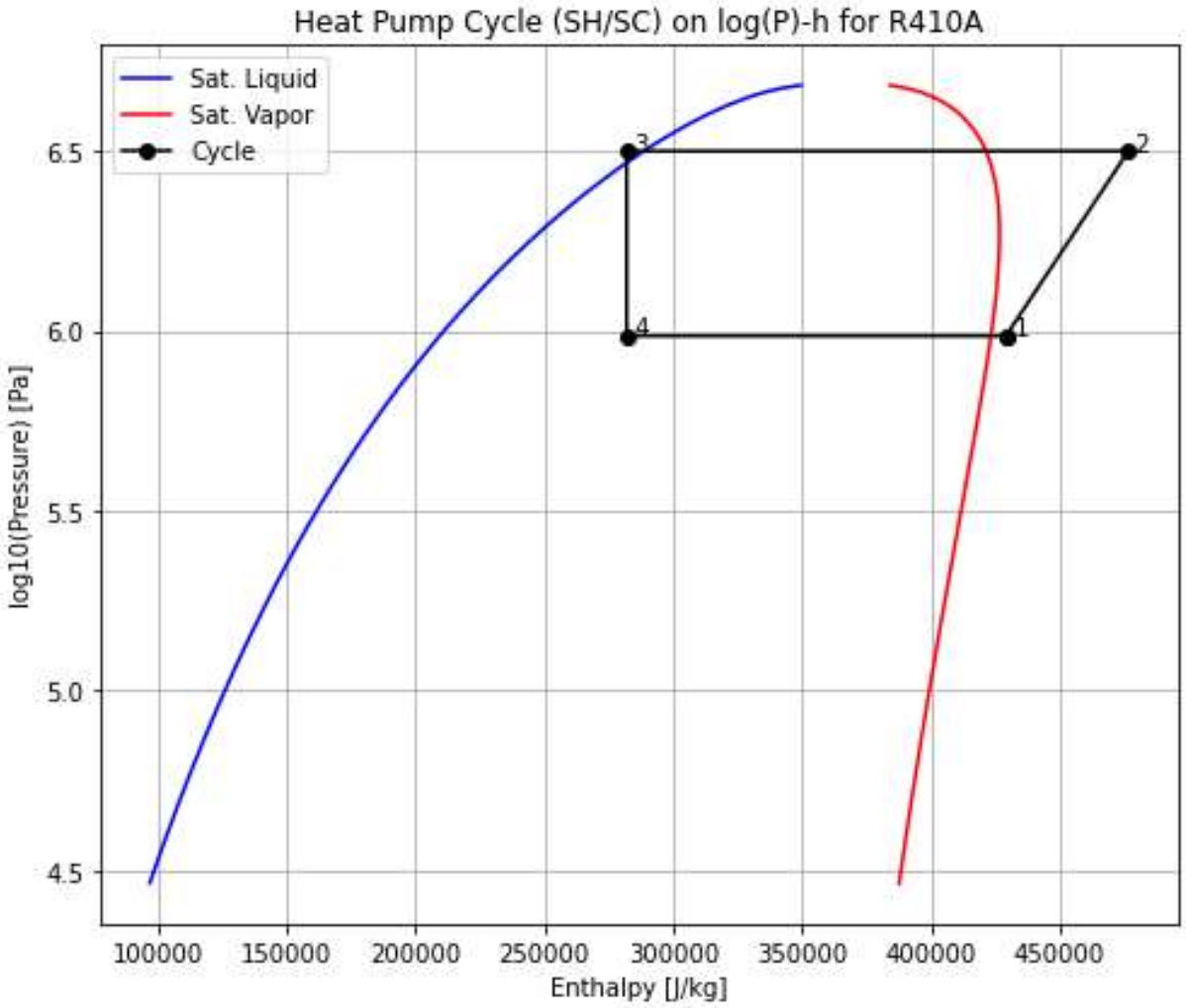

Figure 6 - Heat pump cycle on logP-H diagram with four key states.

The primary objective of the script is to find T_{evap}, T_{cond} and m_{ref} in a system consisting of a compressor heat pump and two heat exchangers so that the following three equations are satisfied:

- **Evaporator Heat Balance**:

$$Q_{evap,UA} - Q_{evap,ref} = 0,$$

where
$Q_{evap,UA} = UA_e \times LMTD_{evap}$ on the water side,
and
$Q_{evap,ref} = m_{ref}\,(h_1 - h_4)$ on the refrigerant side.

- **Condenser Heat Balance**:

$$Q_{cond,UA} - Q_{cond,ref} = 0,$$

where
$Q_{cond,UA} = UA_c \times LMTD_{cond}$ on the **water side**,
and
$Q_{cond,ref} = m_{ref}\,(h_2 - h_3)$ on the **refrigerant side**.

- **Load Water Outlet Temperature Setpoint**:

$$T_{load,out} - T_{load,out,target} = 0.$$

Meanwhile,
$T_{load,out} = T_{load,in} + (Q_{cond,ref}/(m_{load}\, cp_{water}))$.

And similarly for $T_{ground,out}$ based on $Q_{evap,ref}$.

Subcooling & Superheating

- **Evaporator outlet** (State 1):

$T1 = Tevap + \Delta TSHT$.
Therefore, enthalpy $h_1 = h(pevap, T_1)$.

- **Condenser outlet** (State 3):

$T_3 = Tcond - \Delta T_{SCT}$.
So $h_3 = h(p_{cond}, T_3)$.

Isentropic Compression with Efficiency

- We calculate the **isentropic** enthalpy h_{2s} from (p_{evap}, s_1) to p_{cond}.
- Actual h_2 is: $h_2 = h_1 + (h_{2s} - h_1)/\eta_{isentropic}$.

- **Isenthalpic Expansion**
  - $h_4 = h_3$.
- **UA-LMTD** for Each Heat Exchanger**
  - **Evaporator**: $Q_{evap}, UA = UA_e \times LMTD_{evap}$, $LMTD_{evap} = (\Delta T_1 - \Delta T_2)/\ln(\Delta T_1/\Delta T_2)$, $\Delta T_1 = (T_{ground,in} - T_{evap})$, $\Delta T_2 = (T_{ground,out} - T_{evap})$.
  - **Condenser**: $Q_{cond,UA} = UA_c \times LMTD_{cond}$.
- **Solver**
  - The code calls solver script from scipy library, passing the vector of unknowns [T_{evap}, T_{cond}, $\dot{m}_{ref}$] to residual function. Solver tries to driven each residual to near zero. After succession the list of variables is returned

4.2. Heat Pump Mathematical Model Simulation Results

The next step after developing the mathematical model for the heat pump was to obtain simulation results under nominal operating conditions. For the selected heat pump model, these are T_l = 65 degC, T_s=10 degC, m_l = 0.45 kg/s, m_s= 2.3 kg/s, refrigerant R410A. The following results were obtained for the parameters thus assumed:

Table 1 - Simulation model results

T_{evap}	degC	0.342
T_{cond}	degC	70.1
m_{ref}	kg/s	0.215
Q_{cond}	kW	37.7
W_{comp}	kW	15.7
COP	-	2.4

For these assumptions, the heat pump does not meet the COP requirement of at least 4. However, it must be remembered that the required COP level is an annual average for RESHeat operation, the case shown above refers to nominal conditions, the actual operating conditions will be better, resulting in a higher COP level.

In order to verify this, a multi-parameter analysis was carried out to obtain a solution matrix which makes it possible to determine at which operating conditions the heat pump will meet the project requirements.

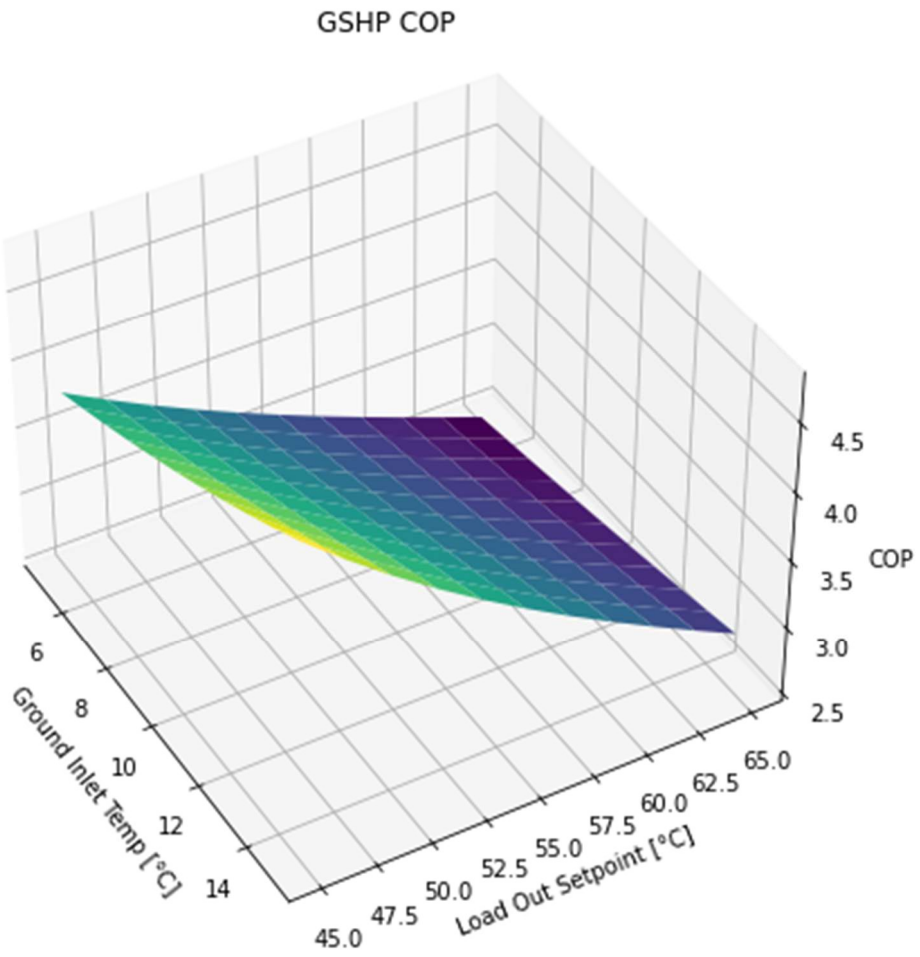

Figure 7 - Multiparam COP results

Figure 7 obtained in multiparam optimisation suggest that there are areas where heat pump works with COP above required threshold. Below is the summary table with COP results of the analysis.

Table 2 - Multiparam results matrix

	45	**47**	**49**	**51**	**53**	**55**	**57**	**59**	**61**	**63**	**65**
5	3.82	3.66	3.50	3.36	3.22	3.08	2.96	2.84	2.72	2.60	2.49
6.5	3.95	3.77	3.60	3.45	3.30	3.16	3.03	2.90	2.78	2.66	2.54
8	4.07	3.89	3.71	3.55	3.39	3.25	3.11	2.97	2.85	2.72	2.60
9.5	4.21	4.01	3.83	3.66	3.49	3.34	3.19	3.05	2.92	2.78	2.66
11	4.36	4.15	3.95	3.77	3.59	3.43	3.28	3.13	2.99	2.85	2.72
13	4.52	4.29	4.08	3.89	3.70	3.53	3.37	3.21	3.06	2.92	2.78
14	4.69	4.45	4.22	4.01	3.82	3.64	3.46	3.30	3.14	2.99	2.85
16	4.88	4.61	4.37	4.15	3.94	3.75	3.57	3.39	3.23	3.07	2.92
17	5.07	4.79	4.53	4.30	4.07	3.87	3.68	3.49	3.32	3.15	2.99
19	5.29	4.98	4.71	4.45	4.22	4.00	3.79	3.60	3.42	3.24	3.07
20	5.52	5.19	4.89	4.62	4.37	4.13	3.91	3.71	3.52	3.33	3.15

As demonstrated in the above table, the temperature of the source has a substantial impact on the COP. A key finding of the research is that, in order to achieve the desired design parameters, it is essential to increase the temperature of the heat pump source. The findings of the research demonstrate that achieving the requisite COP is challenging at typical domestic hot water temperatures. A comparable scenario is evident in the case of central heating systems, which are employed in existing buildings equipped with traditional heating systems that demand comparatively high flow temperatures. The only viable solution to achieve the required heat pump coefficient of performance (COP) is to periodically reduce the temperature of the load during periods of lower heat demand, while utilising waste and solar energy to raise the temperature of the source.

The temperature range employed in the multi-parameter analysis was the basis for the formulation of a two-parameter Ordinary Least Squares (OLS) regression model [25]. Multiple linear regression (MLR) is a statistical technique employed for the modelling of the relationship between one dependent variable (frequently termed the response or outcome) and a minimum of two independent variables (often referred to as predictors, explanatory variables, or features). This model represents an extension of simple linear regression, which involves only a single predictor. [26]. It is important to note that this method is not without its limitations. In order to ensure the reliability of multiple linear regression, it is customary to make certain assumptions:

- Linearity: The relationship between each predictor x_i and the outcome y is assumed to be linear (in the parameters).
- Independence of Errors: The error terms ε are independent of each other (no autocorrelation).
- Homoscedasticity (Constant Variance): The errors have constant variance (the spread of the residuals does not systematically change with the predictor values).
- Normality of Errors: The error terms ε are usually assumed to be normally distributed around zero, especially important for small sample sizes or for constructing confidence intervals.
- No or Minimal Multicollinearity: The predictors should not be perfectly (or excessively) correlated with one another, as high correlation makes it difficult to isolate the effect of each predictor.

The ordinary least squares (OLS) method is most commonly used to estimate the parameters (βi) in a multiple linear regression model. OLS finds the set of βi values that minimize the sum of squared residuals, i.e., $Minimize\ \sum_{n=1}^{n}(y_i - \hat{y}_i)^2$, where y_i is the observed value and $\hat{y}_i$ is the model's predicted value for the i-th data point. To check how well the multiple linear regression model fits the data, several metrics and diagnostic techniques are used:

- Coefficient of Determination (R^2): Represents the proportion of variance in y explained by the model.
- Adjusted R^2: Adjusted for the number of predictors in the model; it penalizes excessive use of variables that do not improve the model significantly.
- Residual Analysis: Plotting residuals against fitted values or predictors to visually check for non-linearity, non-constant variance, or outliers.
- Statistical Tests (F-test, t-tests): Used to assess the overall significance of the regression model and the significance of individual coefficients, respectively.

The interpretation of results can indicate the parameters that have the greatest influence on the COP value. A linear model was fitted to visualise the partial effects of T_{source} and T_{load} on COP:

$$COP = \beta_0 + \beta_1 \times T_{source} + \beta_2 \times T_{Load}$$

Where:

$$\beta_0 = 7.55, \qquad \beta_1 = 0.0729, \qquad \beta_2 = -0.0882$$

And:

$$R^2 = 0.97, \qquad Adj.R^2 = 0.969$$

Results of t-test for parameters:

	Std. err	t	P>|t|
β_0	0.097	77.68	0.0
β_1	0.002	32.517	0.0
β_2	0.002	-52.444	0.0

The resulting formula can be interpreted as follows: for a range of source temperatures from 5 to 20 and load temperatures from 45 to 65 degrees, an increase in the source temperature at a constant load temperature results in an increase in the coefficient of performance (COP) of 0.0729, while an increase in the load temperature by one degree at a constant source temperature results in a decrease in the COP of -0.0882. Upon interpretation of the coefficients, it becomes evident that the impact of the load temperature on the COP is marginally higher, albeit negative.

However, both coefficients demonstrate a comparable degree of influence on the COP parameter. The results of the t-test indicate that the individual parameters are highly significant and have a low standard error. Which indicates that for the given temperature range, the resulting model can be approximated with a low margin of error using a multi-parameter linear equation.

Based on the data obtained from the above analysis of the developed heat pump model, it is necessary to determine on which days of the year the heat pump will operate and what the expected temperature obtained from the ground heat exchanger will be. Weather data from the meteorological station located next to the ZBK building and from temperature sensors placed in the ground were used for the analysis.

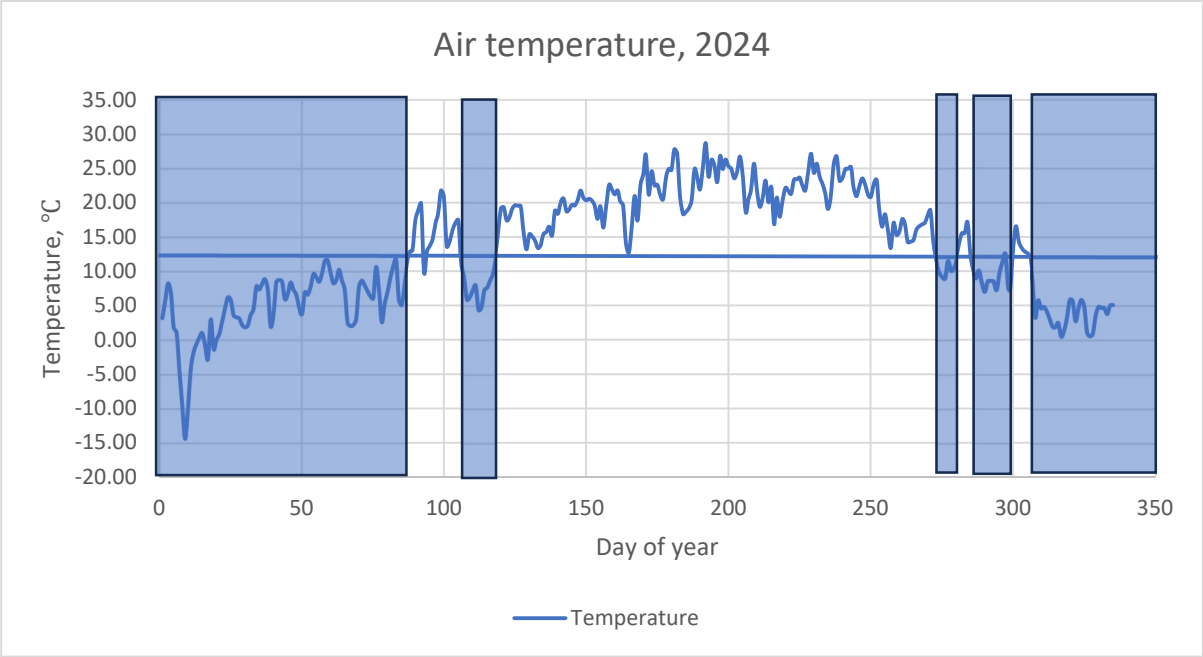

Figure 8 - Outside Air Temperature

Based on the assumption that the central heating is only active when the outside temperature is 12 degrees Celsius or less, a heat pump will be required to provide heat for the central heating on the days marked on the graph above. The number of days when central heating will be required is 150.

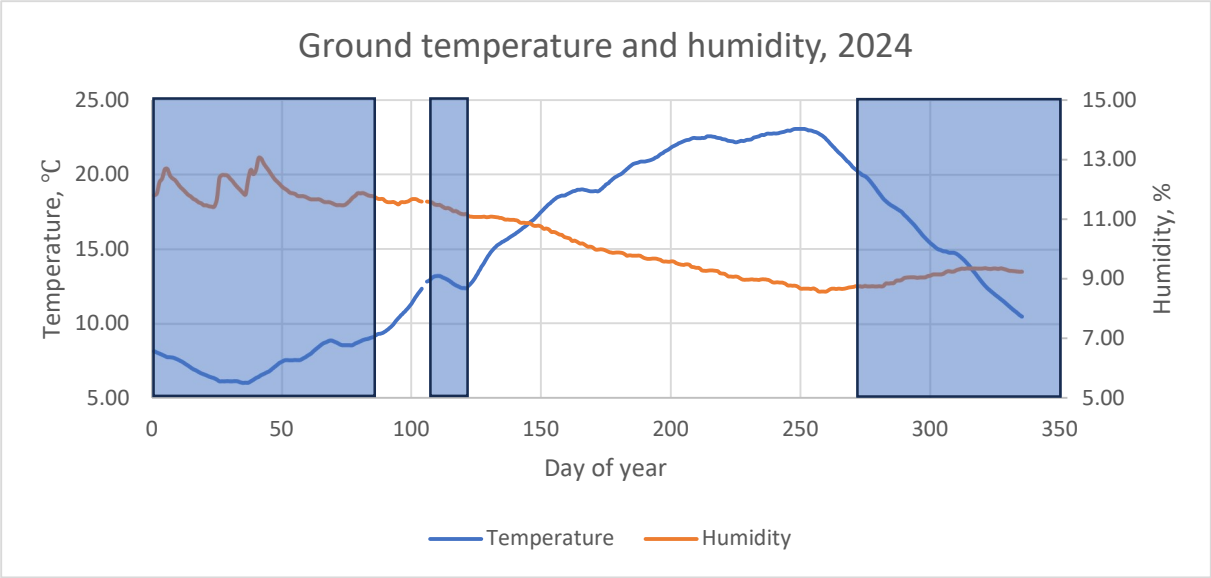

Figure 9 - Ground humidity and temperature

Based on the previous analysis of the days when central heating will be required and the data collected from the sensors placed in the ground, it is possible to determine at what ground temperatures the ground heat exchanger will operate and what the expected temperatures of the circulating water leaving the ground heat exchanger and therefore the source temperatures for the heat pump are. The average ground temperature during this period was 10.4 degrees Celsius.

The outlet temperature of the heat pump and the parameters of the ground heat exchanger must be considered when determining the temperature, which will be slightly lower than the ground temperature depending on the flow rate. Consequently, the ensuing coefficient of performance (COP) can be anticipated. The result obtained in this way will then be compared with the heat pump model to determine what level of coefficient of performance (COP) can be expected for the assumed temperatures of the load.

Table 3 - Matrix of COP Simulation Results

	45	47	49	51	53	55	57	59	61	63	65
5	3.82	3.66	3.50	3.36	3.22	3.08	2.96	2.84	2.72	2.60	2.49
6.5	3.95	3.77	3.60	3.45	3.30	3.16	3.03	2.90	2.78	2.66	2.54
8	4.07	3.89	3.71	3.55	3.39	3.25	3.11	2.97	2.85	2.72	2.60
9.5	4.21	4.01	3.83	3.66	3.49	3.34	3.19	3.05	2.92	2.78	2.66
11	4.36	4.15	3.95	3.77	3.59	3.43	3.28	3.13	2.99	2.85	2.72
13	4.52	4.29	4.08	3.89	3.70	3.53	3.37	3.21	3.06	2.92	2.78
14	4.69	4.45	4.22	4.01	3.82	3.64	3.46	3.30	3.14	2.99	2.85
16	4.88	4.61	4.37	4.15	3.94	3.75	3.57	3.39	3.23	3.07	2.92
17	5.07	4.79	4.53	4.30	4.07	3.87	3.68	3.49	3.32	3.15	2.99
19	5.29	4.98	4.71	4.45	4.22	4.00	3.79	3.60	3.42	3.24	3.07
20	5.52	5.19	4.89	4.62	4.37	4.13	3.91	3.71	3.52	3.33	3.15

The above data shows that in order to maintain the COP at the level of 4 required in the programme, it is necessary to keep the temperature of the load at a low level not exceeding 47 degrees Celsius. If a higher load temperature is required, it will be necessary to increase the source temperature by recovering heat from PVT panels or using heat from solar collectors.

5. Simulation and Manufacturer Laboratory Test Differences

The subsequent stage of the research will entail a comparison of the simulation results with the laboratory specifications of the selected heat pump, as provided by the manufacturer. This comparison will be made for the temperature range defined in the manufacturer's specifications.

Table 4 - Comparision of the simulation results and laboratory data

Source Inlet Temperature, ℃	Load Inlet Temperature, ℃	COP Simulated	COP from Specs	Difference, %
0	29.2	3.9	4.6	17.7%
0	43.8	2.9	3.4	16.5%
0	50.2	2.6	2.8	9.5%
0	55.0	2.3	2.4	3.4%
5	29.2	4.4	5.3	21.3%
5	43.8	3.2	3.8	20.1%
5	50.2	2.8	3.2	15.4%
5	55.0	2.5	2.6	4.8%
10	29.2	5.0	6.0	21.2%
10	43.8	3.5	4.3	24.0%
10	50.2	3.0	3.5	17.2%

10	55.0	2.7	2.9	8.4%
15	29.2	5.7	6.9	21.0%
15	43.8	3.8	4.8	25.9%
15	50.2	3.3	3.8	16.4%
15	55.0	2.9	3.2	10.2%
20	29.2	6.7	8.1	20.5%
20	43.8	4.3	5.3	24.3%
20	50.2	3.6	4.2	17.1%
20	55.0	3.2	3.4	7.6%
25	29.2	8.1	9.6	17.9%
25	43.8	4.8	6.0	24.2%
25	50.2	4.0	4.7	17.7%
25	55.0	3.5	3.8	9.6%

5.1. Origins of the differences

As it has been demonstrated that for all temperature ranges, the COP in the laboratory specification of the pump manufacturer is higher than that obtained in the simulation. The range of the COP difference is between 3.4% and 25.9%. The most significant differences are usually observed for the smallest differences between the source and load temperatures. It can thus be concluded that the bigger the temperature difference between the source and load, the closer the simulation results are to those obtained in the manufacturer's specification.

The disparities may be attributable to a number of factors. The simulation utilises compressor and performance models that are more conservative or idealised in nature, deviating from the manufacturer's optimised rating conditions. It is noteworthy that manufacturer COP data is frequently obtained under "best-case" or standard rating conditions. The employment of more detailed simulation models can lead to the introduction of pressure losses or other minor inefficiencies that may not be fully captured in manufacturer data.

Manufacturers rate heat pumps under standardized laboratory conditions. In a lab, ambient temperatures, humidity, and operating cycles are tightly controlled. These conditions are often idealized – for example, moderate humidity (to avoid coil icing) and no wind or solar effects. In the real world, conditions fluctuate and are often more extreme. As a result, real-world performance is usually lower than lab ratings. [27] In practice, this means a heat pump might

achieve its rated Coefficient of Performance (COP) or efficiency only when operating in a narrow band of conditions similar to the lab test.

Examples of Condition Differences: In standardized tests [28, 29], indoor and outdoor temperatures are fixed (e.g. 21.1°C indoors, 8.3°C outdoors for a nominal heating test). Humidity is set at a standard level, and there is no random wind affecting the outdoor unit. By contrast, field conditions introduce variables: wind can cool or stress the outdoor coil, sun can heat the unit, occupants may set varying thermostats, etc. Laboratory tests also often run the equipment in steady-state without frequent cycling or defrost interruptions. In reality, a heat pump will cycle on/off and perform defrosts in cold weather, further lowering the effective efficiency [30]. All these factors mean a simulation that attempts to mimic real usage may predict lower performance than the spec (as the specification is based on fixed lab conditions), whereas a simulation that assumes lab-like steady conditions might overpredict performance seen in the field.

Another difference is that manufacturers' lab tests usually exclude installation-related losses. For example, ducted heat pumps are tested with a short, straight duct and a low static pressure. In a home, ducts may be long, leaky, or have higher resistance. New testing standards have increased the required external static pressure to better reflect real installations [31]. Previously, the low static pressures in lab tests made fans work easier than they would in a house, boosting efficiency. SEER2 certification standard require now higher pressure loss, resembling real life conditions. This change was specifically made because lab ratings were optimistic – they didn't account for typical duct restrictions. In summary, simulations that consider realistic duct and installation effects will diverge from specs that assume a near-perfect setup.

5.2. Idealised models vs. real-time operation

Simulation tools inevitably simplify certain aspects of heat pump operation. Models often assume ideal or calibrated performance for components such as compressors and heat exchangers, which may not capture all real-world inefficiencies. For example, a model may use a compressor map provided by the manufacturer or an equation fitted to laboratory data. If the simulation assumes that the compressor follows an ideal polynomial performance curve, or that the heat exchangers have a uniform temperature distribution, the results may differ from actual behaviour. Heat exchanger performance is sometimes modelled with fixed efficiencies or

correlations that don't account for refrigerant maldistribution or oil films, potentially leading to optimistic capacity or efficiency predictions in the simulation.

Many building energy simulations ignore certain losses to simplify modelling. If a manufacturer's specification doesn't include duct losses either, then both are on equal footing in this respect. However, if the simulation also ignores other secondary losses (fan heat, auxiliary heaters, etc.) or assumes perfect refrigerant charge, it may overestimate performance compared to a realistic scenario.

Simulations often assume steady-state operation at each condition, unless a detailed transient model is used. Manufacturer ratings are also steady-state (except for seasonal metrics such as HSPF, which include cycling). However, real heat pumps cycle on and off with load, incurring efficiency penalties during start-up and shut-down. If the simulation model does not include a part-load degradation factor, it may not capture these losses. In fact, part-load performance data for specific units is rarely published. This means that many simulations simply assume that the heat pump achieves steady-state efficiency even at part load, or use a generic degradation coefficient. Differences in these assumptions (or the lack of cycling in the simulation) can cause simulated seasonal performance to differ from the manufacturer's seasonal ratings.

Another modelling assumption is how the unit is controlled. Simulations may assume that the heat pump is always operating at optimal settings (e.g. optimal defrost timing, ideal thermostat operation, no unnecessary auxiliary heat use). Real units have control algorithms that may prioritise comfort or reliability over efficiency (e.g. more frequent use of electric backup heating to maintain indoor temperature). If the simulation doesn't model these control behaviours accurately, its results will differ from both the manufacturer's specifications and real-world performance. In summary, simplifications in compressor/fan models, omitted losses and assumed ideal control in simulations can all lead to discrepancies with specifications.

5.3. Existing literature about simulation and controlled laboratory data

Researchers have compared detailed heat pump simulations with manufacturer or laboratory data to identify the gaps. In a validation study [32], the Oak Ridge National Lab simulation tool was used to predict the performance of various heat pumps and the results were compared with manufacturers' test data. The differences were generally within about 5-8% on average for capacity and efficiency. For example, for a standard 35°C cooling test, the simulation was very close (within ~5%). However, some differences exceeded the commonly accepted tolerance of

5%. In a few cases, there were differences of over 10% - for some models, the simulated efficiency was significantly off until the model was further refined. At very low outdoor temperatures (the -8.3°C heating test condition), the average simulation error increased to around 7-8% for capacity and 7% for COP. This is probably because it's harder to model phenomena such as frost and refrigerant properties at extremes. The takeaway is that even with a sophisticated model and input from the manufacturer, simulated performance can vary by up to 5-10% from laboratory specifications, especially at the edges of the operating range. These studies highlight the need to adjust and calibrate simulations if you want to reproduce the exact spec numbers.

Field monitoring projects provide a different perspective - they compare the performance of installed heat pumps with the rated values. Often simulations are used to predict performance in the field, and then measured data is compared. A US Department of Energy (DOE) field evaluation of cold-climate heat pump (CCHP) prototypes [33] found that the units did not always achieve their lab-rated efficiencies in real homes. For example, the median COP observed at outdoor temperatures of -18 to -15 °C was about 1.9. In the lab, the same units had to meet a COP requirement of 2.1 (and some aimed for 2.4) at 15°C. So the field COP was about 10-20% lower than the optimised lab value. Nevertheless, the field performance was better than many conventional heat pumps and above the minimum standards (most units stayed above COP 1.75 at -15°C).

Manufacturers know the specific test conditions (e.g. 35°C outdoor/26.6°C indoor for EER, or -8.3°C outdoor for low temperature heating COP). They can design the system (or at least program the controls) to perform extremely well at these points, sometimes at the expense of other points. For example, they might size the outdoor coil a little larger so that the system's COP for the HSPF test procedure is maximised at an outdoor temperature of 8.3°C. But the same sizing might not be optimal at -12.2°C (where the unit might be undersized for refrigerant charge, etc.). This type of tuning can cause simulations to under-predict performance at the design point if the model doesn't capture the manufacturer's secret sauce, but over-predict performance at off-design points where the real unit has not been optimised as much.

As mentioned, prior to 2023, test standards allowed relatively low external static pressures for ducted units. Manufacturers would publish high SEER and HSPF values achieved with, say, 25 Pa external static (very low). In a normal home, the static could be 125 Pa or more, which would reduce airflow and efficiency. The new SEER2 standard forces testing at higher static to avoid this optimisation trick. But for older ratings, a simulation using a realistic static pressure

will show lower performance than the specification measured at unrealistically light conditions. This is a clear case of manufacturers optimising lab conditions to increase the rating, and including a real condition (higher static) in a model immediately makes a difference - a more conservative, realistic efficiency number. For heating, manufacturers test the heat pump alone, but in cold weather real systems often need electrical resistance backup. Manufacturers also specify cut-off temperatures (e.g. "will run down to -15°C"). In the laboratory, they can run it at these temperatures without ever using the auxiliary heater (as this would ruin the COP rating). In the field, homeowners or installers often set a switchover balance point where the system uses auxiliary heat below, say, 0°C. A simulation might include this control (to maintain comfort), causing the seasonal performance to drop (as the resistance heat COP = 1). The manufacturer's HSPF assumes a certain algorithm for accounting for auxiliary heat (following a standard climate bin method), but if the real control strategy is different, that's another deviation. In short, manufacturers try to put their unit in the best possible light for specs, whereas simulations may test the unit more practically or under less 'forgiving' conditions.

6. Simulation of RESHeat in TRNSYS software

The proposed RESHeat system in Krakow consists of the following equipment

- Solar collectors,
- Stationary photovoltaic and photovoltaic-thermal (PV-T) panels,
- Ground Source Heat Pump (GSHP),
- A domestic hot water (DHW) tank and a central heating (CH) tank,
- Borehole heat exchangers,
- Underground heat storage tank,
- Radiators,
- SCADA system,

The system schematics are shown in Figure 10. The demo site is located in the northern hemisphere with a temperate climate. Therefore, only the heating system is required during the year. In the system, stationary photovoltaic panels and photovoltaic/thermal (PV/T) panels provide the electricity consumed by the heat pump and control system.

(a)

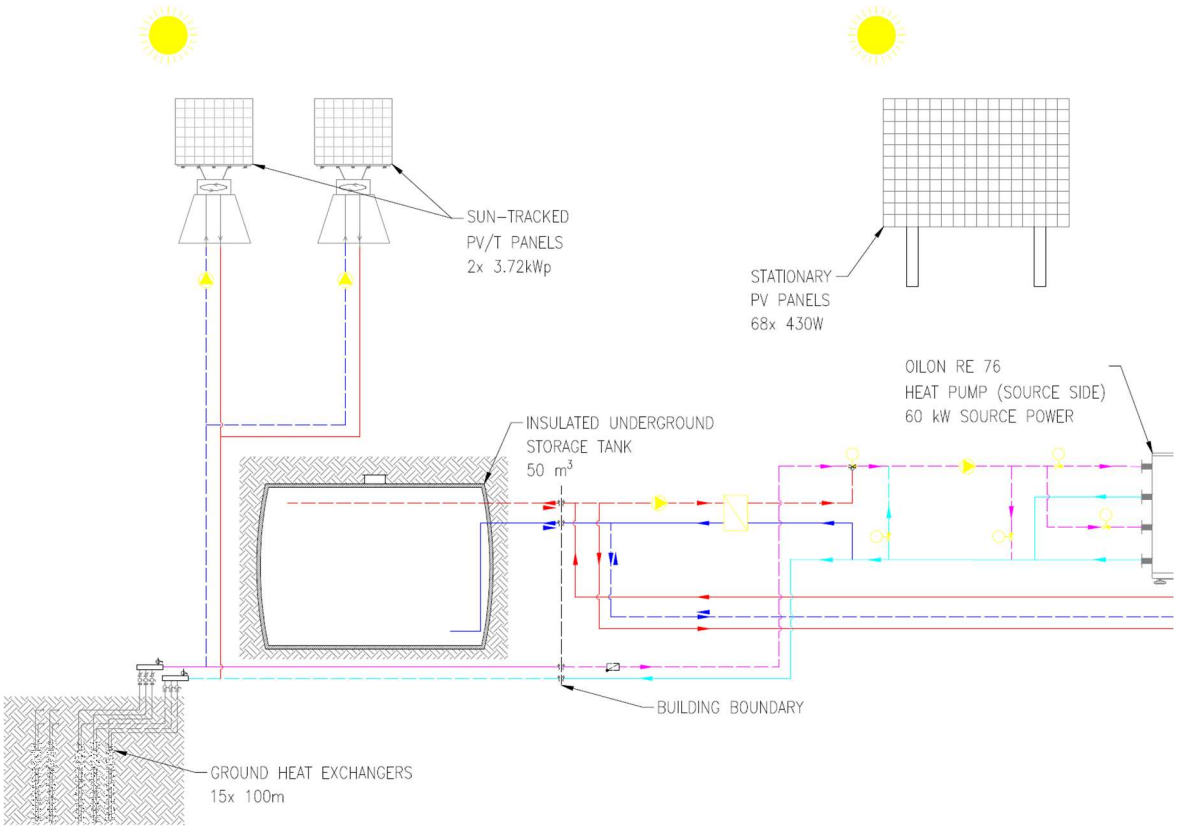

(b)

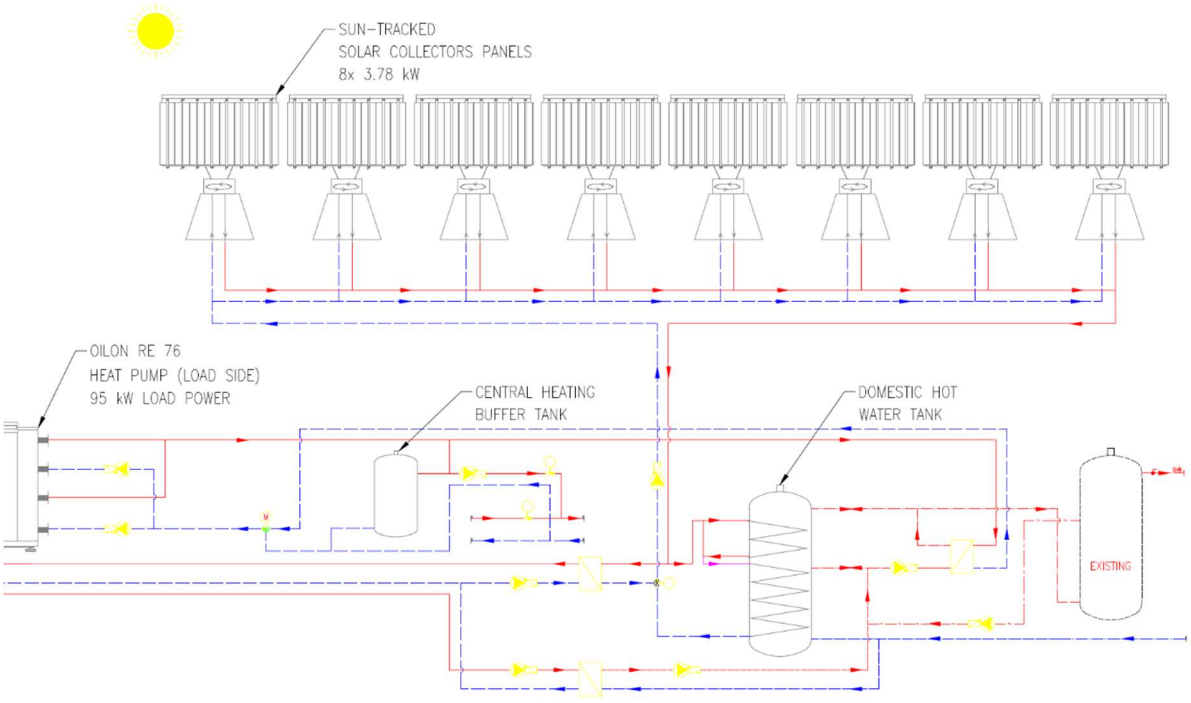

Figure 10 - Schematic diagram of the system in Krakow, (a) heat source part of the heat pump system, (b) heat load part of the heat pump system

The heat produced by the solar panels is stored in an underground heat storage tank (UGS) and used by the system. In winter, when the temperature from the solar collectors is insufficient, the heat pump will make up the deficit. Excess heat from the solar collectors and the PV-T system is stored in a ground heat exchanger. The stored heat is used by the heat pump during the winter period to keep the COP as high as possible.

As part of the RESHeat project, the following elements have been modelled in TRNSYS:

- Heating demand of the building
- Tracking PV/T panels
- Stationary PV panels
- Tracking solar collectors
- Water to water heat pump
- Radiators
- Buffer tanks
- Underground heat storage
- Ground heat exchanger

The thesis describes the mathematical models of all simulated elements and their parameters.

6.1. Assumptions of the numerical TRNSYS simulation

TRNSYS has an open and modular structure. It is possible to extend the contents of the software by adding new component models using the most common programming languages (C, C++, FORTRAN, etc.) according to the specific needs of the user. Furthermore, TRNSYS can easily be combined with other software for processing input or output data (Microsoft Excel, Matlab, EES, Python, etc.).

The modular structure is created by combining individual component models (Types) into a complete model. Each type represents an element of the installation, such as pumps, pipes, chillers and solar panels, as well as the building, weather and schedule. These are then linked together in the TRNSYS environment, just as they would be in a real installation. The entire programme is essentially a collection of energy system components organised around a simulation module (solver). Each component is described by a mathematical model within the TRNSYS simulation environment. The simulation components (types) contains a black box description of the component, including inputs, outputs and parameters (Figure 11).

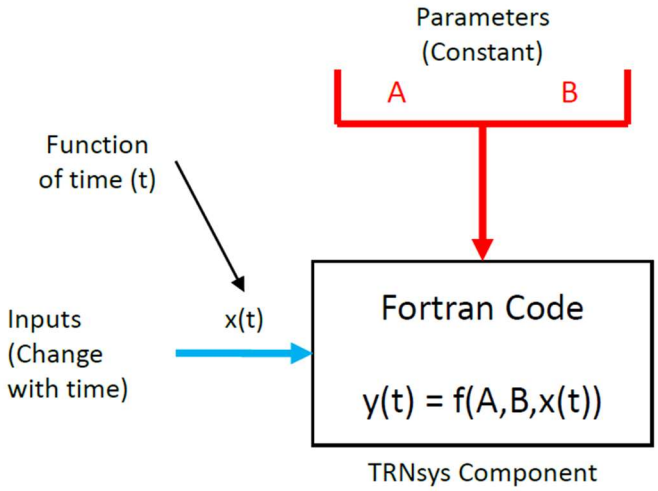

Figure 11 - TRNSYS type/object

The following section presents mathematical models that describe the types used to simulate the RESHeat system in TRNSYS.

6.1.1. Thermal model of the building

The geometrical and thermophysical characterisation of buildings and the assessment of the building's energy requirements are carried out using the TRNSYS3D and TRNBuild add-ons.

The first step in modelling the building is to define and draw the thermal zones in TRNSYS3D (SketchUp plugin). Once the geometric model was ready, the .idf file was imported into TRNSYS Building. For each thermal zone, it is necessary to determine the initial values of internal temperature and relative humidity, as well as the data needed to assess the overall characteristics of the zone, such as infiltration rate, internal gains and comfort parameters of the building occupants. It also identifies the thermo-physical properties of the walls and windows that define the zone under consideration. A building model from the TRNSYS (Simulation Studio) workspace is imported to the TRNSYS Workspace and defined by Type 56.

Heating and cooling equipment are modelled as separate components in Simulation Studio. Therefore the output from the Type 56 zones can be used as input to the appliance models, which in turn produce input to the Type 56 zones for heating and cooling.

6.1.2. PV-T solar collector

One of the main components of the RESHeat system is a cooled photovoltaic panel. TRNSYS Type 560 was used to model this type of panel. This component is designed to model an uncooled solar collector that generates energy from embedded photovoltaic (PV) cells while

providing heat to a fluid stream flowing through tubes connected to an absorber plate located beneath the PV cells (see Figure 12). The model is based on linear coefficients that describe the efficiency of the PV cells as a function of cell temperature and incident solar radiation.

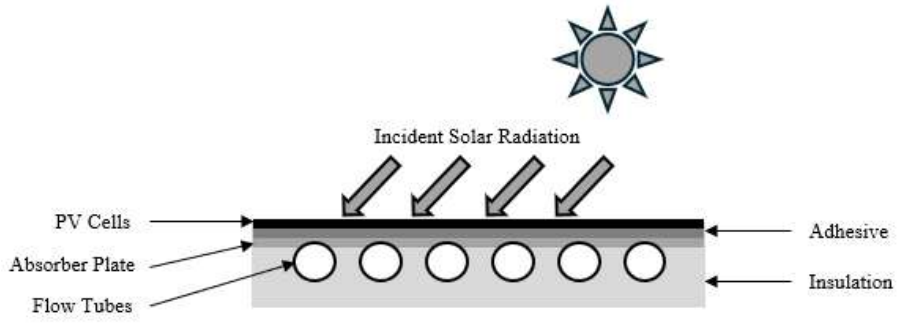

Figure 12 - Cross-section through a PV/T panel [56]

By means of the energy balance on the collector surface (1), the energy balance assumed for a different-dimensional section along the absorber plate, the energy balance on the base (unribbed) surface of the absorber plate, and the energy balance assumed around a different-dimensional section of fluid moving through the collector (in the y-direction), the mathematical function of the PVT panel can be described.

$$\dot{q}_{abs}=\dot{q}_{l,conv}+\dot{q}_{l,rad}+\dot{q}_{l,PV} \rightarrow plate \quad (1)$$

At any point along the surface, the energy balance at the collector (PV cell) surface is the difference between the absorbed net solar radiation ($\dot{q}_{abs}$) and the convective, radiative and conduction losses to the panel (respectively: $\dot{q}_{l,conv}$, $\dot{q}_{l,rad}$, $\dot{q}_{l,PV} \rightarrow plate$) according to (1) and (2) (Fig. 13).

$$0 =\dot{q}_{abs}-h_{outer}(T_{PV}-T_{amb})-h_{rad}(T_{PV}-T_{sky})-(T_{PV}-T_{abs})/R_T \quad (2)$$

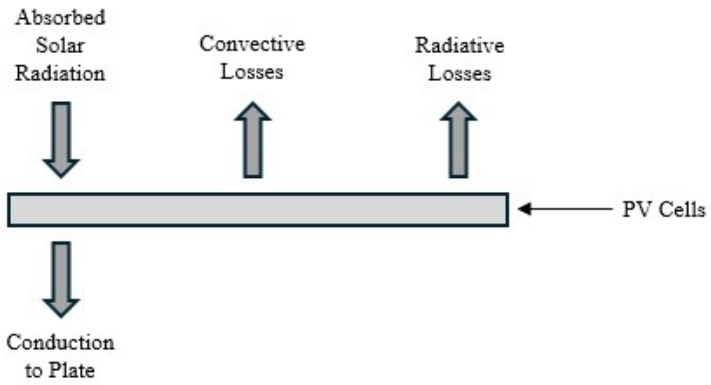

Figure 13 - PV/T panel energy balance [56]

The energy balance assumed for a section of varying size including the absorber plate, at any point including the plate away from the pipe section, shows the following relationship (3) (assuming the plate is thin and made of conductive material):

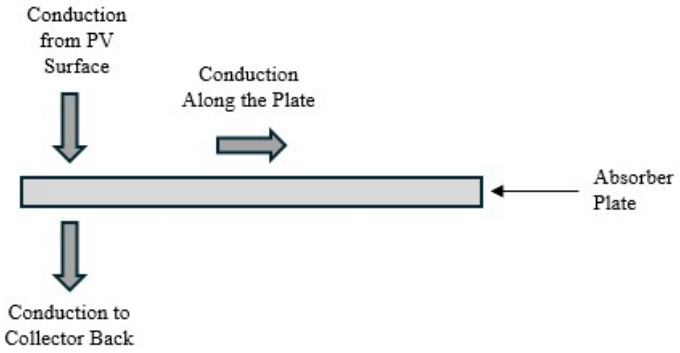

Figure 14 - Absorber energy balance [56]

$$k\lambda(d_2\, T_{abs}/d_{x2}\,) = {}_(T_{abs}\, - T_{back})/R_B\, - (T_{PV}\, - T_{abs})/R_{\,T} \tag{3}$$

The energy balance for the entire collector can also be written as (4):

$$= Q_{abs}Q_{l,\,conv}+Q_{l,\,rad}+Q_{l,\,back}+Q_{\,u} \tag{4}$$

6.1.3. Stationary PV panel

The model is used to represent the performance of stationary panels over the course of a year. In case of mono and polycrystalic photovoltaic panels the electrical performance model can be utilised. For this a four-parameter model can be used, which assumes that in short circuit conditions the slope of the current voltage equals to zero:

$$(dI/dV)_{v=0} = 0 \tag{5}$$

Both insolation and temperature affect the IV characteristics of a photovoltaic cell. The current-voltage equation can be written as follows:

$$I = I_L\, - I_o\, [exp((q/\gamma kT_c\,)(V+IR_s\,)) - 1] \tag{6}$$

where q is the charge constant of the electron, k is the Boltzmann constant, T_c is the temperature of the module. Additionally, V and I represents the module voltage and current respectively. R_s and γ are constants. The current I_L have linearly dependence on the solar irradiance:

$$L\, = II_{L,\,ref}(G_T\, /G_{T,\,ref}) \tag{7}$$

where G_T is the total incident radiation on the PV panel, $G_{T,ref}$ is the incident radiation under reference conditions. The reverse current of the diode I_o is a temperature-dependent quantity:

$$I_o / I_{o,ref} = (T_c / T_{c,ref})^3 \quad (8)$$

The module temperature is calculated using the following equation.

$$\tau\alpha/U_L = (T_{c,NOCT} - T_{a,NOCT})/G_{T,NOCT} \quad (9)$$

where $\tau\alpha$ is the transmission-absorption product of the module and UL is the thermal loss coefficient of the matrix, $T_{c,NOCT}$ is the module's temperature under normal operating cell conditions (NOCT), $T_{a,NOCT}$ is the ambient temperature(20 °C), and $G_{T,NOCT}$ is the solar irradiance under NOCT conditions(800 $W/m2\ K$). Assuming this factor remains constant, the module temperature at any given time can be calculated as follows:

$$T_c = T_a + ((1-\eta_c / \tau\alpha)/(G_T\ \tau\alpha)/U)L \quad (10)$$

where η_c is the conversion efficiency of the module in question, which varies depending on the ambient conditions.

6.1.4. Solar collector

One of the key components of the RESHeat project is the solar collector. The solar collector used is a vacuum tube type, represented by Type 71 in the TRNSYS software, which uses the standard linear efficiency equation. This model requires input data for the collector area, the specific heat of the fluid, the inlet temperature and flow rate, the ambient temperature, the incident radiation and the angle. Solar collectors use a mixture of water and propylene glycol as the working fluid. The rate at which a solar collector extracts useful energy is calculated using the following equation:

$$Q_{useful} = \dot{m} * c_p * (Tout - T_{in}) \quad (11)$$

where Q_{useful} is the energy gained by the collector, $\dot{m}$ is the mass flow rate, cp is the specific heat capacity of the working fluid and $Tout$ and Tin are the outlet and inlet temperatures of the solar collector respectively.

The Hottel-Whiller equation is used to calculate the overall thermal efficiency of a solar collector:

$$\eta = Q_{useful}/(A * I_T) = (\dot{m} * c_p * (T_{out} - T_{in}))/A * I_T = a_0 - a_1\ (\Delta T)/I_T - a_2\ (\Delta T)^2 / I_T \quad (12)$$

where η is the thermal efficiency, A is the total gross area of the collector, I_T is the total radiation incident on the solar collector. a_0 is the maximum collector efficiency, a_1 is the negative first-order coefficient in the collector efficiency equation and a_2 is the negative second-order coefficient in the collector efficiency equation. ΔT is the temperature difference between the inlet temperature of the collector fluid and the ambient temperature.

The optical efficiency of a solar collector can be expressed as follows:

$$\frac{(\tau\alpha)}{(\tau\alpha)_n} = \frac{I_{bT}\frac{(\tau\alpha)_b}{(\tau\alpha)_n} + I_d\frac{(\tau\alpha)_d}{(\tau\alpha)_n} + \rho_g I\left(\frac{1-\cos\beta}{2}\right)\frac{(\tau\alpha)_g}{(\tau\alpha)_n}}{I_T} \quad (13)$$

Where $\tau\alpha$ is the product of the shield's transmittance and the absorber's absorption, $(\tau\alpha)_n$ is $(\tau\alpha)$ at normal tilt, I_{bT} is the incident beam on the solar collector, $(\tau\alpha)_b$ is $(\tau\alpha)$ for the radiation beam. Additionally, I_d is the diffuse horizontal radiation, $(\tau\alpha)_d$ is $(\tau\alpha)$ for diffuse sky radiation, ρ_g is the ground reflectance, I is the total horizontal radiation, β is the inclination of the collector above the horizontal plane, and $(\tau\alpha)_g$ is $(\tau\alpha)$ for ground reflected radiation.

6.1.5. Water-to-Water Heat Pump

Two different heat pumps, which were supplied by OILON, will be used at the demonstration sites in Krakow and Limanowa. A variable-speed water-to-water compressor heat pump was used for the modelling, which allows the supply-side output temperature to be modified. TRNSYS used Type 1323, a single-stage, variable-speed, water-to-water heat pump. This model calculates the outlet temperature on the supply side of the heat pump assuming full capacity operation. If the outlet temperature exceeds the setpoint in heating or cooling mode, the model calculates the partial load required for the heat pump to reach the supply-side setpoint temperature. The model is based on external (array) data provided by the user. These arrays contain several inlet temperatures for both the heat source and the heat load. For each pair of source and load temperatures, coefficients are given for the nominal capacity and electricity demand multiplication factors. Therefore, the program used two heat pump datasheets (RE33 and RE76) for modelling.

Below is a table of performance factors for different temperatures for the RE 76 pump, where a factor of 1.00 indicates nominal conditions:

Table 5 - Table of heating capacity factors

Source temperature \ Load temperature	55	50.2	43.8	29.2
25	1.33	1.33	1.32	1.31
20	1.22	1.20	1.20	1.19
15	1.10	1.09	1.09	1.07
10	1.00	0.99	0.98	0.95
5	0.90	0.89	0.88	0.85
0	0.81	0.79	0.78	0.75

Another matrix needed to be implemented in the model is a table showing electricity demand:

Table 6 - Table of electricity consumption factors

Source temperature \ Load temperature	55	50.2	43.8	29.2
25	1.02	0.82	0.64	0.40
20	1.04	0.83	0.66	0.42
15	1.00	0.84	0.66	0.45
10	1.00	0.82	0.66	0.46
5	1.01	0.80	0.67	0.46
0	0.98	0.82	0.66	0.47

By comparing the above matrices, we can obtain a table of the dependence of the COP on the temperatures of the heat load and heat sources:

Table 7 - Table of COPs Multiplier

Source temperature \ Load temperature	55	50.2	43.8	29.2
25	1.31	1.62	2.07	3.31
20	1.17	1.45	1.83	2.79
15	1.10	1.31	1.66	2.38
10	1.00	1.21	1.48	2.07
5	0.90	1.10	1.31	1.83
0	0.83	0.97	1.17	1.59

Varying conditions can be simulated for the operation of the heat pump by implementing performance and electricity demand matrices that have been suitably prepared. Additionally, the parameters of a pump operating under nominal conditions need to be implemented in the model.

Table 8 - Parameters of pump RE 76

RE 76 Performance Characteristic	
Heating Capacity	95 kW
Power Consumption	32.8 kW
COP	2.9
Heat Sink (Condenser)	
Type of Heating Medium	Water
Heat Load Inlet Temperature	55.0 °C
Heat Load Outlet Temperature	65.0 °C
Flow Rate	2.3 l/s
Pressure Loss in Heat Exchanger	134 kPa
Heat Source (Evaporator)	
Type of Coolant	Water-Propylene Glycol (35%)
Heat Source Inlet Temperature	10.0 °C
Heat Source Outlet Temperature	5.0 °C
Flow Rate	3.1 l/s
Pressure Loss in Heat Exchanger	241 kPa

6.1.6. Radiators

Type 1231 was used to model radiators. This model represents heating devices that provide heat through a combination of radiation and natural convection. The amount of heat transferred by the radiator (q) to the environment depends on the difference between the room air temperature (T_a) and the average temperature of the appliance (T_s). It also depends on the appliance's characteristics, which are represented by two constants, c and n, where n depends

on the appliance's type. The values of n for different types of heating appliance are shown in the table below.

Table 9 - Correction coefficients for heaters

Cast-Iron Radiator	1.3
Baseboard Radiation	1.4
Convectors	1.5
Ceiling Heating and Floor Cooling Panels	1
Floor Heating and Ceiling Cooling Panels	1.1
Finned-Tube Units	varies with temperatures

The c-factor is a correction factor issued by the manufacturer or calculated from the design values for the unit using Equation 15.

$$q = c(T_s - T_a)^n \tag{14}$$

$$c = \frac{q_{design}}{(T_{s,design} - T_{a,design})^n} \tag{15}$$

Where T_s is the surface temperature of the device, defined as:

$$T_s = \frac{T_{water,in} + T_{water,out}}{2} \tag{16}$$

The total heat energy transferred to the water flow is calculated as:

$$q_{water} = \dot{m} C_p (T_{water,in} - T_{water,out}) \tag{17}$$

Given the room temperature (T_a), the inlet water temperature ($T_{w,in}$) and the water mass flow rate (m), the outlet water temperature ($T_{w,out}$) must be adjusted until the heat flow from the water stream into the room (q_{water}) equals the target value (q).

6.1.7. Heat buffers

The RESHeat project uses a fixed-volume storage tank containing a submerged heat exchanger. This component is a cylindrical tank configured vertically. The fluid in the accumulation tank exchanges heat with the fluid in the heat exchanger and with the surroundings through heat losses from the top, bottom and rim surfaces. It also exchanges heat with up to three flow streams that flow in and out of the accumulation tank. This type of buffer allows heat to be transferred with three flow streams. Two of these streams mix with the storage fluid, while the third transfers heat to/from the storage tank via an immersed heat exchanger. The temperature change in the tank and heat exchanger over time can be modelled using differential equations.

$$\frac{dT_{tank}}{dt} = \frac{\left(Q_{in,tank} - Q_{out,tank}\right)}{C_{tank}} \quad (18)$$

$$\frac{dT_{hx}}{dt} = \frac{\left(Q_{in,hx} - Q_{out,hx}\right)}{C_{hx}} \quad (19)$$

Where $Q_{in,\,tank}$ and $Qout,\,tank$ denote heat transferred to and from the tank, respectively, and are functions of ambient temperature, inlet fluid conditions and flow rate, and heat exchanger temperature. $Q_{in,hx}$ and $Qout,hx$ are the heat transferred to and from the heat exchanger, respectively, and are functions of the inlet fluid temperature, the flow rate to the heat exchanger, and the tank temperature. As far as the heat exchanger is concerned, the outlet temperature at any point in time can be taken as the average temperature of the heat exchanger node that contains the outlet at a given time step. The heat exchanger and the storage tank interact thermally by natural convection of heat exchange from the external surface of the heat exchanger to the fluid in the tank.

6.1.8. Underground heat storage

The main problem with ground source heat pump heating systems is that the ground's heating capacity reduces over many years of operation. After the heating season, when a large amount of heat has been extracted from the ground, there is insufficient time for the ground to restore its heat capacity. Consequently, the COP of the heat pump can decrease by up to 10–15% each year that it is in operation, and the electricity consumption of the heat pump compressor increases. Manufacturers of heat pumps declare the COP measured under laboratory conditions, but operational reality is different, with energy consumption potentially 30% higher than declared (especially in the absence of groundwater). In the RESHeat project, waste heat from PVT panels and solar collectors is used to regenerate the thermal capacity of the ground. When the medium temperature is below 40°C and cannot be used to heat domestic water, the waste heat is sent to a ground heat exchanger.

The insulated tank stores thermal energy for heating domestic hot water. Connected to vacuum solar collectors with a solar tracking system, the tank can achieve water temperatures of up to 80°C. The insulated tank can also be used as a peak heat source when the outdoor temperature is very low in winter. During autumn and winter, when the output temperature from the solar collectors is below 40°C, waste heat is used to regenerate the ground via a ground heat exchanger.

The underground energy storage model was established in Trynsys. The following differential equations describe the underground energy storage model:

$$\rho_w c_w \frac{\pi D^2}{4} L \frac{dT}{d\tau} = Q_{solPV} - Q_{HP} - Q_{ground} \quad (20)$$

where ρ_w is the density of water, c_w is the specific heat of water, D is the outside diameter of the tank, L is the length of the tank, T is the temperature of the water in the tank. In addition, Q_{solPV}, Q_{solSC}, and Q_{HP} are respectively the heat supplied to the tank by the PV/T panels, the heat supplied to the tank by the solar panels and the heat absorbed by the heat pump and transferred to the building. Q_{ground} denote the heat exchanged with the ground by the tank.

6.1.9. Ground Heat Exchanger

In the RESHeat project, a U-shaped ground heat exchanger is used for facilities in Poland. A heat medium flows through the exchanger, giving off or absorbing heat depending on the temperatures of the medium and the ground. In a typical ground heat exchanger application, a vertical borehole is first drilled into the ground. The heat exchanger is then inserted into the borehole. The upper part of the exchanger is usually located several metres below ground level. Finally, the borehole is filled with backfill material, either native soil or another type of fill. A U-tube heat exchanger is shown in Figure 15.

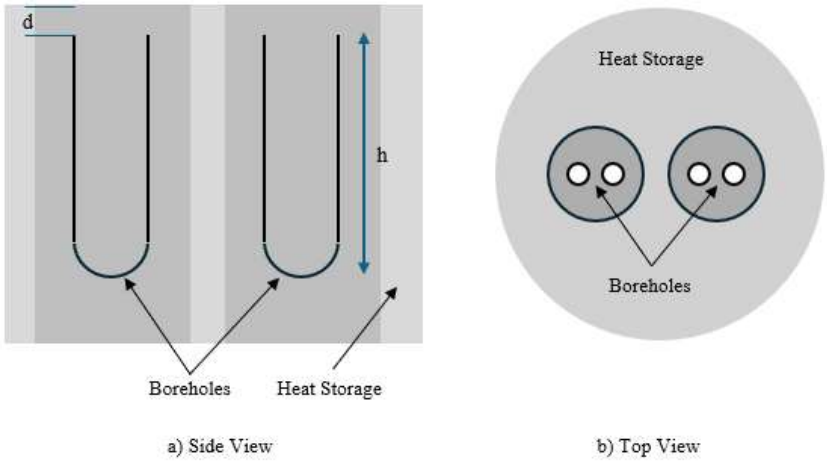

Figure 15 - Typical U-shaped ground heat exchanger [57]

Heat exchange occurs when there is a temperature difference between the heat transfer fluid and the surrounding ground. The fluid will lose or gain energy and its temperature will vary along the flow path through the volume of the storage tank. The amplitude of the temperature change depends, among other things, on the flow rate of the fluid. If the transient conditions in the fluid are neglected, the heat balance equation for the heat transfer fluid can be written as:

$$cp_f q_{fp} \frac{\partial T}{\partial x} + \alpha_p (T_f - T_a) = 0 \tag{21}$$

$$cp_f q_v \frac{\partial T}{\partial x} + \alpha_v (T_f - T_a) = 0 \tag{22}$$

where cp_f is the volumetric heat capacity of the fluid, q_{fp} is the flow rate of the fluid, T_f (s,t) is the temperature of the fluid, α is the heat transfer coefficient between the fluid and a point in the surrounding ground with temperature T_a . The first expression is the heat balance per unit length of pipe (subscript p), while the second takes into account the balance per unit volume in the reservoir (subscript v). The length coordinate along the flow path is x.

6.2. Base simulation configuration

The first step was to prepare and analyse the simulation results of the system under baseline conditions, i.e. with nominal system parameters and an assumed (historical) energy demand.

6.2.1. Weather data

Simulation of the system operation was carried out using Meteonorm meteorological data for the measuring station Kraków-Balice. Meteonorm is a database of historical meteorological data that has been prepared in an accessible form for use with various renewable energy simulation programmes. Meteonorm is based on data from the Global Energy Balance Archive (GEBA), which is a central database for instrumentally measured energy fluxes at the Earth's surface. The GEBA is maintained by the Institute for Climate and Atmospheric Sciences at ETH Zurich. It stores the monthly means of the various energy balance components observed at stations distributed worldwide.

As the Meteonorm data are prepared on the basis of historical data and normalised, i.e. they represent the most likely atmospheric conditions to occur at a given time, their use allows simulations to be carried out for the likeliest atmospheric conditions to occur in the future. In this way, it is possible to prepare a baseline simulation for a newly built system and predict what the expected conditions will be.

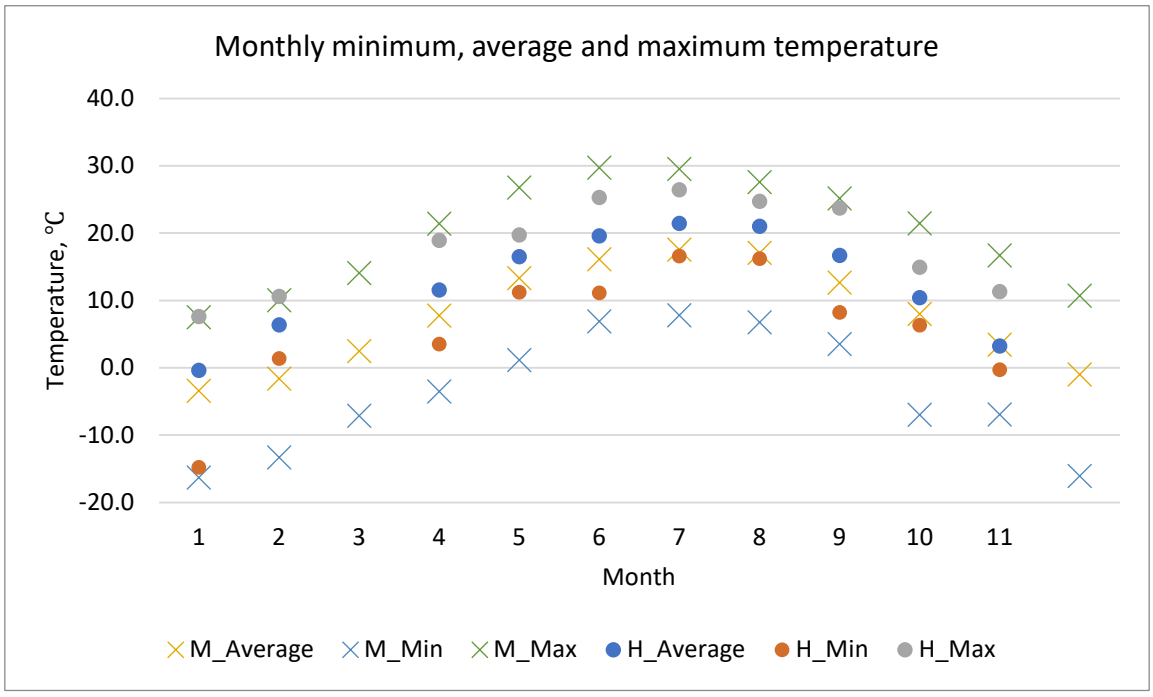

Figure 16 - Monthly statistics of historical and statistical data

The graph above illustrates a comparison between historical meteorological data and statistical meteonorm data. On average, the meteonorm temperature is 3 degrees lower than the historical data from 2023, with February exhibiting a 8-degree discrepancy. However, it is important to note that February 2023 was characterised by unusually high temperatures, and therefore, should not be directly compared with statistical data. The mean values of meteonorm and historical data exhibit a comparable pattern and temperature distribution. Consequently, statistical data can be employed as an initial simulation for system design and improvements.

6.2.2. Building geometry

The building consists of 3 functional floors, a garage which is partly underground and an unoccupied attic. The ground floor consists of 6 flats and the other functional floors of 8 flats. The total usable space is 1015 m2 not including stairways and technical spaces.

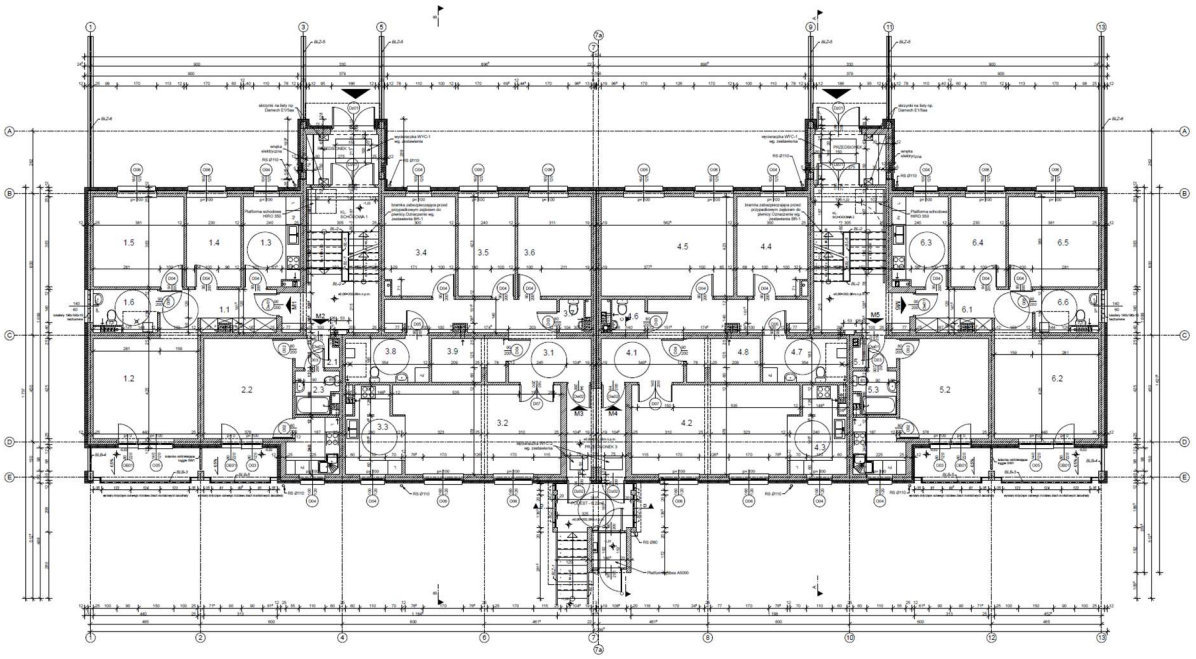

Figure 17 - Layout of ground floor

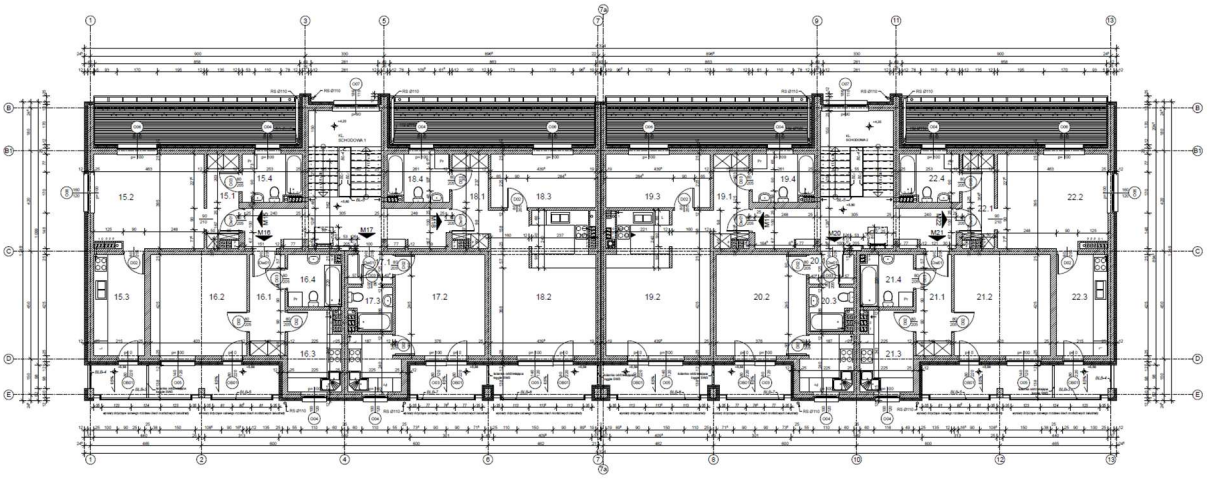

Figure 18 - Layout of 2nd floor

A thermal zone must be defined for each apartment, for which it is necessary to determine the initial values of internal temperature and relative humidity, as well as the data required to assess the overall characteristics of the zone, such as infiltration rate, internal gains and occupant comfort parameters. The thermo-physical properties of the walls and windows defining the zone under consideration are also specified. Figure 19 shows the building model B1 developed in Sketchup.

(a) (b)

Figure 19 - ZBK building model: a) photograph, b) TRNSYS model

The energy production efficiency for a medium-sized residential building with a condensing gas boiler (CH and DHW efficiency) based on Polish law Dz.U. 2014 item 888 is 0.83 and 0.55 for CH and DHW, respectively. The thermal properties of building partitions, glazing and are given in Table 1. The partitions shown in Table 1 are based on the existing building partitions shown in Figure 20.

Table 10 - B1 Building partitions

Partition	Thickness, m	U, W/m².K
External wall	0.39	0.22
External non-insulated roof	0.04	2.90
insulated roof	0.20	0.18
Ceiling above the last floor	0.33	0.21
Internal wall	0.28	0.99
Internal ceiling	0.27	0.55
External window	-	1.10

The infiltration rate for residential dwellings is calculated using the infiltration rates of the components of the envelope. The infiltration values for each component are taken from the SSPC 90.1 Envelope Subcommittee standard [34]. This standard includes infiltration rates for opaque components such as roofs, floors and doors. It also includes information for glazed elements such as windows, skylights and sliding glass doors. Building average infiltration has been calculated as 0.30 1/h.

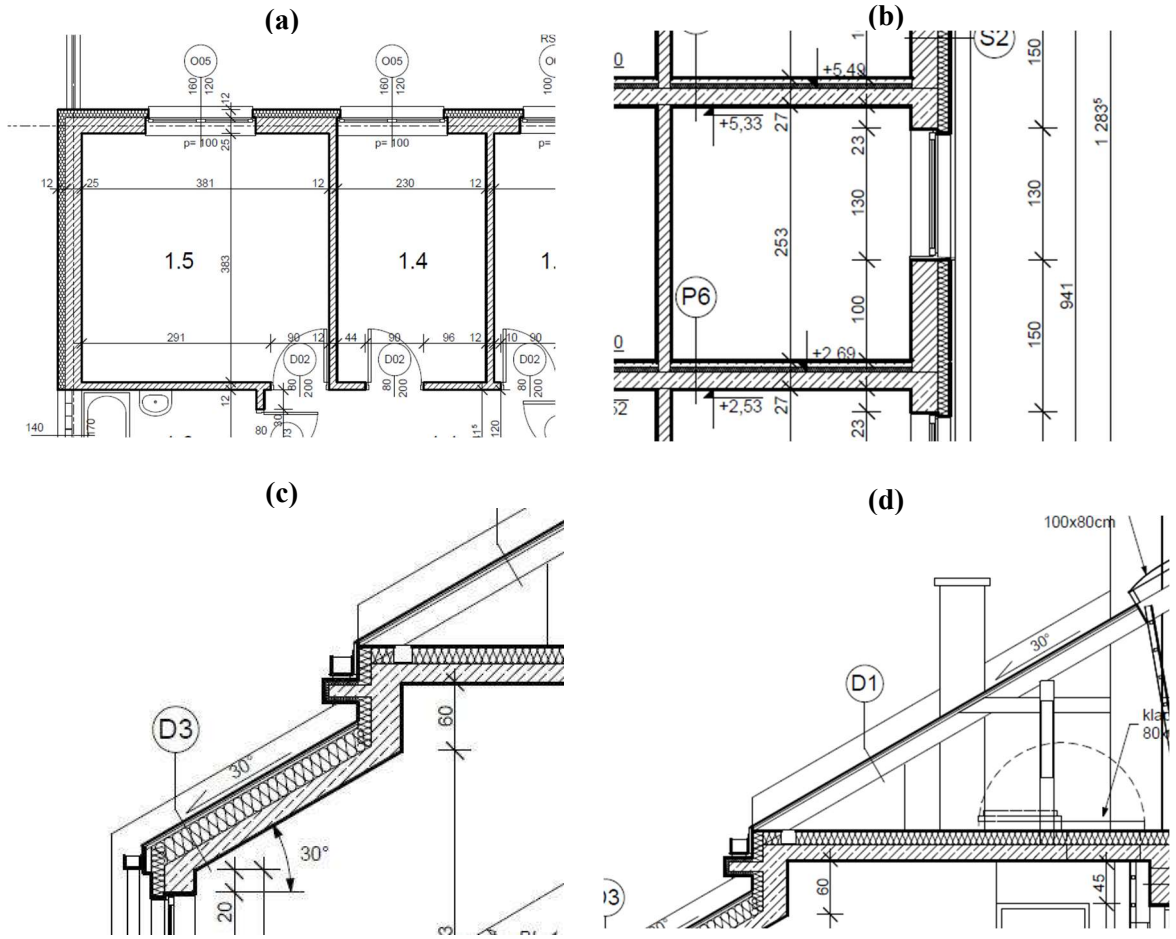

Figure 20 - Building partitions from as-built layouts: a) External wall, b) Ceiling, c) Insulated roof, d) Insulated ceiling and uninsulated roof

6.2.3. RESHeat Components

The RESHeat system represents a further evolution of the SOPSAR system that was previously installed in the manufacturing facility in Limanowa. The RESHeat system, which has been installed in the B1 building, comprises the following components:

- Eight sun-tracked solar collectors with a total thermal energy output of 30.4 kW
- Twenty-four PV/T panels (twelve panels in series) with 10.4 kWe electrical power output and 5.6 kWt thermal power output
- Sixty-eight PV panels with a total electrical power output of 30 kW
- Fifteen boreholes (each 102 m length)
- An Oilon heat pump (95 kW of heating capacity)
- A central heating buffer tank
- A domestic hot water tank
- An underground heat storage tank (with a capacity of 50 m^3)

Figure 21 illustrates the components of the RESHeat system during installation.

(a)

(b)

(c)

(d)

(e)

(f)

Figure 21 - RESHeat system components installed and planned to be installed in ZBK: a) Sun tracking solar collectors, b) sun tracking PV/T panels, c) stationary PV panels, d) underground heat storage tank, e) Oilon RE 76 heat pump, f) boiler room and hydraulic connections

The RESHeat system employs two primary heat sources: solar collectors and a heat pump. The control system is designed to optimise the utilisation of the renewable energy source, namely the solar collectors. The surplus heat generated by the solar collectors is stored in an underground storage tank. The entire control system is based on the following assumptions:

- In Case 1, the temperature at the outlet of the collectors is sufficient to heat the domestic hot water tank and the central heating storage tank, and the heat pump is inactive.
- In Case 2, the water temperature in the buffer storage tank is sufficient, but the temperature at the outlet of the collectors is too low. The stored heat is then utilised.
- In the third case, when the temperature of the storage tanks is insufficient, the temperature of the water at the outlet of the collectors is also below the operating temperature. In this instance, the heat stored in the underground tank is utilised.
- In the fourth case, when the temperature of all storage tanks and the fluid in the underground storage tank is below the required level, and the temperature of the water at the outlet of the collectors is also insufficient, the heat pump is activated to ensure that the circulation fluid reaches the correct temperature.

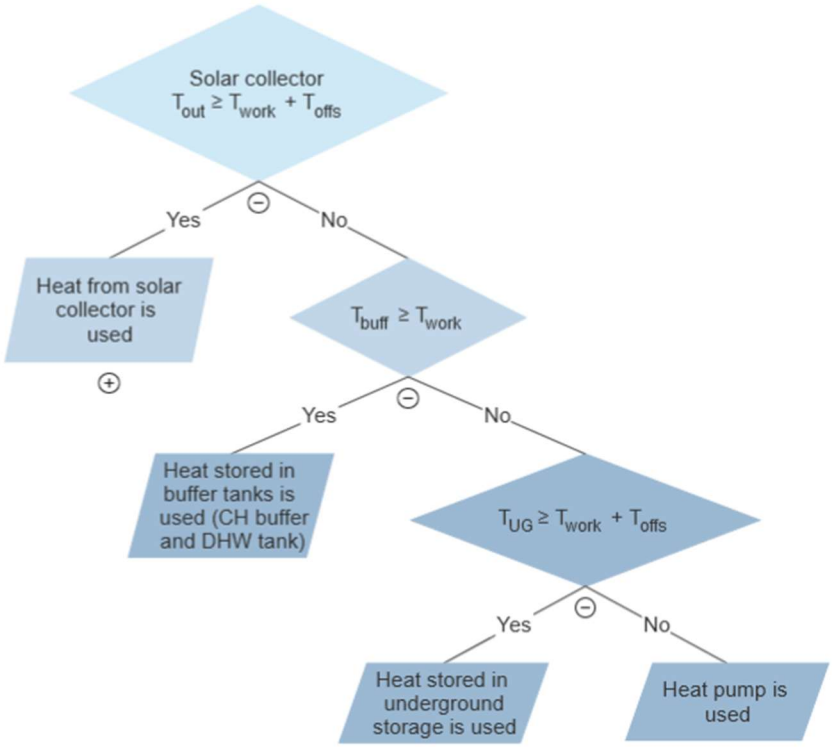

Figure 22 - RESHeat controls decision tree

Figure 22 illustrates the decision tree for the RESHeat project control strategy, wherein T_{out} represents the outlet temperature of the solar collectors, T_{buff} denotes the temperature within the water tanks, and T_{UG} signifies the temperature within the underground buffer. The working fluid target temperature (T_{work}) is dependent upon whether there is a demand for CH and DHW or only for DHW. In the event that a demand is present for both target temperatures, the target temperature is set at 60°C. Conversely, in the event that only DHW is required, the target

temperature is lowered to 40°C. T_{offs} represents the temperature differential requisite for enabling heat transfer between fluids within the system via the heat exchangers. The control algorithm imposes limits on the duration of operation of the heat pump, which represents the primary energy-consuming component of the RESHeat system. Furthermore, the thermostats responsible for controlling the system are set to minimise the average inlet temperature of the medium on the load side of the heat pump, thereby increasing its average COP.

The data sheets for the RE 76 pump were provided by an OILON company and are presented in Table 7. In addition to the data sheet for the heat pump, OILON provided a tool for creating a COP, heating capacity, and energy consumption curve for different temperatures on the load and source sides. In the TRNSYS software, the model "type 1323" was selected from the HVAC library to represent the heat pump. The heat pump type RE 76 was installed at a demo building in Krakow, Poland, and its specifications are shown below.

Table 11 - OILON RE 76 HP Parameters

Parameters	Value
Fluid specific heat – source, kJ/kg.K	3.70
Fluid specific heat – load, kJ/kg.K	4.19
Fluid density – source, kg/m^3	1024.33
Fluid density – load, kg/m^3	1000.00
Nominal heating capacity, kW	95
Nominal energy usage, kW	32.76
Nominal flow – source, l/s	5.14
Nominal flow – load, l/s	2.57

Based on laboratory data provided by the OILON company, a COP curve was prepared for four load temperatures and six source temperatures. The COP dependency matrix for the heat pump is provided in Table 12.

Table 12 - COP/Heating Capacity Matrix

	Load Outlet, °C	**65**	**58.4**	**49.7**	**34.5**
	Load Inlet, °C	**55**	**50.2**	**43.8**	**29.2**
Source Outlet, °C	**Source Inlet, °C**	**COP/Heating Capacity, kW**			
20	25	3.80 / 126.60	4.70 / 126.00	6.00 / 125.60	9.60 / 124.50
15	20	3.40 / 115.50	4.20 / 114.30	5.30 / 114.00	8.10 / 112.60
10	15	3.20 / 104.80	3.80 / 104.00	4.80 / 103.30	6.90 / 101.20
5	10	2.90 / 95.00	3.50 / 93.90	4.30 / 92.70	6.00 / 90.60
0	5	2.60 / 85.80	3.20 / 84.30	3.80 / 83.20	5.30 / 80.70
-5	0	2.40 / 77.30	2.80 / 75.50	3.40 / 73.80	4.60 / 71.50

The heat pump electricity consumption matrix is shown in Table 13.

Table 13 - Electricity consumption matrix

	Load Outlet, °C	**65**	**58.4**	**49.7**	**34.5**
	Load Inlet, °C	**55**	**50.2**	**43.8**	**29.2**
Source Outlet, °C	**Source Inlet, °C**	**Electricity Consumption, kW**			
20	25	33.32	26.81	20.93	12.97
15	20	33.97	27.21	21.51	13.90
10	15	32.75	27.37	21.52	14.67
5	10	32.76	26.83	21.56	15.10
0	5	33.00	26.34	21.89	15.23
-5	0	32.21	26.96	21.71	15.54

The COP matrix shows that a COP greater than 4.0 is achievable for different sets of load and source temperatures. The COP is strongly correlated with the load temperature and by reducing the load temperature it is possible to achieve the required COP level of 4.

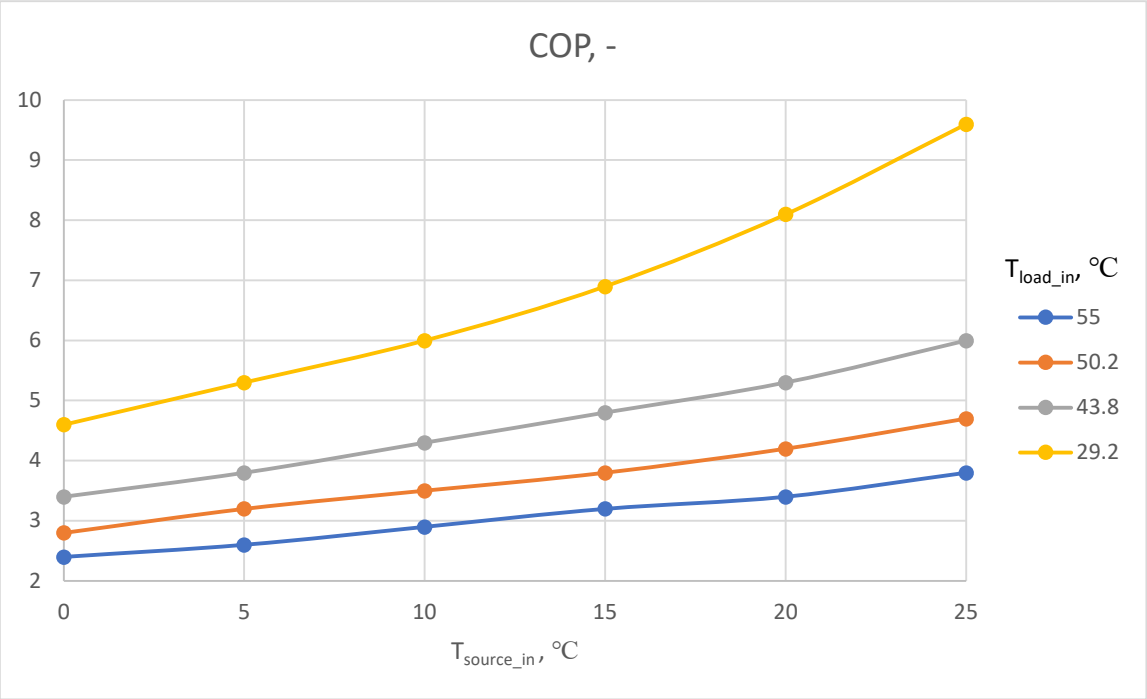

Figure 23 - COP to Load and Source Temperature

The heating capacity matrix shows that the heating capacity is strongly dependent on the temperature of the source, in practice it is very little affected by the temperature of the load.

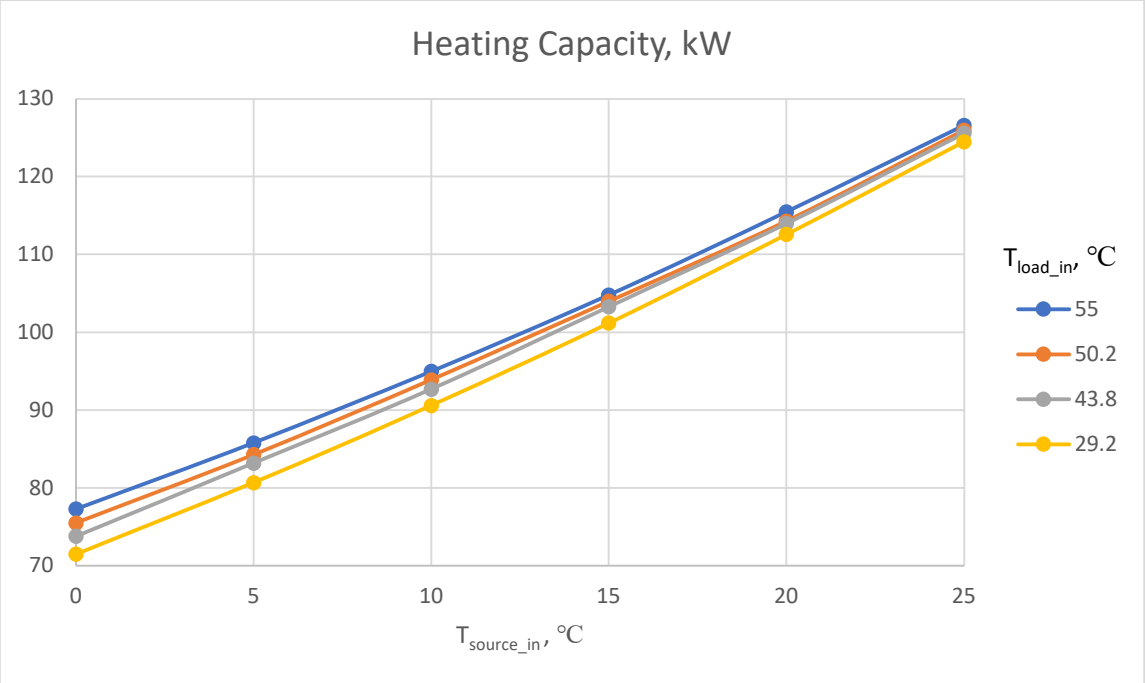

Figure 24 - Heating Capacity to Load and Source Temperature

The wide range of data made it possible to carry out simulations under different load and source conditions and to aim the system design at the best possible performance before

implementing the system. This correlation is proved by many studies. Maivel and Kurnitski [35] et al. In their paper, the investigation focused on the impact of return water temperature in radiator-based domestic heat pump systems on the condensing temperature of the heat pump and, consequently, its seasonal performance factor (SPF). Seasonal Performance Factor (SPF) is average COP through whole year for a heat pump in heating mode. Therefore it is a good indicator for overall system performance. Three calculation methods were utilised: an analytical model, a dynamic simulation (IDA-ESBO), and a correlation equation derived from laboratory tests. The findings demonstrated a high degree of correlation between the IDA-ESBO model and the analytical model. However, the correlation-based calculation underscored the significance of lower return temperatures in enhancing SPF.

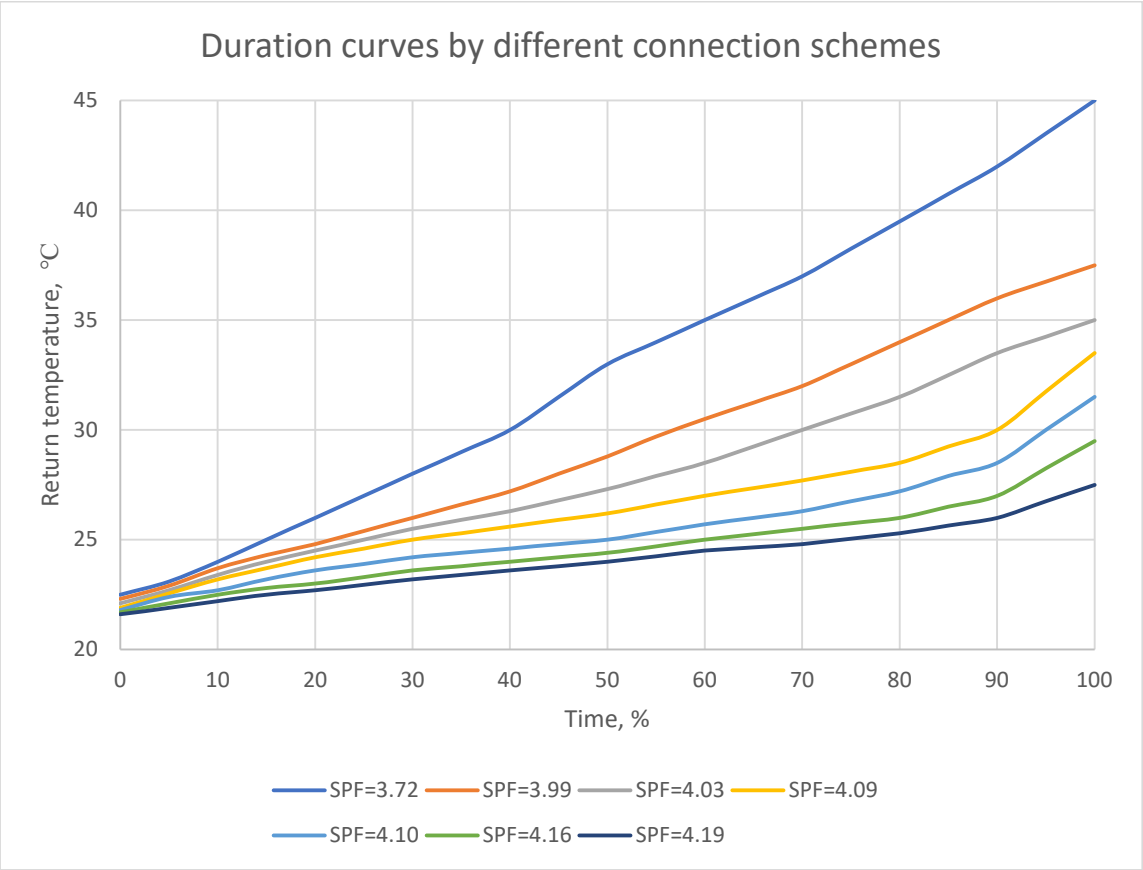

Figure 25 - Return temperature for different connection types with corresponding SPF values [8].

Of the four common connection schemes, the direct connection scheme, which yields the lowest return temperature, provided the highest SPF. Accuracy was further improved by adjusting for correct flow rates, as fixed-flow assumptions underestimated the SPF by about 4.5%. The study concluded that simplifying assumptions about return temperatures and condensing conditions can lead to an underestimation of SPF of more than 10% in radiator-

heated domestic heat pump systems. This emphasises the need for precise calculation methods to capture the full efficiency potential.

In general, the results of Maivel and Kurnitski's research are consistent with the findings presented in Figure 19. The factor that most influences the COP is the return temperature from the heating system, which in my research is the return load temperature in the heat pump thermodynamic cycle.

Fatouh et al. [36] examine how increasing the condenser water inlet temperature affects the performance of a heat pump system when other operating conditions remain fixed. As the inlet temperature rises, the condensing pressure increases while the evaporating pressure decreases slightly. This results in an increased pressure ratio, lower volumetric efficiency and reduced refrigerant mass flow. Consequently, the system's cooling capacity diminishes while the compressor's workload and specific work input increase. The outcome of this process is a decline in the system's overall coefficient of performance (COP) as the condenser inlet temperature increases. Notwithstanding, the condenser outlet water temperatures remain elevated to the extent that they are suitable for a variety of domestic and industrial applications, and the chilled water produced is still adequate for cooling purposes.

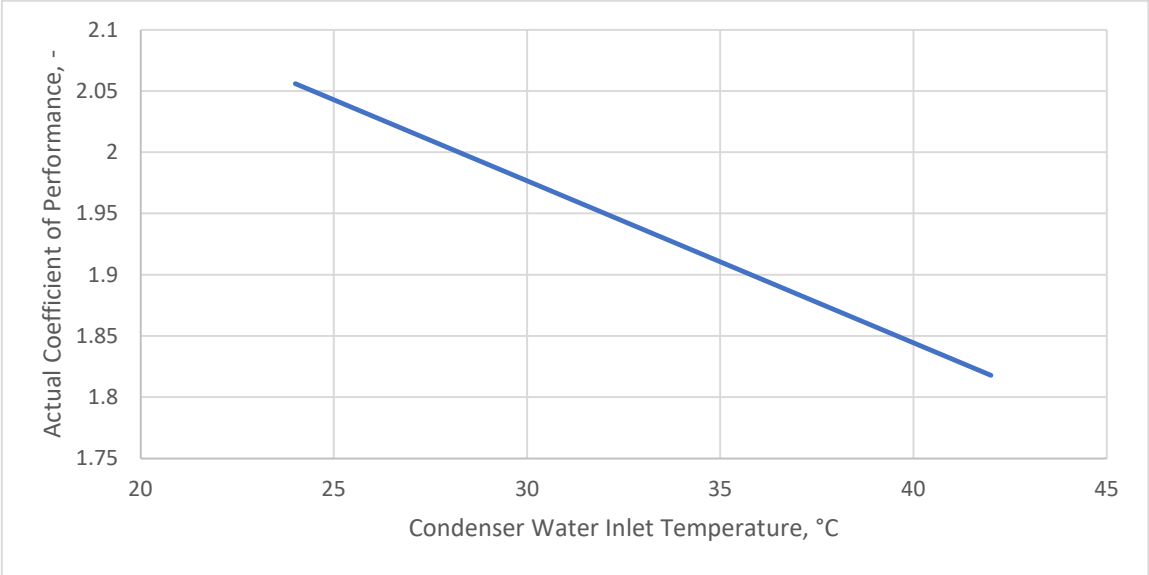

Figure 26 - Condenser inlet temperature and COP

It has been demonstrated that there is a direct correlation between the evaporator water inlet temperature and the overall performance of the heat pump system. By increasing the evaporator water inlet temperature from 14°C to 26°C, whilst maintaining a constant flow rate, there is a demonstrable improvement in the performance of the system in several key areas. Firstly, it is

important to note that the pressure ratio decreases as the increase in evaporating pressure exceeds that of the condensing pressure. This reduced pressure ratio enhances volumetric efficiency, leading to a significant increase of approximately 36% in the refrigerant mass flow rate. Whilst the enthalpy differences through the evaporator and condenser, and the compressor's specific work input, decline slightly, the significant increase in refrigerant mass flow rate compensates for these reductions.

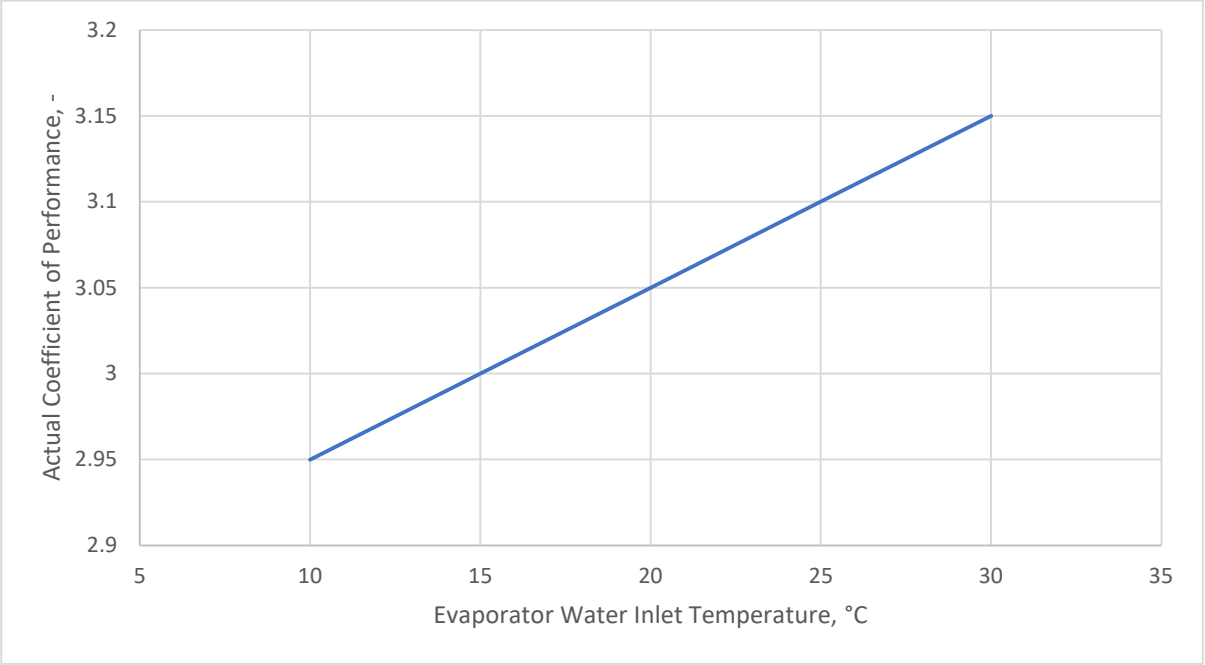

Figure 27 - Evaporator inlet temperature and COP

Consequently, both the heating and cooling loads increase, enabling higher outlet water temperatures in the condenser and providing enhanced heating capacity for a variety of applications. It is important to note that even the chilled water temperature from the evaporator remains at an appropriately low level. The system's coefficient of performance (COP) improves as the increase in heating and cooling capacities is greater than the increase in compressor power input. Over the examined temperature range, the COP increases from approximately 3.7 to around 4.0. In essence, increasing the evaporator water inlet temperature improves system efficiency, enabling the heat pump to provide more effective heating and cooling while keeping energy consumption reasonable.

6.3. TRNSYS Model

All components of the RESHeat system have been accurately modelled in TRNSYS based on manufacturer specifications, weather data, architecture, and relevant standards. Illustrations showing the most important components of the system are shown below.

The figure below shows the heat pump, which is the most important part of the RESHeat system. The heat pump is reproduced in the simulation with all the necessary components, such as circulating water pumps, a ground heat exchanger, and an additional heat exchanger for when the heat transport medium changes (from glycol mix to water).

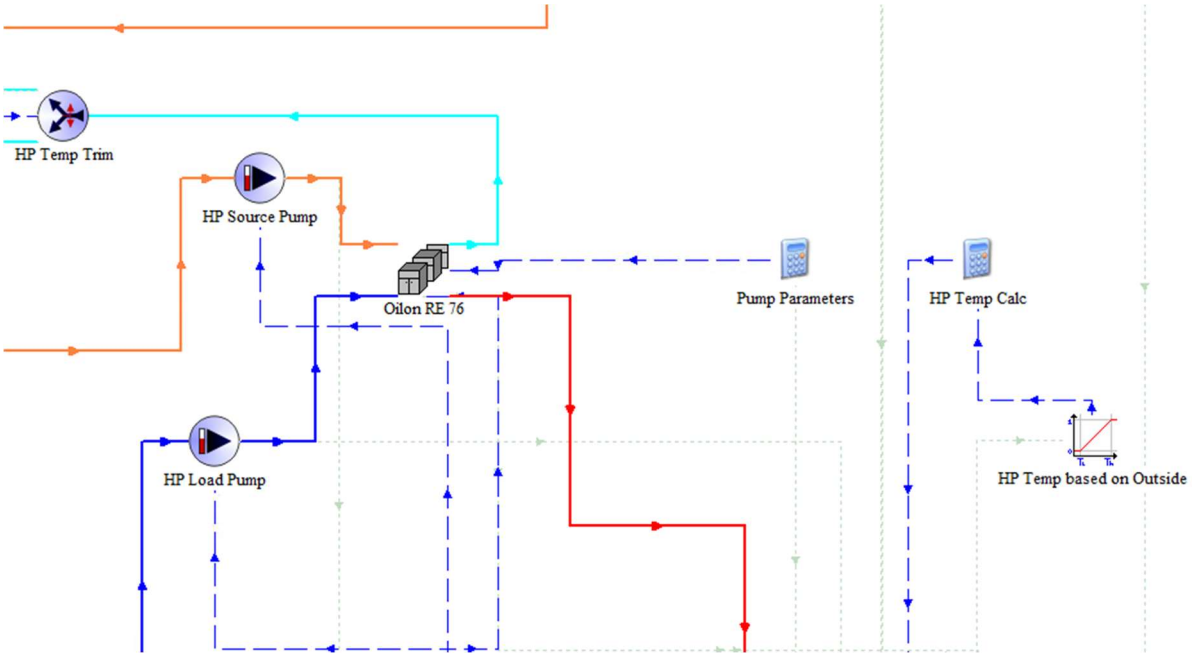

Figure 28 - Heat Pump Simulation

The ZBK building simulation is shown below. The building simulation was created by generating a geometric model incorporating all partitions and windows. This model uses weather data such as temperature, solar radiation and wind profile, as well as partition specifications, to calculate heat losses or gains and thus the necessary heat load for central heating.

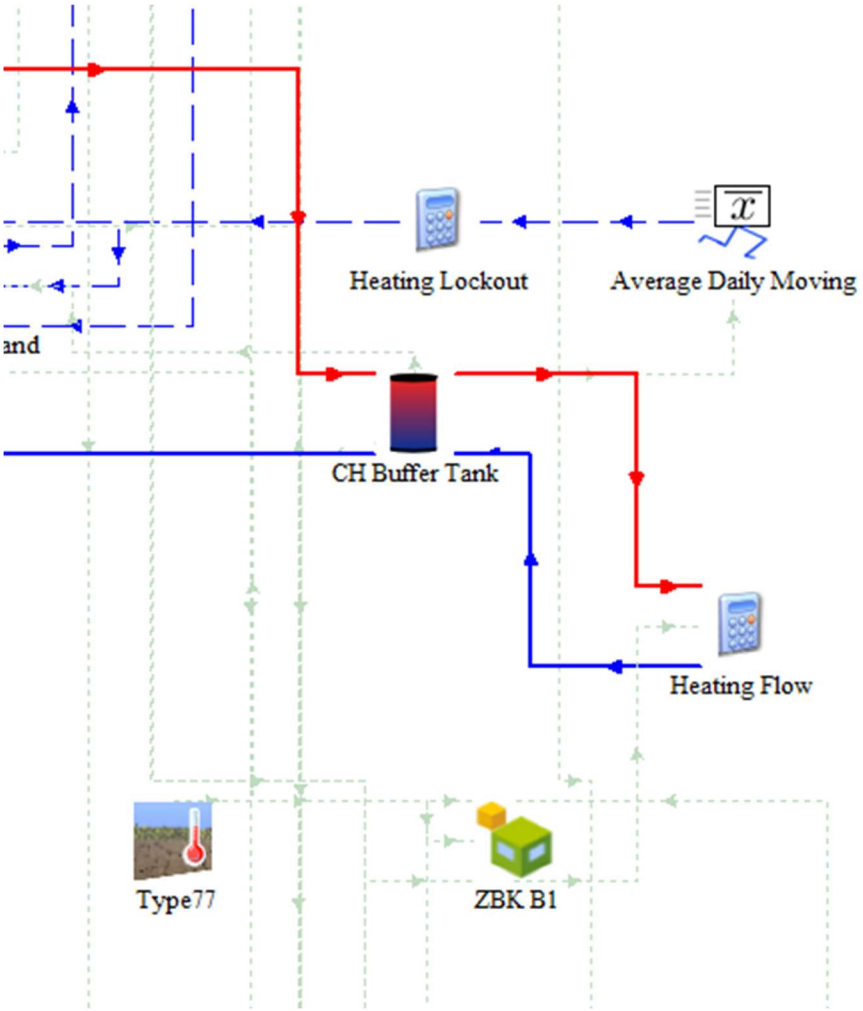

Figure 29 - Building Simulation and Central Heating Buffer Tank

The next figure shows the preparation of domestic hot water. This is also one of the most important parts of the simulation, as the DHW preparation system has been retrofitted and requires a high temperature from the heat pump, which significantly decreases its performance. The daily hot and cold water usage is set to represent a typical daily water usage profile.

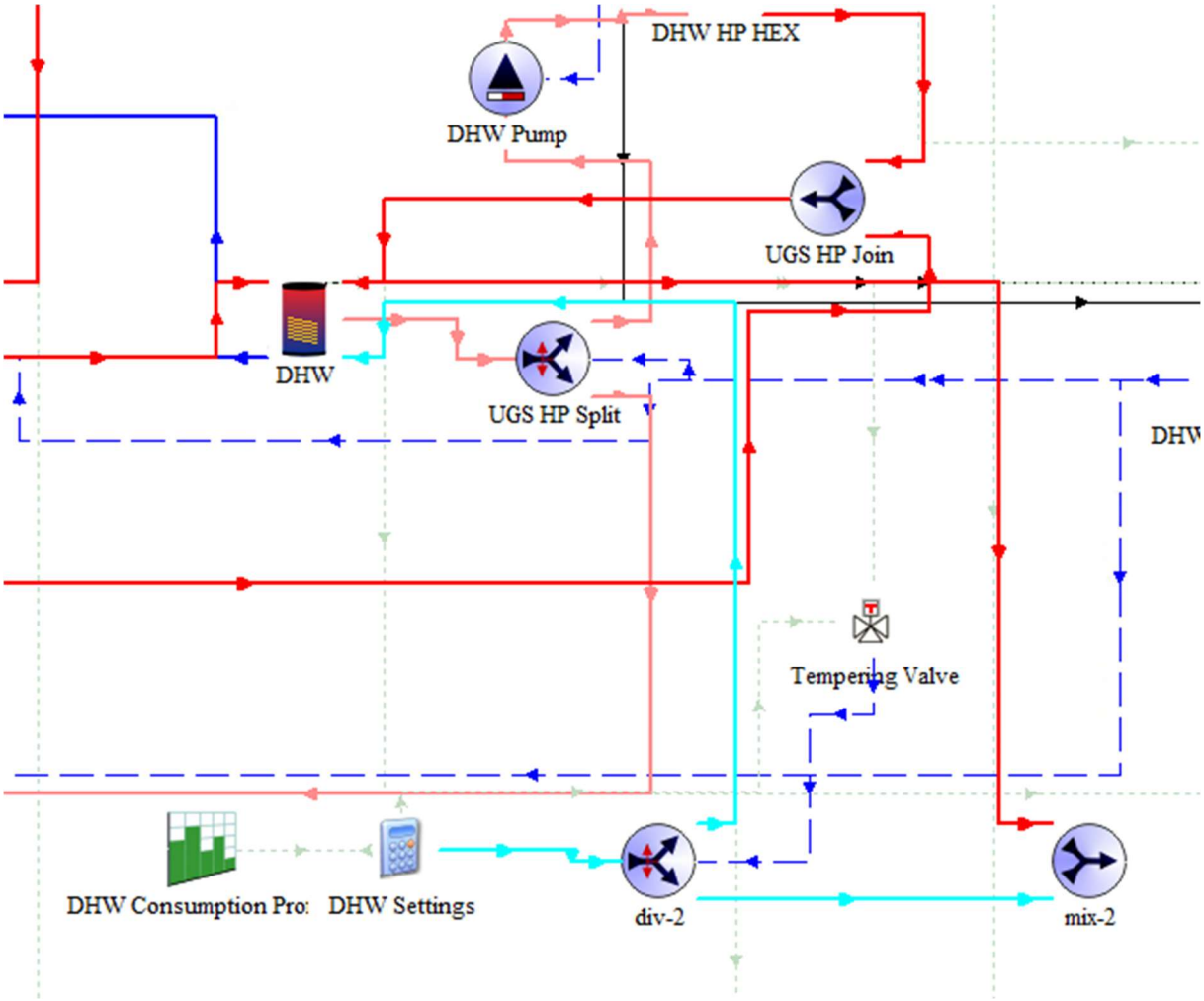

Figure 30 - Domestic Hot Water (DHW) Preparation

The following figure shows a simulation of a ground heat exchanger functioning as a heat source for a heat pump. This simulation was based on local ground parameters and meteorological data.

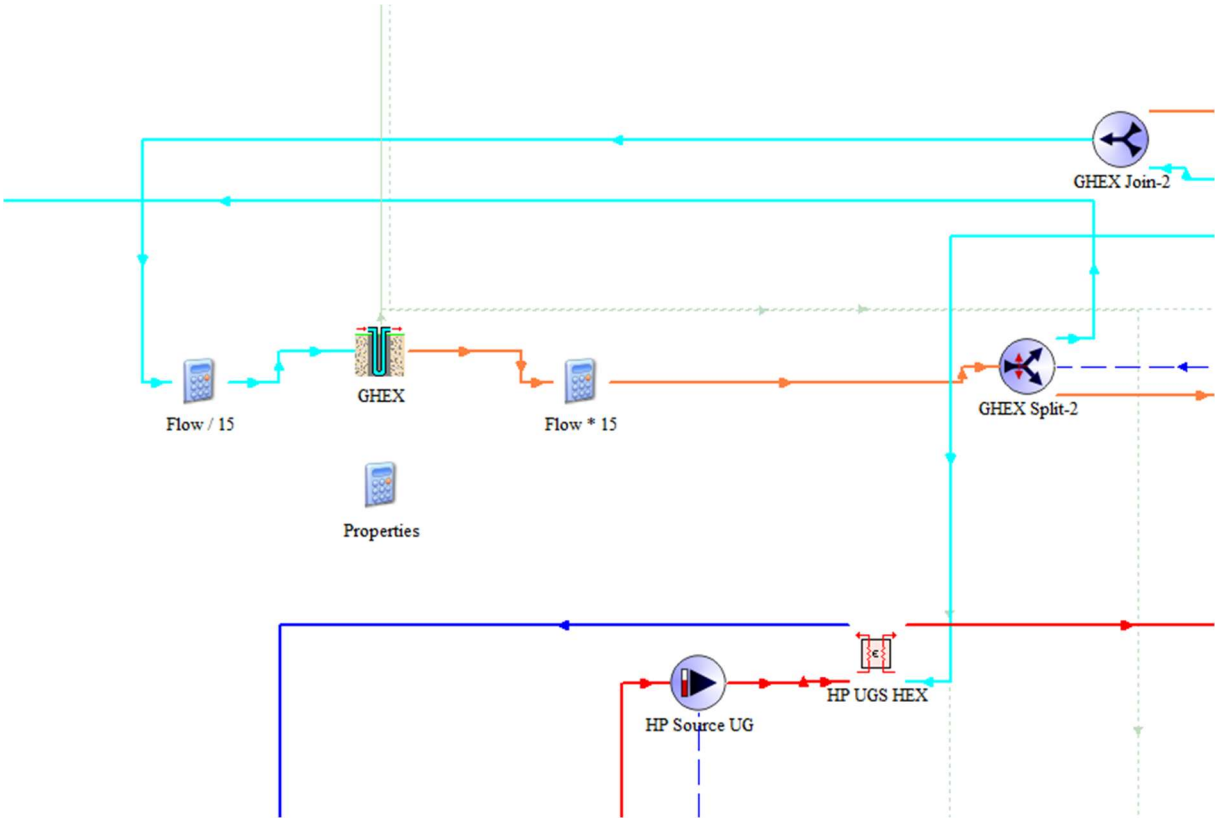

Figure 31 - Ground Heat Exchanger Simulation

The next figure shows PV/T panels, which can be used to generate both heat and electricity.

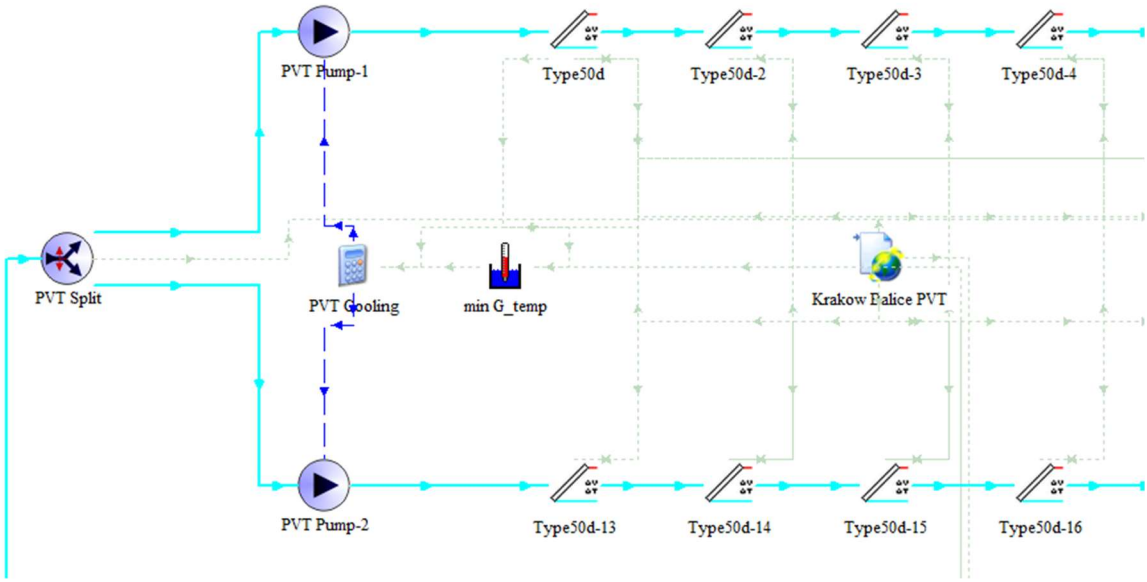

Figure 32 - PVT Panels Simulation and Weather Data

The next figure shows both underground heat storage and solar collectors. Excess heat produced by solar collectors is stored in ground heat storage.

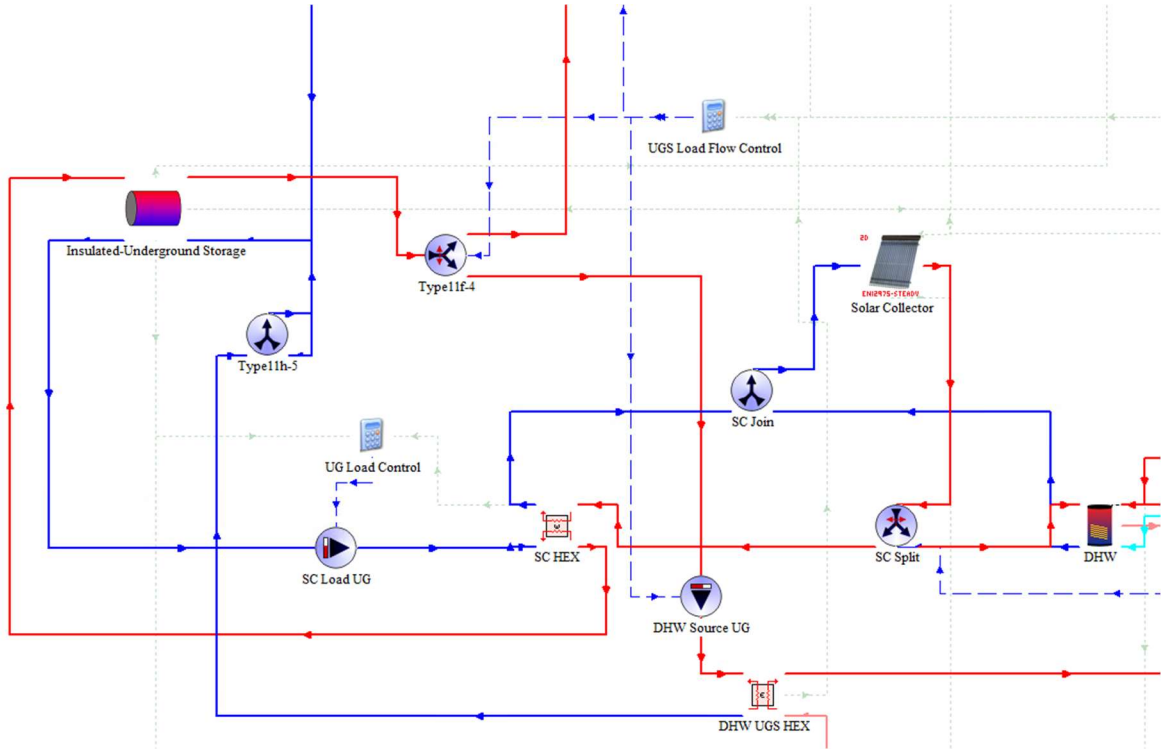

Figure 33 - Underground Heat Storage and Sollar Collectors

The last picture shows the various model settings and the simulation results plotters.

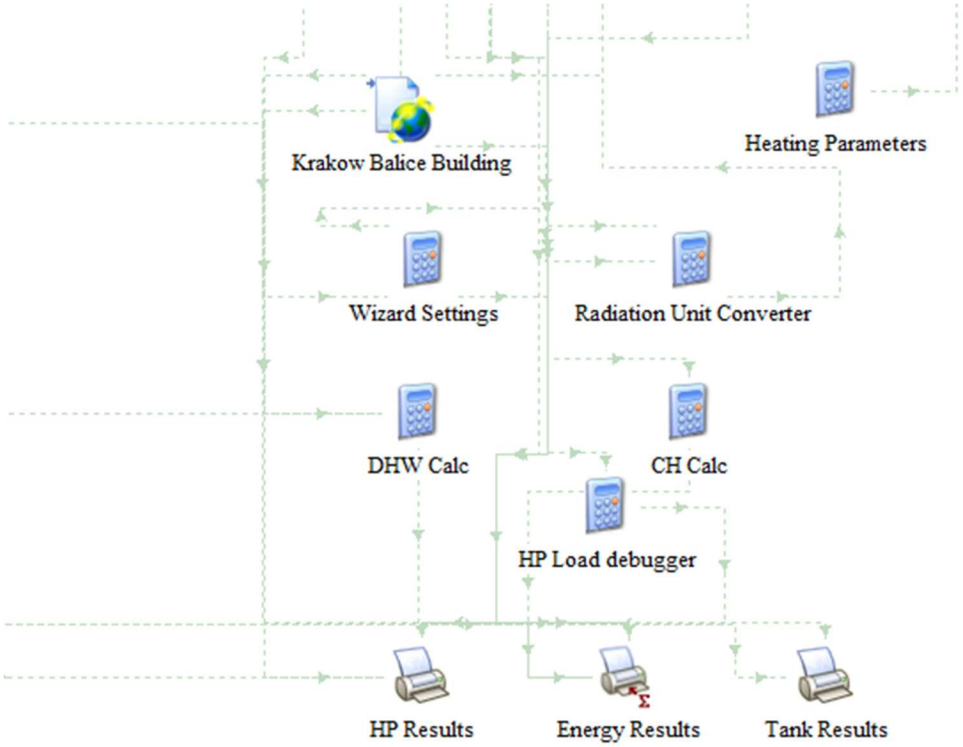

Figure 34 - Model Settings and Output Results Plotters

6.4. Simulation results

The following section presents the findings of the simulation conducted in the B1 building of the ZBK over the course of a year.

Figure 35 illustrates the annual history of the average air temperatures on each day, along with the average temperature of the water in the underground storage tank. As can be observed, the mean temperature of the underground storage tank for the winter and autumn period remains at approximately 60°C, which permits its utilisation for the heating of the building during the nighttime hours. During the daytime, the surplus heat enables the contents of the storage tank to be reheated to the requisite operational temperature.

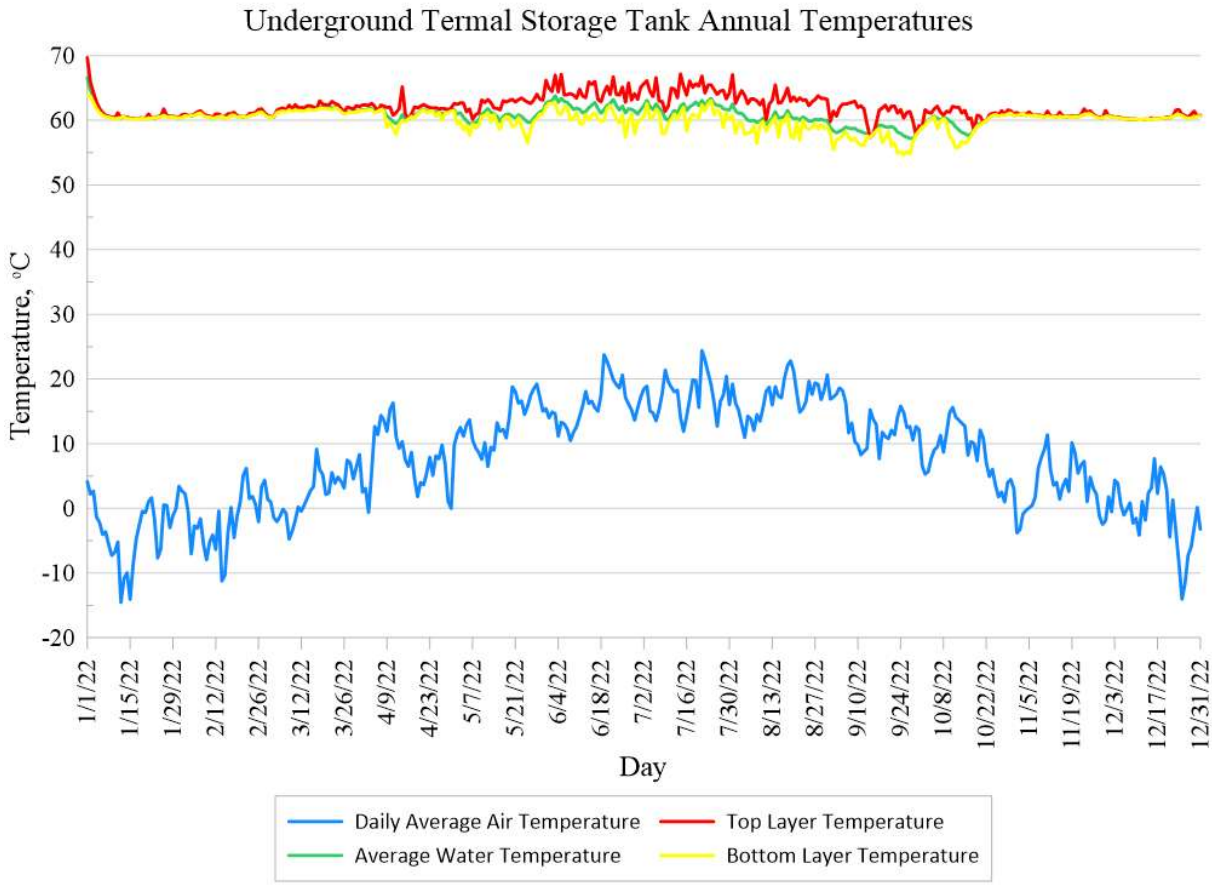

Figure 35 - Underground storage tank daily temperatures

During the spring and summer months, there is a notable increase in the temperature within the storage tank. This is attributable to the considerable surplus heat generated by the solar collectors. By increasing the average temperature in the underground storage tank, it is possible to extend the period during which the heat pump is not in operation, from the end of April to the beginning of October.

Osterman and Stritih [37] described the importance of thermal energy storage (TES) in heat pump-based heating systems. The main advantage of using TES is that it balances the system's operation and increases the amount of time that the HP can run at full capacity throughout the year, thus improving the SPF. TES can improve the performance of domestic heating systems, making them more cost-competitive than traditional gas-fired boilers or fossil fuel heat sources. Jung et al. [38] also emphasise the importance of using TES in residential heating. As in the previous paper, they state that using thermal storage enables the load on the heat pump to be shifted from daytime, when electrical energy processes are at their highest, to night-time, when the heat pump can load the thermal storage with hot water produced when electrical energy processes in the grid are lower. This optimises operating costs. In the proposed system with TES, excess energy is produced during the day using photovoltaics and is used throughout the day and night. The heat stored in the TES also enables the demand for the heat pump to be shifted in the spring and autumn, thereby reducing annual energy consumption and increasing the overall SPF.

Figure 36 illustrates the monthly energy consumption of the heat pump during the year period. When the high temperature in the underground tank and solar collectors is achieved, the energy consumption is minimal.

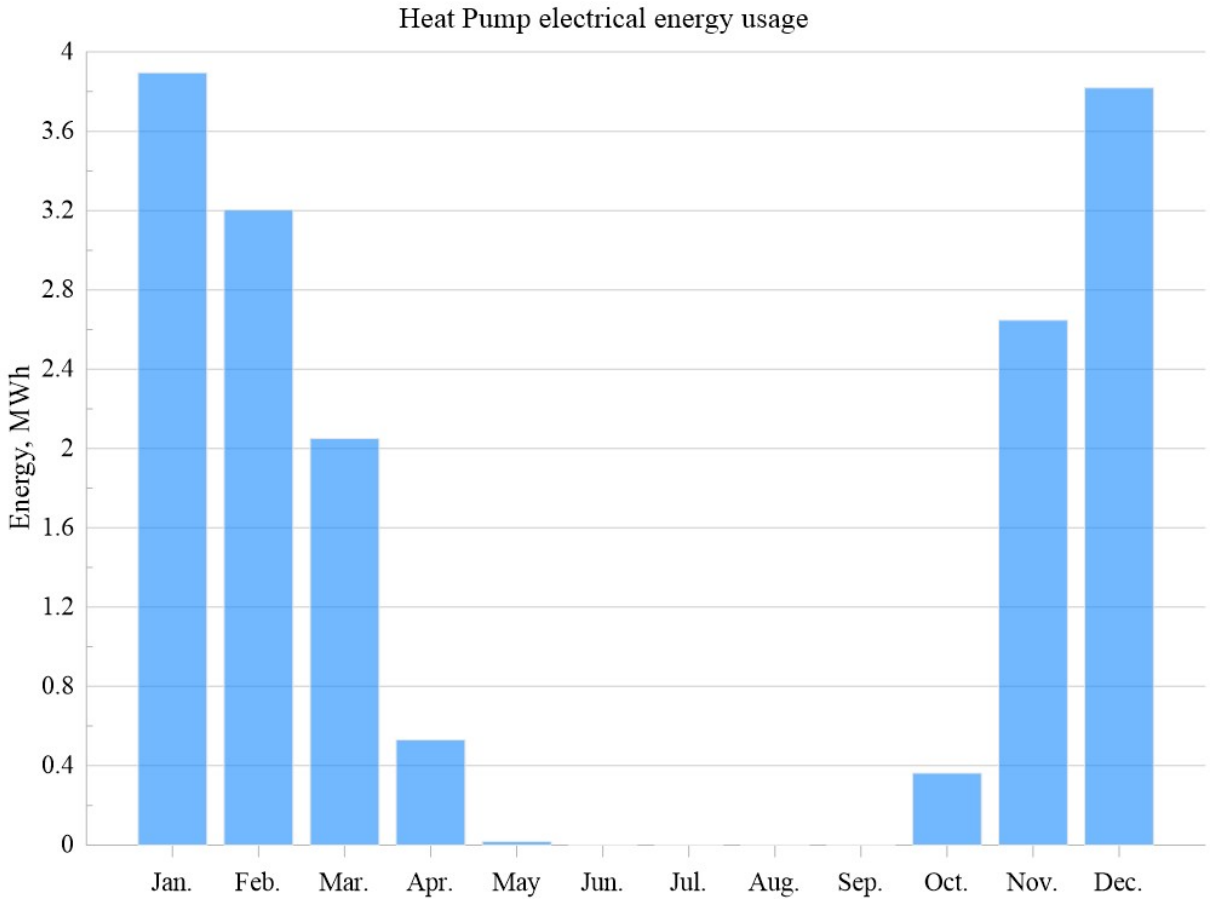

Figure 36. Heat pump monthly energy usage

From the beginning of April to October, the parameters of the storage tank fluid and the amount of heat generated by the solar collectors are sufficient for the heat pump to be rendered unnecessary. Figures 37 and 38 illustrate the periods of April and October, which are of particular significance in this context. During April, the average temperature in the tank rises above 60 degrees Celsius, which allows for the heat pump to be deactivated. Conversely, in October, the temperature in the underground storage tank falls below 60 degrees Celsius, resulting in the heat pump being switched back on.

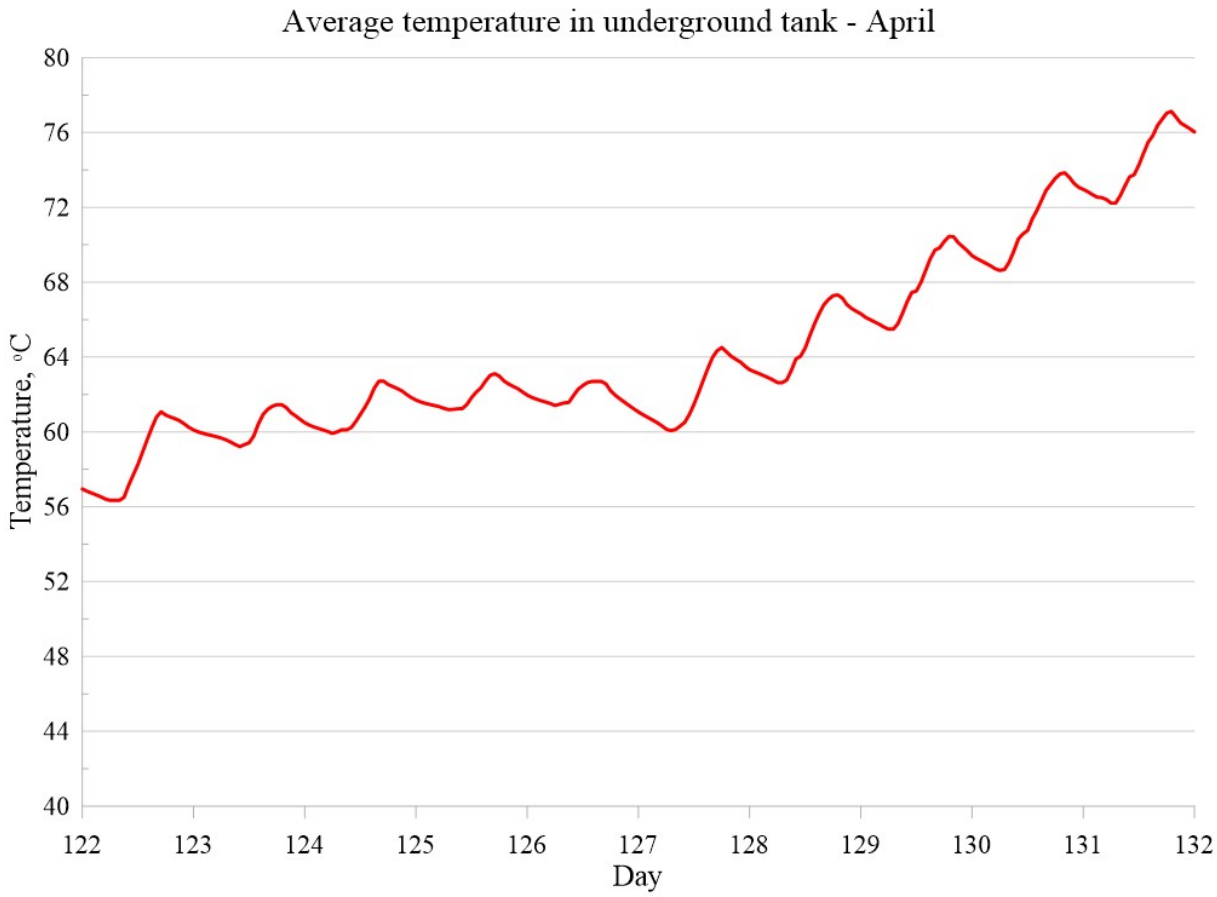

Figure 37. Average temperature in a storage tank - April

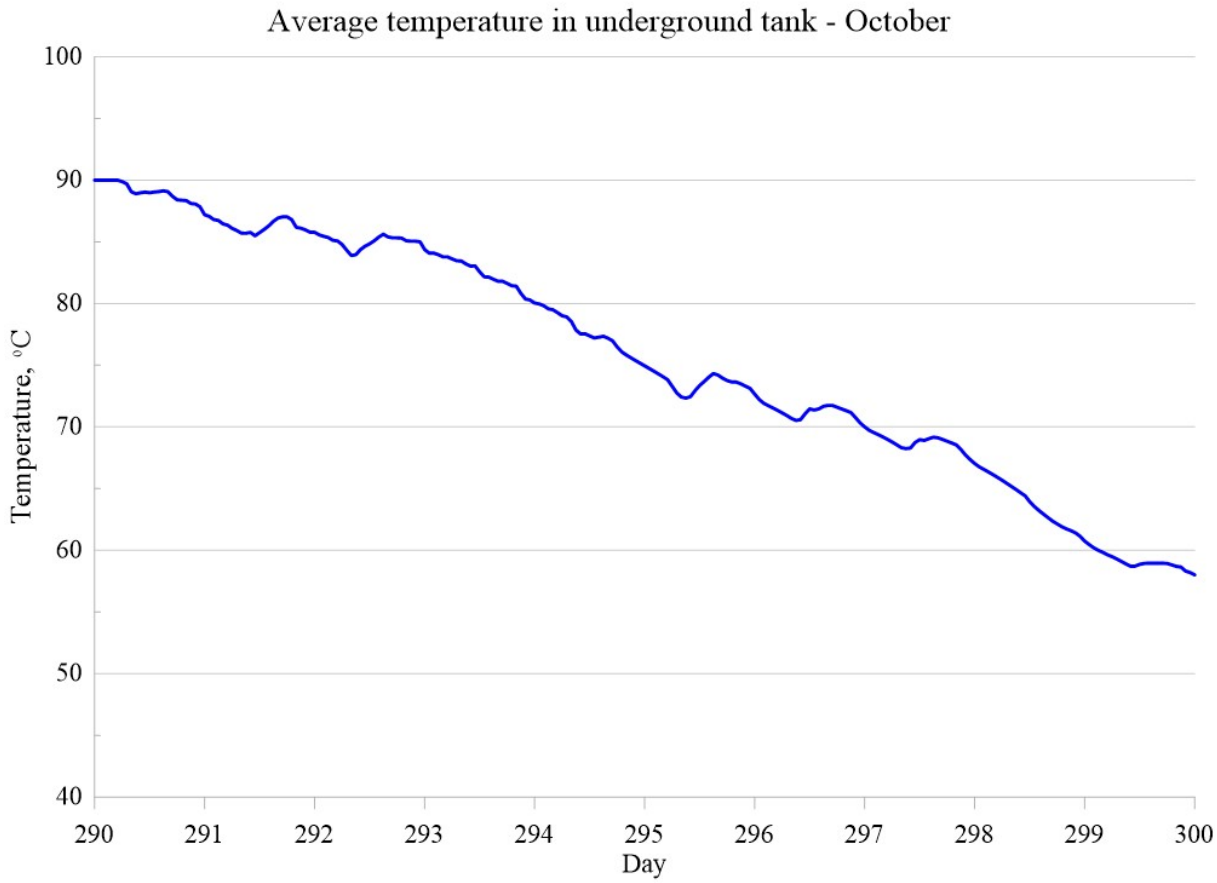

Figure 38. Average temperature in a storage tank - October

The mean COP for heat pumps over the course of a year is greater than 4.0, thus satisfying the RESHeat project's criteria. Figure 39 shows the average COP values for heat pumps each month.

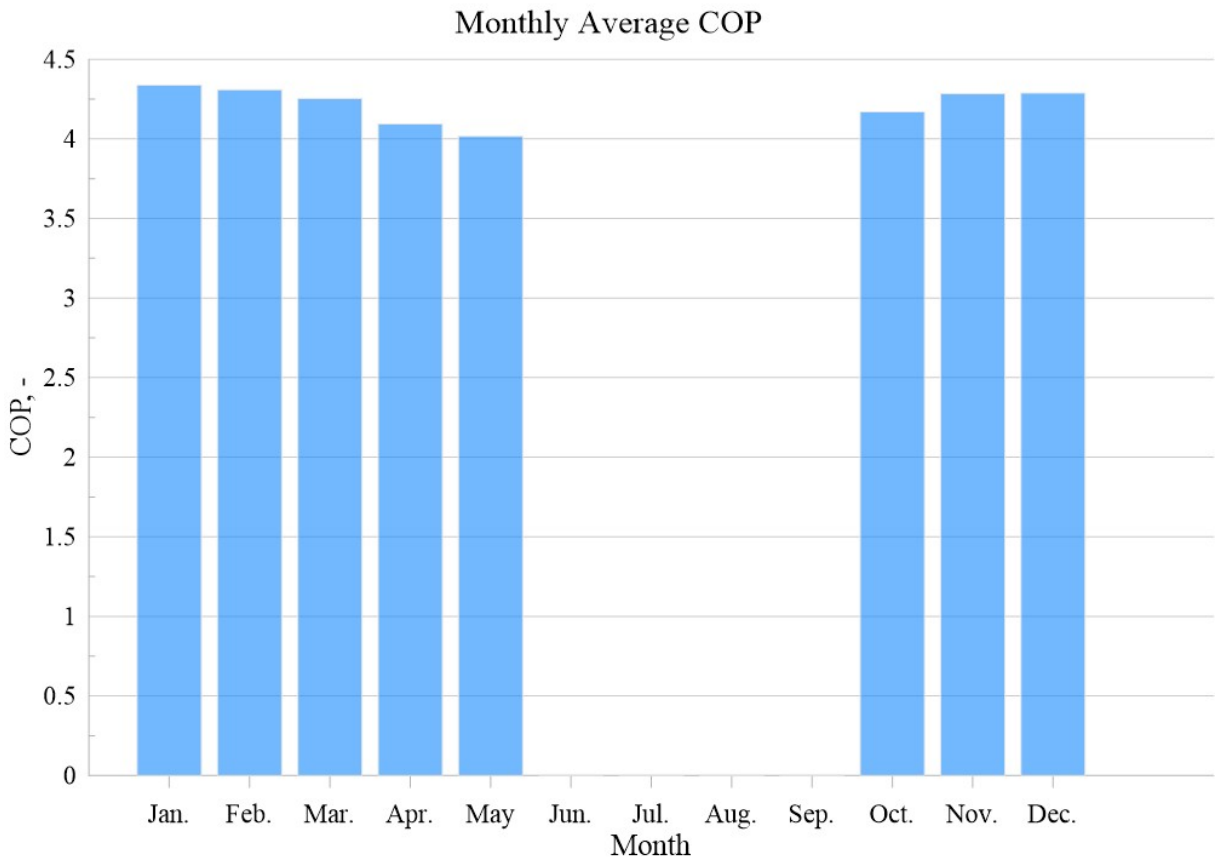

Figure 39. Monthly average heat pump COP

The COP of the heat pump remained relatively constant throughout the year. This is due to the constant temperature and large heat capacity of the ground, which is used as a heat source, as well as the constant average temperature of the load. Figure 40 summarises the electricity demand and the amount produced by the PV and PV/T panels.

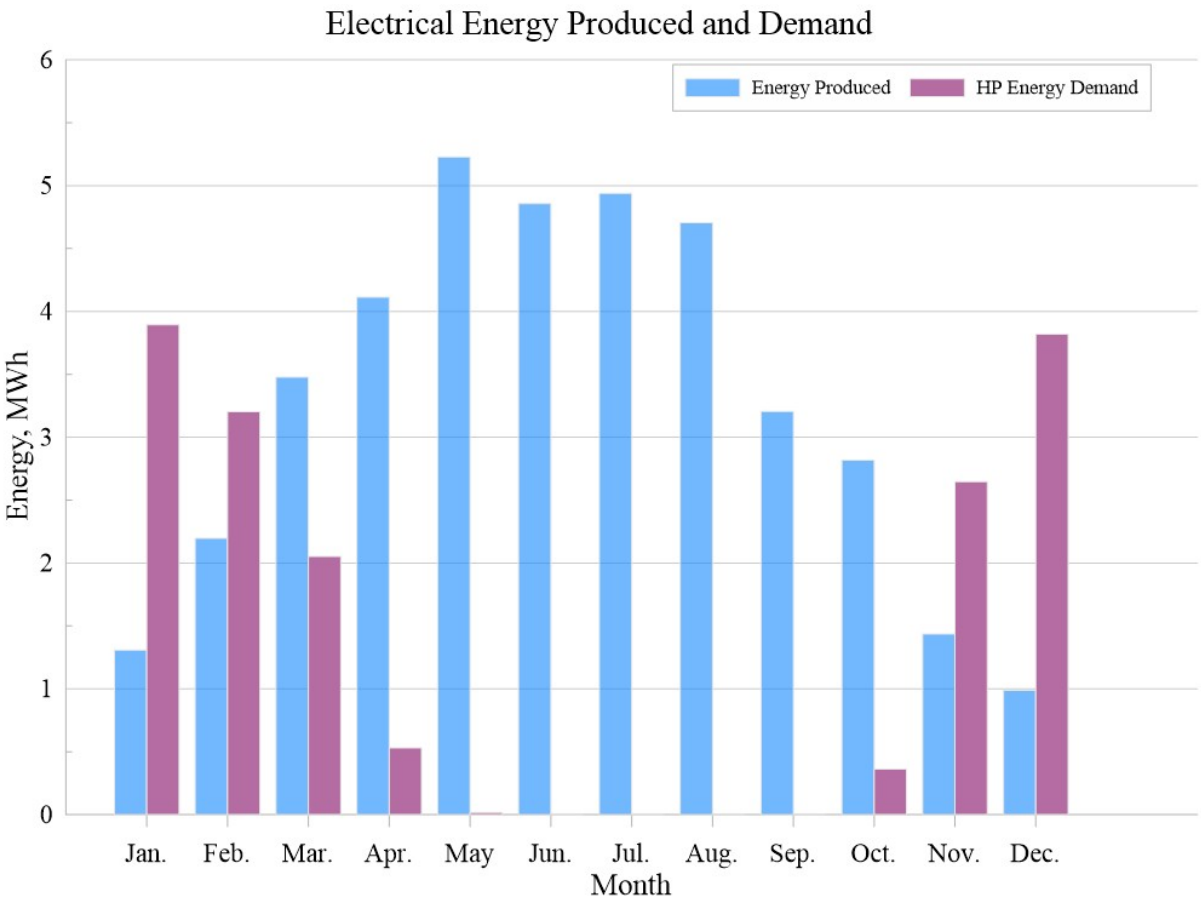

Figure 40. Heat pump electricity demand and PV and PV/T panels electrical energy production

A total of 39.27 MWh of energy is produced over the course of the year, while the electricity demand is 16.53 MWh. Year-round demand coverage is therefore 238%, significantly higher than the European Commission's target of 70%. Figure 41 shows the amount of thermal energy generated by the solar collectors. Over the course of the year, the total energy generated was 41.8 MWh, while the building's energy demand was 109.8 MWh. This equates to 38% of the building's total annual heat demand.

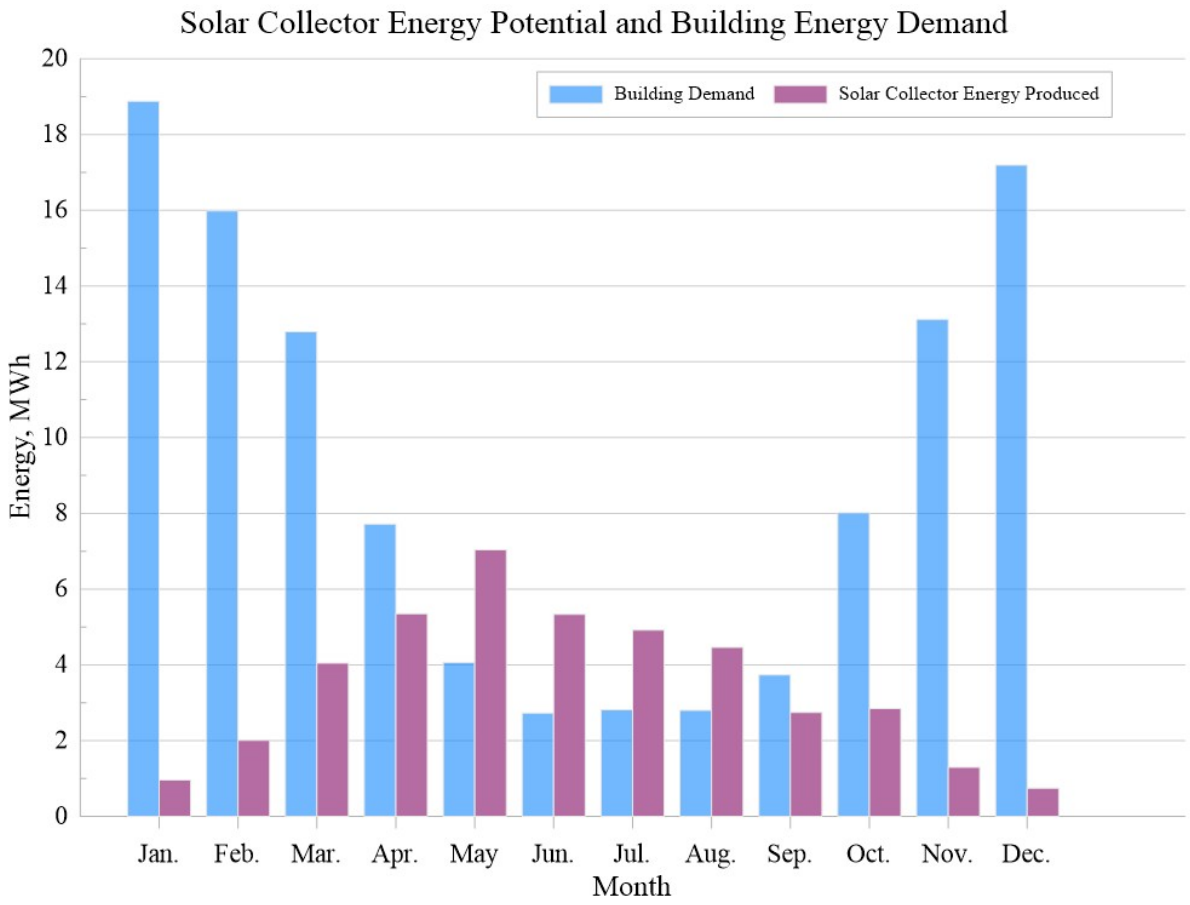

Figure 41. Solar collectors heat gain vs building heating demand

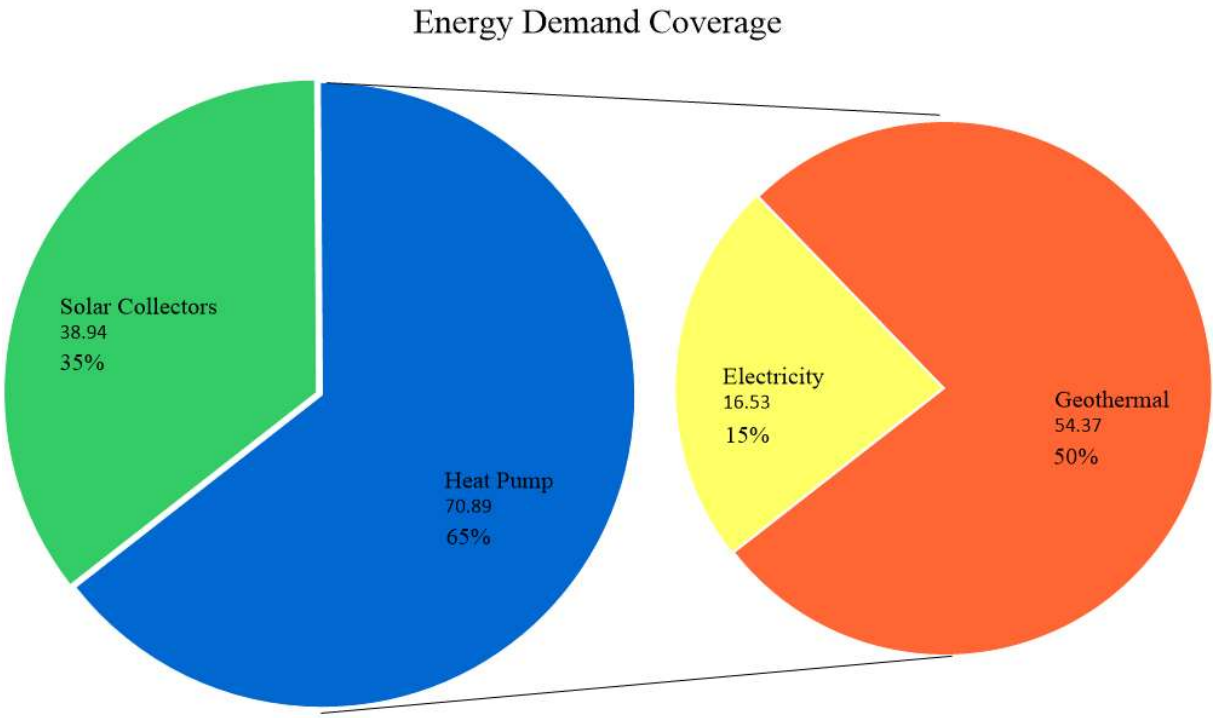

Figure 42. Energy coverage analysis

Figure 42 illustrates that 15% of the heat energy is obtained from electricity, while 50% is derived from energy stored in the ground and extracted via a ground heat exchanger. In fact, only 15% of the demand is met by electricity, which is generated entirely by photovoltaic panels. The remaining energy comes from solar thermal energy and energy stored in the ground.

6.5. Results of the modified system parameters simulations

The impact of system parameters on performance was analysed. The model developed for the RESHeat installation at ZBK was used to simulate different scenarios and verify design assumptions. The following simulations of installations in ZBK buildings were carried out as part of the RESHeat project:

- Analysis of the electricity production of the PV panels and PVT and comparison with the electricity demand of the heat pump installed in the considered system.
- Analysis of the required number of ground exchangers and the impact of their number on system performance.
- Analysis of the impact of the size of the underground heat storage on system performance, heat pump efficiency and demand of heat produced by the heat pump.

- Analysis of the effect of installing an underground heat storage tank and PVT panels on system performance.
- Consideration was given to methods of utilising the excess electricity produced to potentially increase the efficiency of the system by using an electric heater and raising the temperature in the underground storage tank and the heat source.
- The impact of weather control, which controls the temperature of the heat load depending on the outside temperature, on system efficiency was also considered.

The first simulation analysed electricity production and demand in hourly intervals. Below are daily graphs showing the three days with the greatest variation in temperature and solar radiation, which directly impact the amount of electricity produced by the system, as well as the heat demand and, consequently, the electricity consumed by the heat pump.

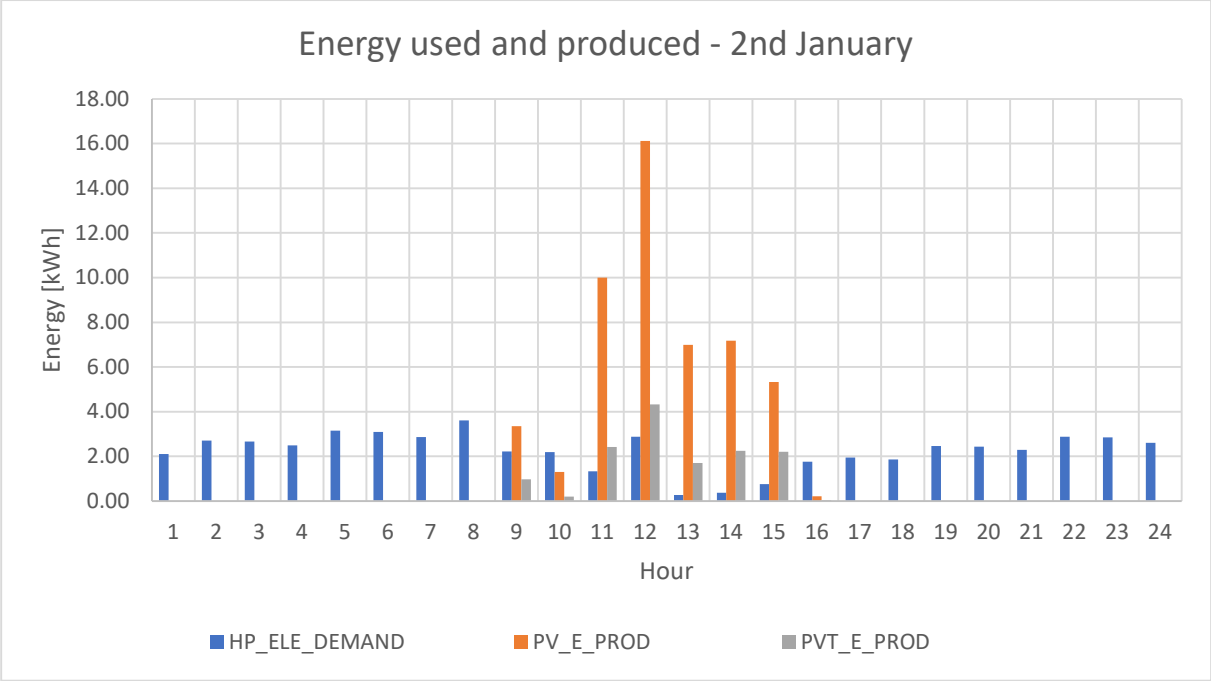

Figure 43 - Energy usage and production analysis for 2nd of January

On each of the days in consideration, the system produced more electricity than was required. On 2 January, the amount of energy produced was 64.6 kWh and the demand was 53.8 kWh.

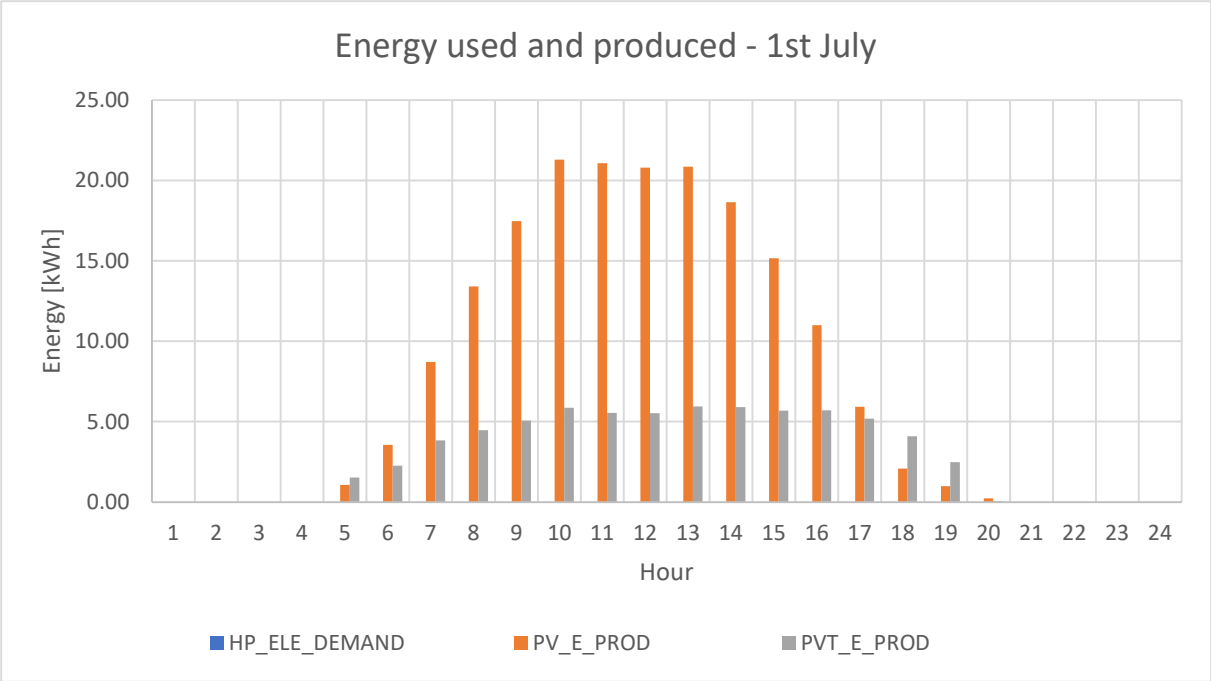

Figure 44 - Energy usage and production analysis for 1st of July

1 July the amount of heat produced was 251.4 kWh and the demand was 0 kWh. 1 October the amount of energy produced was 75.5 kWh and the demand was 53.6 kWh.

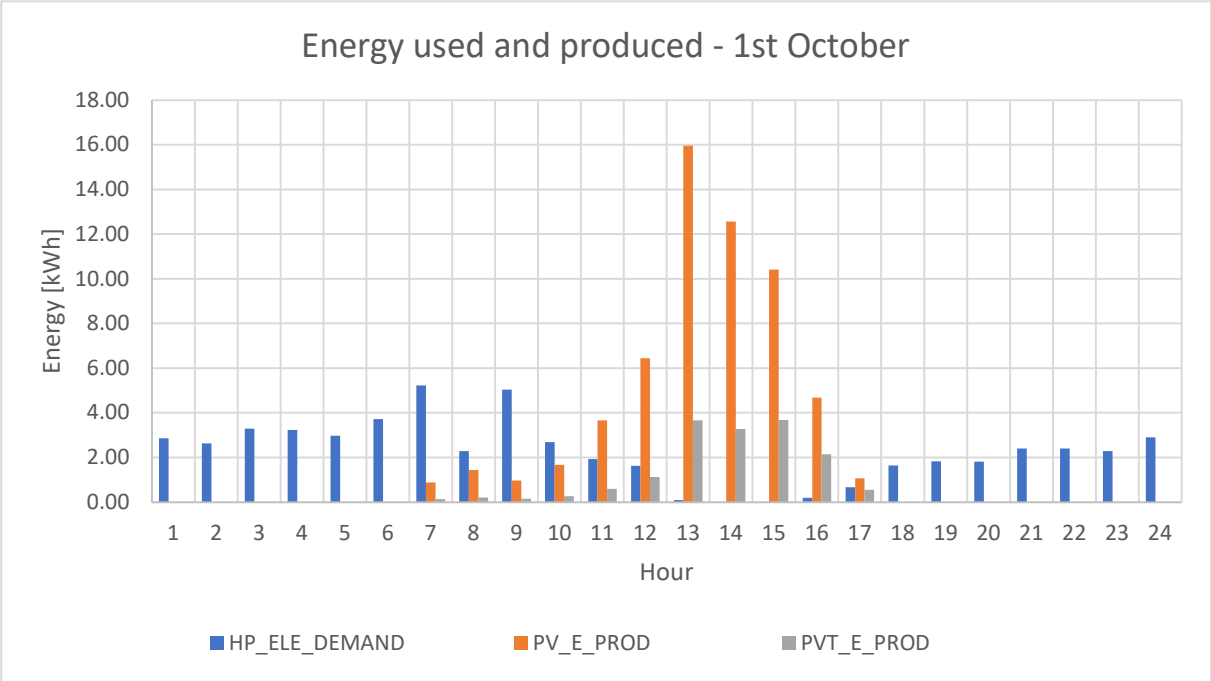

Figure 45 - Energy usage and production analysis for 1st of October

Therefore, it would be beneficial to install an electric energy storage of a size that would cover the daily demand of the system. In this way, the amount of electricity consumed by the

system during the night period would be zero, thus reducing operating costs and the load on the power grid during peak periods.

A further analysis looked at the effect of the number of ground heat exchangers on system efficiency and heat pump source temperature. 5, 10 and 15 exchangers were considered, of which 15 were finally installed in the system. A graph of the average daily heat pump source temperatures over the year is shown below.

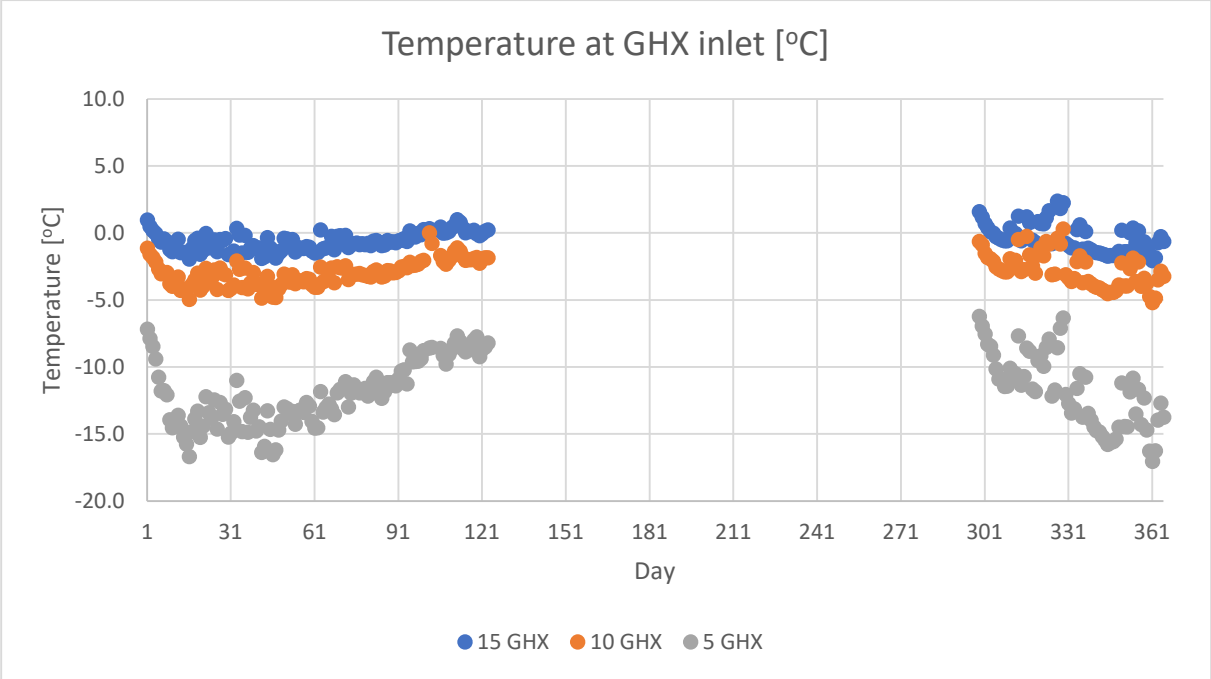

Figure 46 - GHX Inlet Temperatures

As can be seen from the diagrams, the use of fewer than 15 heat exchangers with a heat pump of this size would result in a significant reduction in heat pump source temperature which could result in an emergency shutdown of the system.

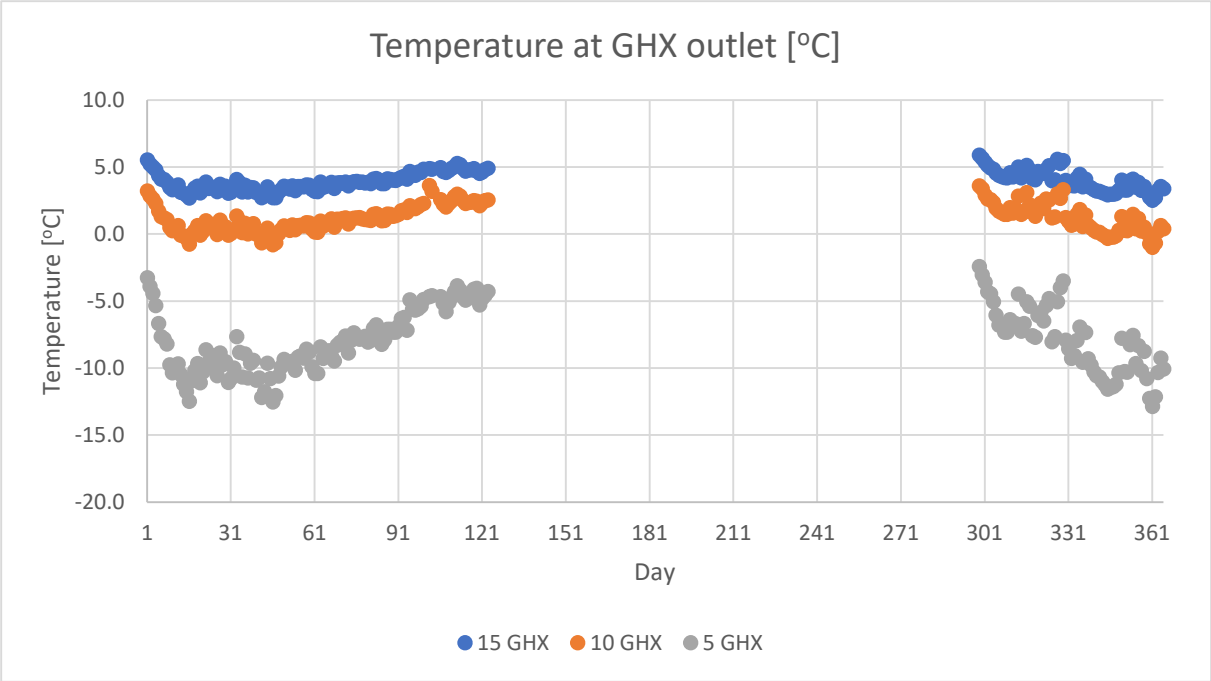

Figure 47 - GHX Outlet Temperatures

In the end, despite technical difficulties, the contractor was recommended to install 15 boreholes in which ground heat exchangers were placed.

Another case considered was the analysis of the impact of underground storage tank size on system performance. Storage tank sizes of 20, 50 and 100 m³ were considered. Ultimately, the decision was made to install a 50 m³ underground storage tank.

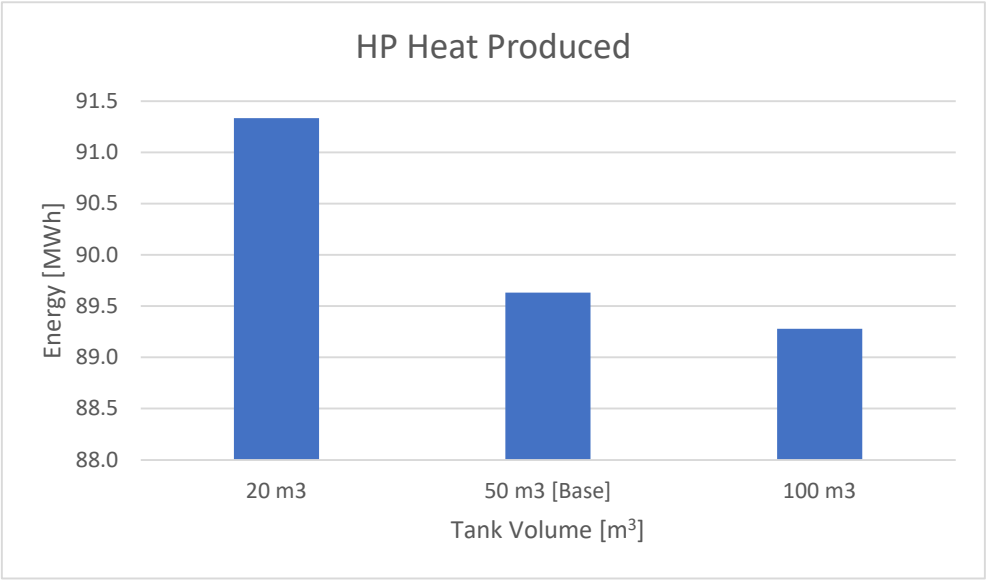

Figure 48 – Tank volume vs Energy Usage

The amount of heat required by the heat pump decreased as the size of the underground storage tank increased. This was by 1.9% and 2.2% for 50 m³ and 100 m³ storage tanks, respectively, compared with 20 m³ storage tanks.

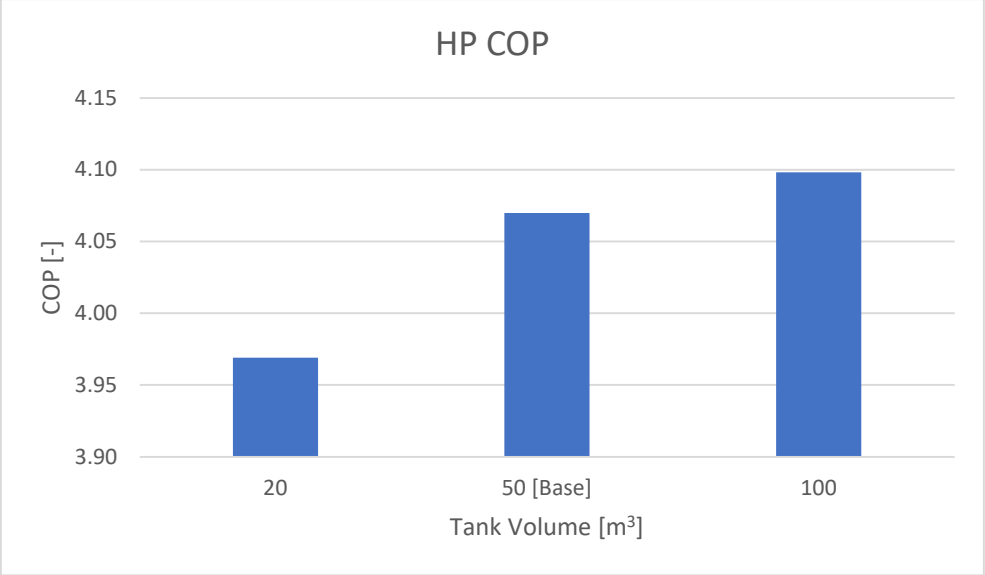

Figure 49 - Tank volume vs COP

The greatest difference in performance was observed at an underground storage volume of up to 50 m³. Above this size, the impact on system performance was much smaller. Increases in COP of 3% and 1%, respectively, were observed for 50 m³ and 100 m³ storage volumes compared to a 20 m³ storage tank.

Another analysis looked at the impact of the use of an underground heat storage tank and PVT panels on system efficiency. Variants without the installed storage tank and a variant without the storage tank and PVT panels were considered.

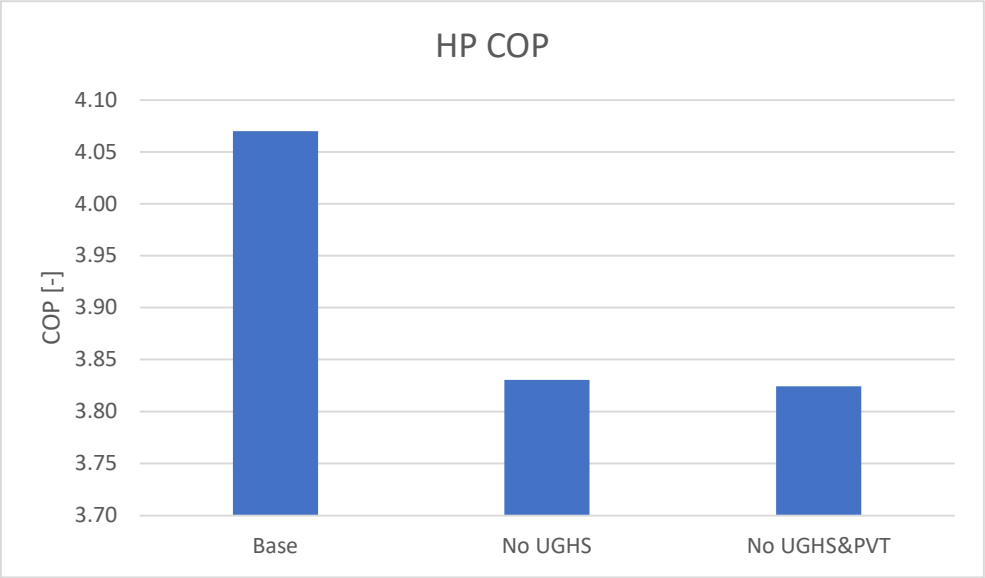

Figure 50 – COP in system without Underground Tank Storage and PVT

The underground heat store had the greatest impact on the efficiency of the system. The absence of the PVT panels and the underground heat exchanger reduced the COP of the system from 4.07 to 3.83. As can be seen, the use of PVT heat recovery does not have a major impact on the efficiency of the system, but the absence of the underground heat exchanger would have resulted in a significant drop in COP.

Next simulation option considered was the possibility of managing the excess electricity produced by PV and PVT panels. Various electric heater sizes were considered to raise the temperature of the water in the underground heat storage tank and thus increase the heat source temperature of the heat pump. The graph below shows the impact of the 3.5 kW, 4 kW and 4.5 kW heaters on the efficiency of the system expressed by the COP.

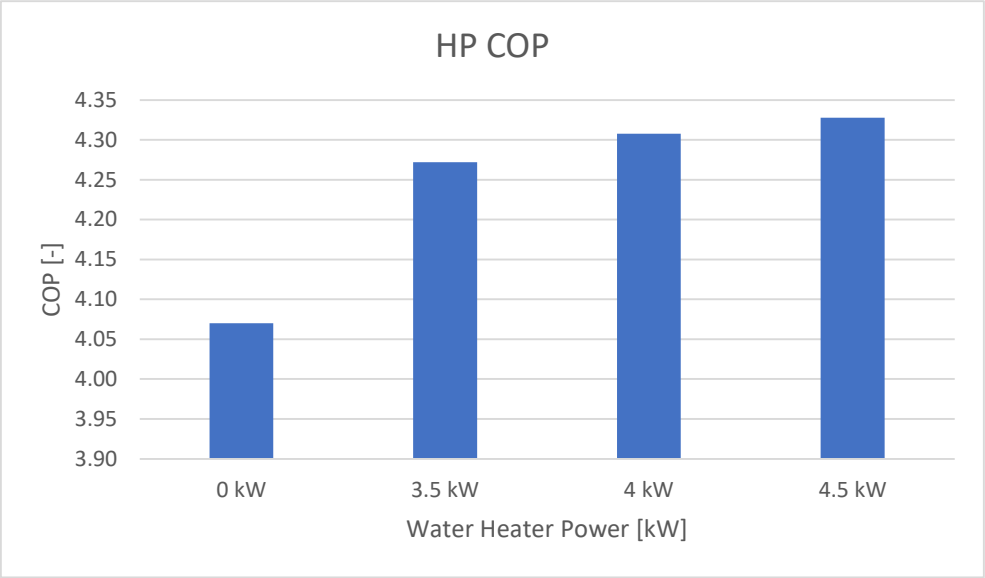

Figure 51 - COP in system with water heater

An increase in COP was observed from a baseline of 4.07 to 4.27 with a 3.5 kW heater, to 4.31 with a 4 kW heater and to 4.33 with a 4.5 kW heater, corresponding to increases in COP of 5%, 5.8% and 6.3%, respectively.

The last simulation considered a variant when weather control was not applied and the heat pump outlet water temperature was a constant 60 degrees Celsius. The temperature of the heat pump outlet water, equivalent to the temperature of the heat pump's heat load temperature, has a significant effect on the COP and therefore on the amount of electricity required to produce a unit of heat. This simulation compares a system with a variable temperature adjusted to the outside temperature and a system with a constant temperature.

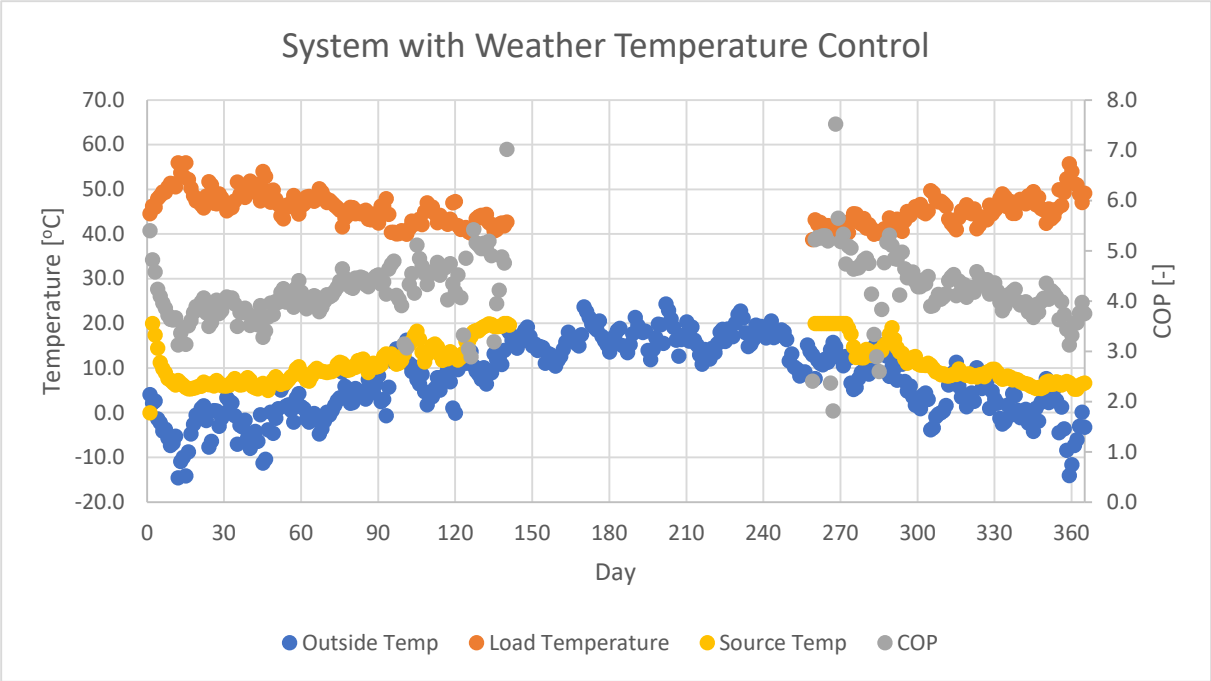

Figure 52 - System with weather temperature control

The graph above shows the situation when a weather controller is installed in the system. As can be seen, the average daily temperature of the heat source rises as the outside temperature increases. The difference between the temperature of the heat source and the heat load, as well as the temperature of the heat load itself, significantly impacts the COP. As this difference increases and the temperature rises, the COP decreases.

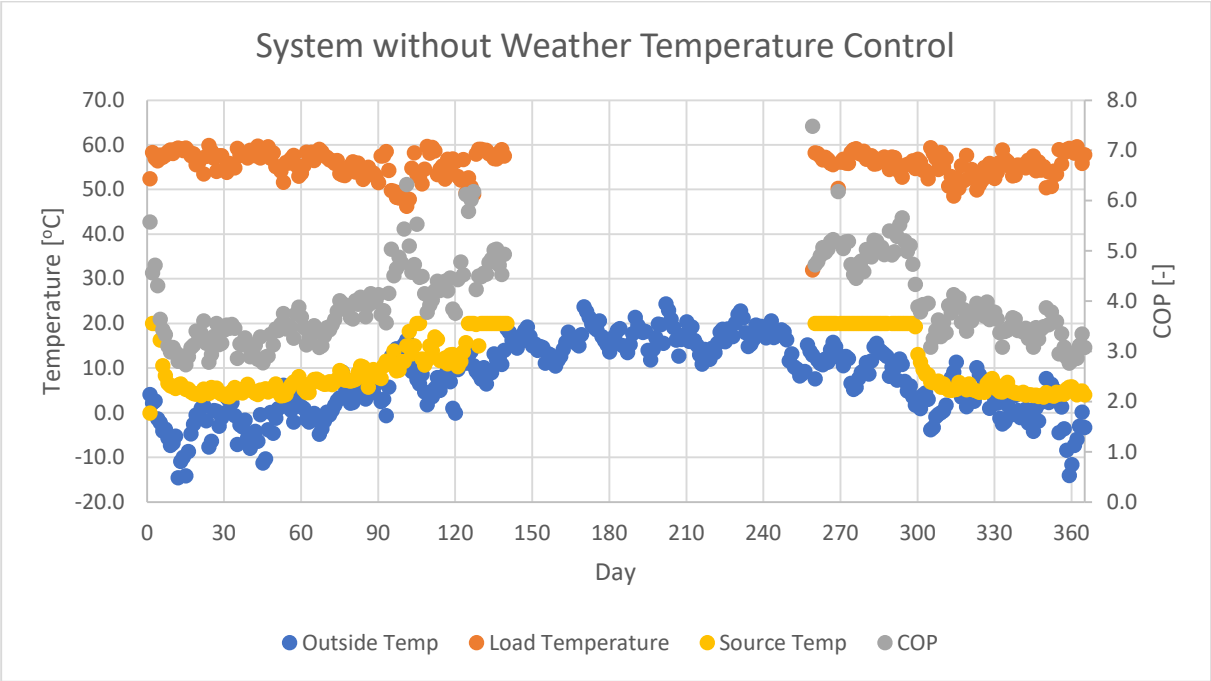

Figure 53 - System without weather temperature control

The next graph shows situations where there was no weather controller in the system, resulting in a relatively constant heat load temperature and therefore a higher average temperature difference, resulting in a lower COP compared to a system with a weather controller.

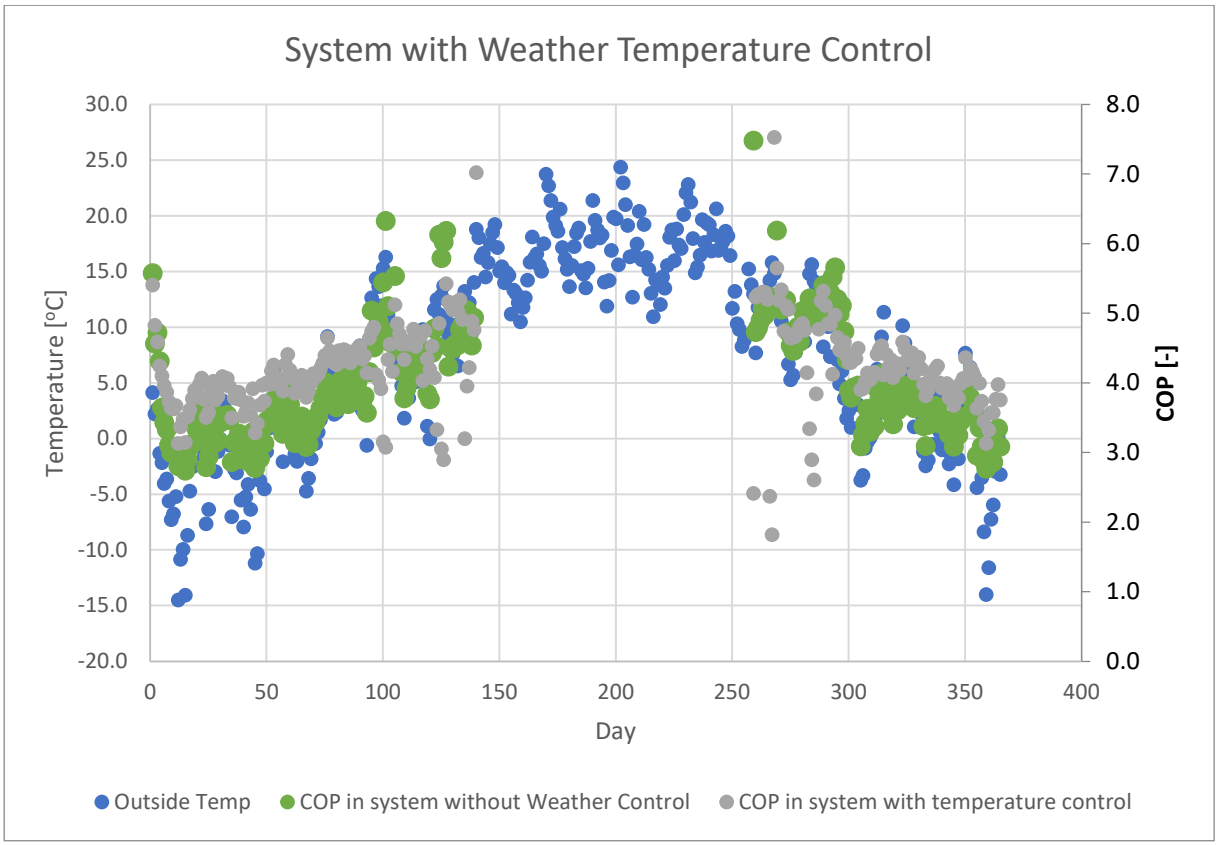

Figure 54 - COP comparision of two systems

The graph above shows a comparison between two systems and the average monthly temperature. As can be seen, the outside temperature has a greater effect on the system without weather control, where low outside temperatures cause it to have lower performance than the system with weather control. In hotter months such as May or September, the difference between these two systems is almost negligible and increases as the outside temperature drops.

7. Results obtained in the real system and their comparison with the simulation results

The next chapter of this thesis will focus on presenting the results of implementing the simulated system in practice. The RESHeat system was commissioned in the B2 ZBK building in June 2023, achieving full functionality by the end of the year. The results presented here cover the period from January to December 2024 and are compared with the corresponding simulation period.

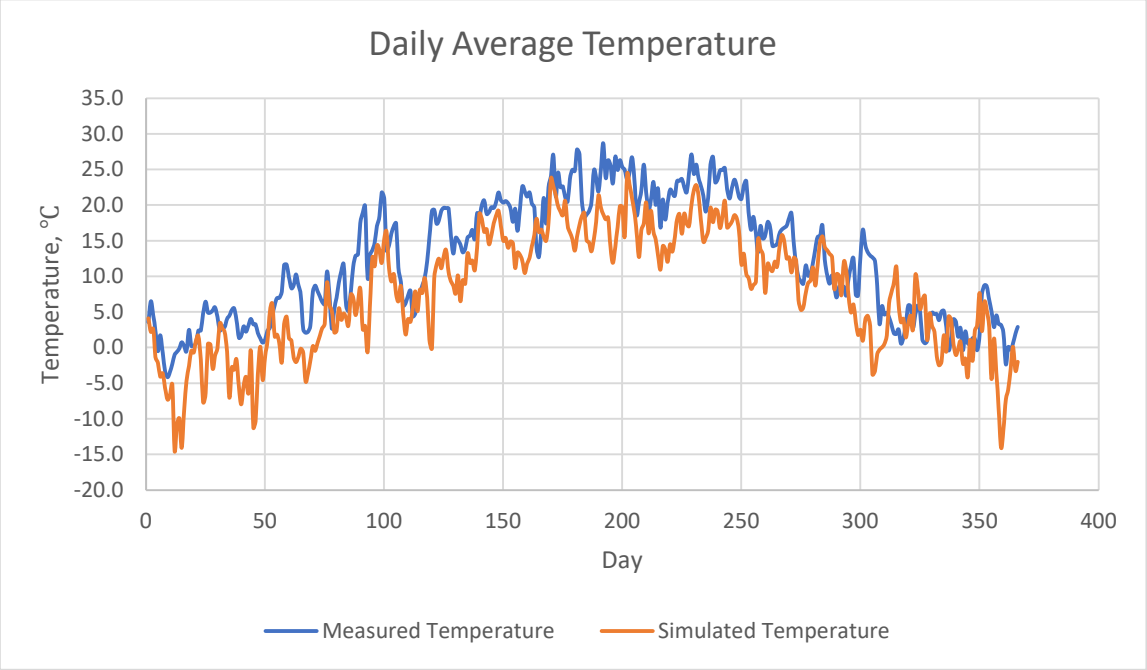

Figure 55 - Yearly Simulated and Measured Temperature Profiles

Following a comparison of the simulated (Meteonorm Data) and measured temperatures, the following conclusions can be drawn:

- The mean bias has been calculated to be -4.6 °C. This indicates that the Meteonorm data is typically lower than the measured, real-life data.
- The mean absolute error (MAE) is 5.3, which indicates that the measured temperature is always above the simulation data (the average bias is close to the MAE).
- RMSE is equivalent to 6.4 and higher than MAE (as anticipated, since it imposes a greater penalty on outliers). It is evident that certain days exhibit a pronounced bias.
- A robust positive correlation of 0.86 was identified, indicating that day-to-day trends in the simulation align with real measurements (i.e., higher measured temperatures tend to coincide with higher Meteonorm temperatures, and vice versa). However, a substantial mismatch remains.

The mean monthly measured temperatures were then compared with those employed in the simulation, in order to illustrate whether the same discrepancies occur for the months, or whether the differences between the measured data and those used in the simulation cancel each other out within a monthly period.

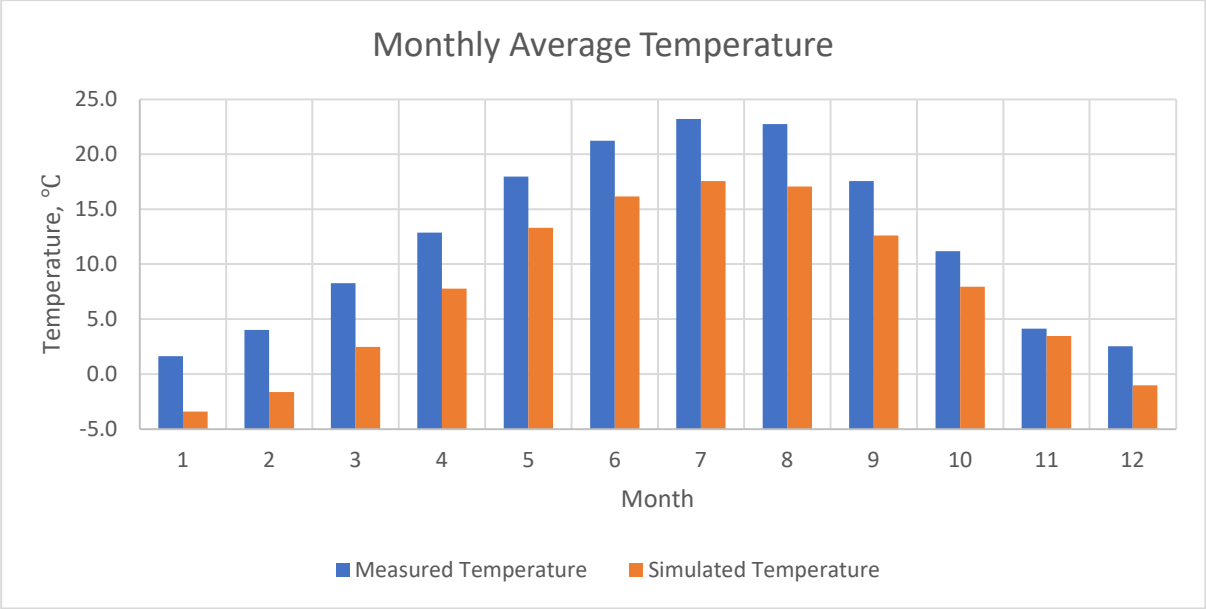

Figure 56 - Monthly average temperature comparison

Temperatures on a monthly average basis show less volatility, but a clear trend can still be seen - simulated temperatures are lower than those measured in 2024. Lower temperatures can result in an overestimation of energy consumption by the simulated system compared to the real system, and reduced operating parameters in the simulated system. The following conclusions can be drawn from the monthly average data:

- The average bias is -4.6, exactly the same as for the daily values. The simulated results are still significantly lower than the measured data.
- The mean absolute error is 4.6, showing that the daily volatility has been removed as it is equal to the bias.
- The RMSE is 4.8, almost the same as the MAE, which means that the outliers have been removed.
- The correlation is 0.98, indicating a very strong correlation between measured and simulated data. It shows that both temperatures closely follow the same pattern, but the measured data have the same offset for almost all months.

This difference may indicate a worrying phenomenon, i.e. that even in the case of energy simulations compared to the actual implementation of the system, the effects of global warming

can be noticed. Meteonorm weather data is based on a 'typical meteorological year' and not on actual measured data. This dataset aims to represent typical meteorological data and is based on averaged historical measurements from this region. This may indicate systematic problems that will occur in all simulations using similar climate data and show the need to update similar data sets in a warming climate.

The next step is to compare and analyse the electricity demand, the amount of heat produced by the heat pump and the COP factor for the simulation and for the measurements taken in the actual installation.

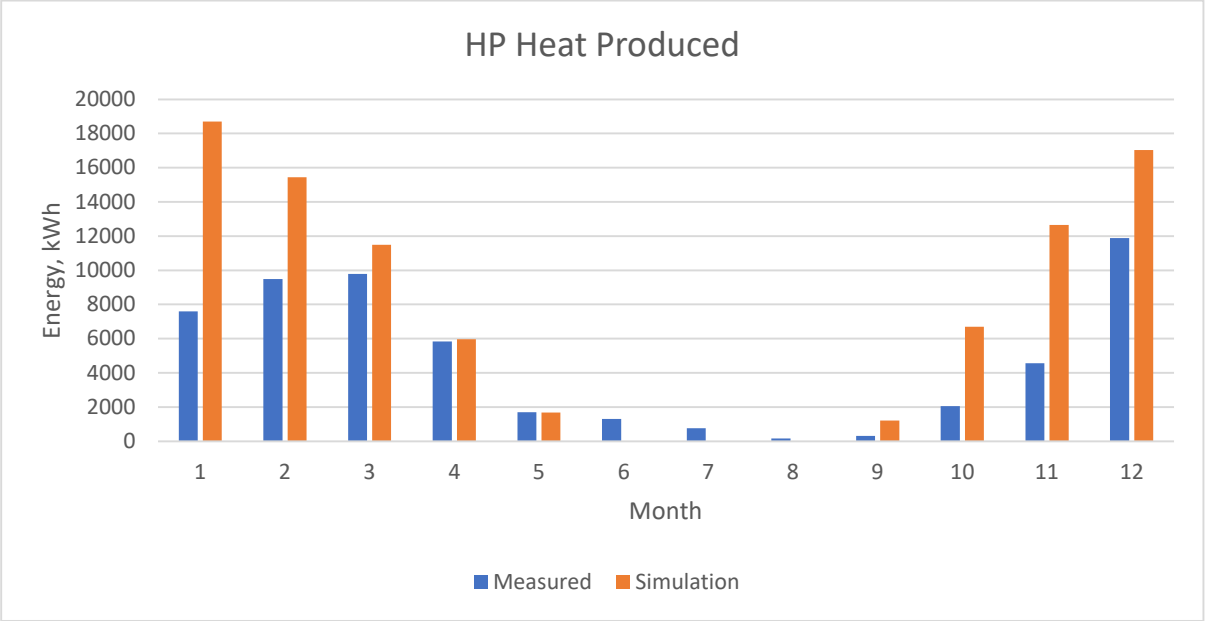

Figure 57 - Heat produced by heat pump comparison

As can be seen, the amount of energy produced by the heat pump (which is directly related to the building's demand for heat for central heating and hot water preparation) is significantly lower in reality than it appeared in the simulation. This may be due to a number of factors, including the difference between the actual temperature and the meteorological data used in the model. The biggest discrepancy can be seen in the first months of the year - January and February, which can also be seen in the difference between the simulation and the actual data of the monthly average temperature for these months. The most surprising thing is the demand for heat in January and February. In these two months, which are the coldest of the year, the demand should be the highest, but it is comparable to March and even slightly lower. This is not entirely consistent with the recorded temperatures because according to the measured monthly average temperatures, January was the coldest of these months.

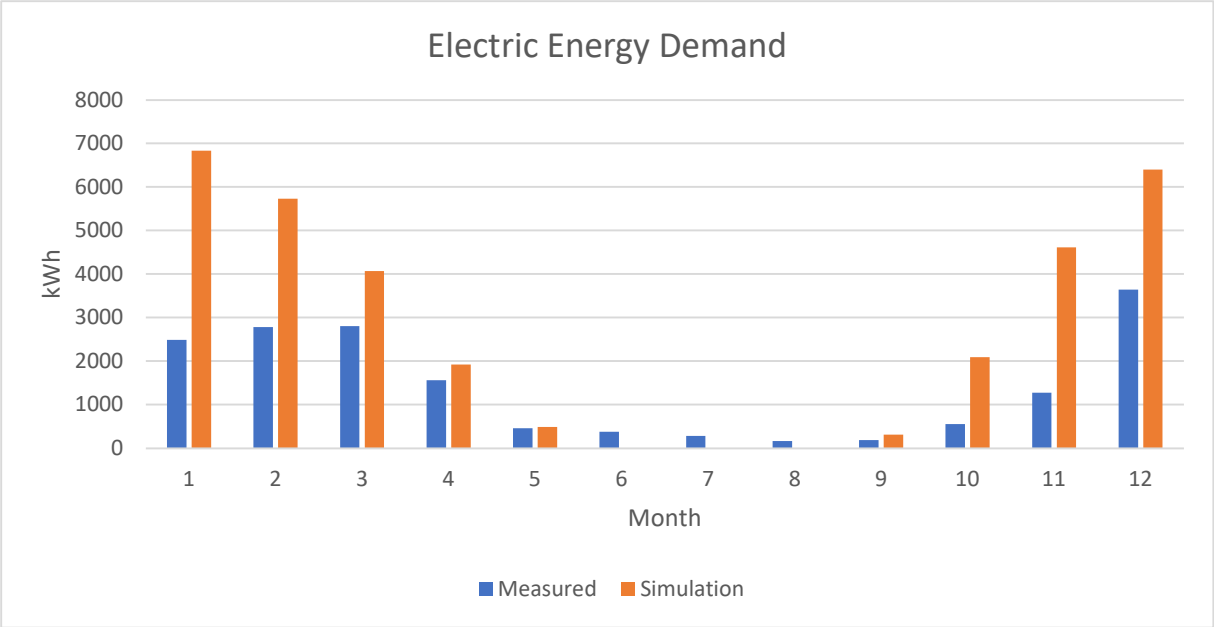

Figure 58 - Electric Energy Demand Comparison

As expected and in line with the amount of heat produced, the demand for electricity is shown. The amount of electricity consumed by the heat pump in the simulation corresponds to the temperatures in the given months. The energy demand in reality is lower than in the simulation but in line with the amount of heat produced.

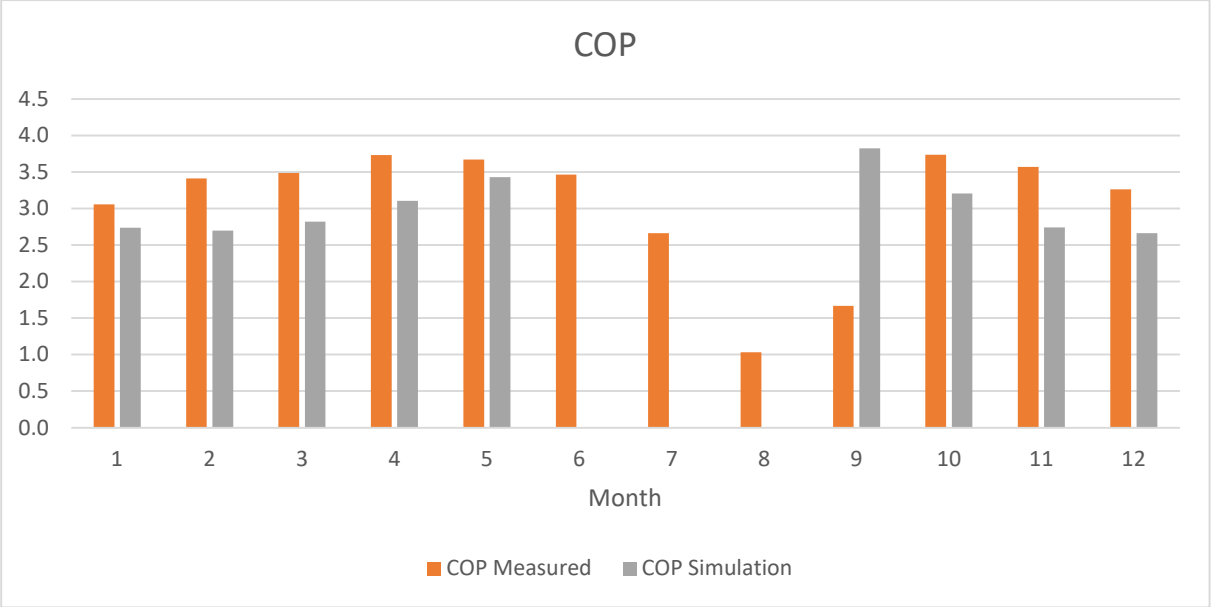

Figure 59 - Monthly average COP comparison

The COP is relatively constant, both in the simulation and in reality. The average COP in the simulation was 2.8, and for the measured data in reality it was 3.3. As expected, both for the simulation and for the real data, the COP is lowest in the autumn and winter months. August is noteworthy for the real data, where there was no demand for heat in the simulation, but in reality

there was, and the pump had to work in extremely unfavourable conditions because the COP was exceptionally low at 1.0. This was probably due to the demand for domestic hot water and the resulting high temperature of the load However, the amount of heat produced that month - 167 kWh - was very low (by comparison, the demand in February was 9,479 kWh). Consequently, when calculating the COP and other efficiency parameters, extreme values should not be directly averaged to an annual average; rather, a weighting appropriate to the frequency of occurrence should be taken into account. The average annual COP in the simulation is 16% lower (2.8 vs. 3.3), which can be justified by the significant difference in outside temperatures.

In the subsequent section of the study, an analysis will be conducted on the temperatures of the circulating water of the heat source and heat load. This analysis may provide a significant explanation for the observed differences in COP and electricity demand. Unfortunately, due to technical reasons caused by sensor failure, temperature measurements for the heat source and load are only available for the first 71 days of the year. Therefore, during this period, they will be combined with the simulation results.

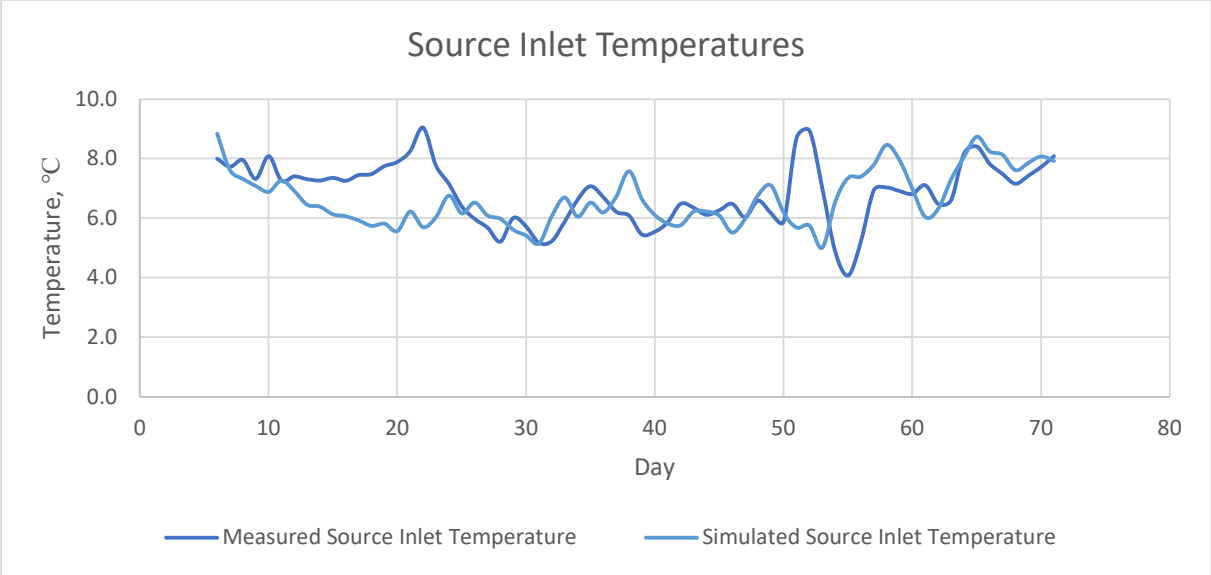

Figure 60 - Source inlet temperatures comparison

The first factor analysed is the temperature of the medium leaving the ground heat exchanger and, consequently, the supply temperature of the heat pump's source. The temperature resulting from the simulation and the temperature measured in reality are similar to each other. The average temperature in the simulation was 6.7°C, whereas in reality it was 6.8°C, which was negligibly higher. The average difference for individual days was 0.2°C. Therefore, we can

conclude that the simulation data and the actual measurements are very similar and will not affect the overall results of the simulation.

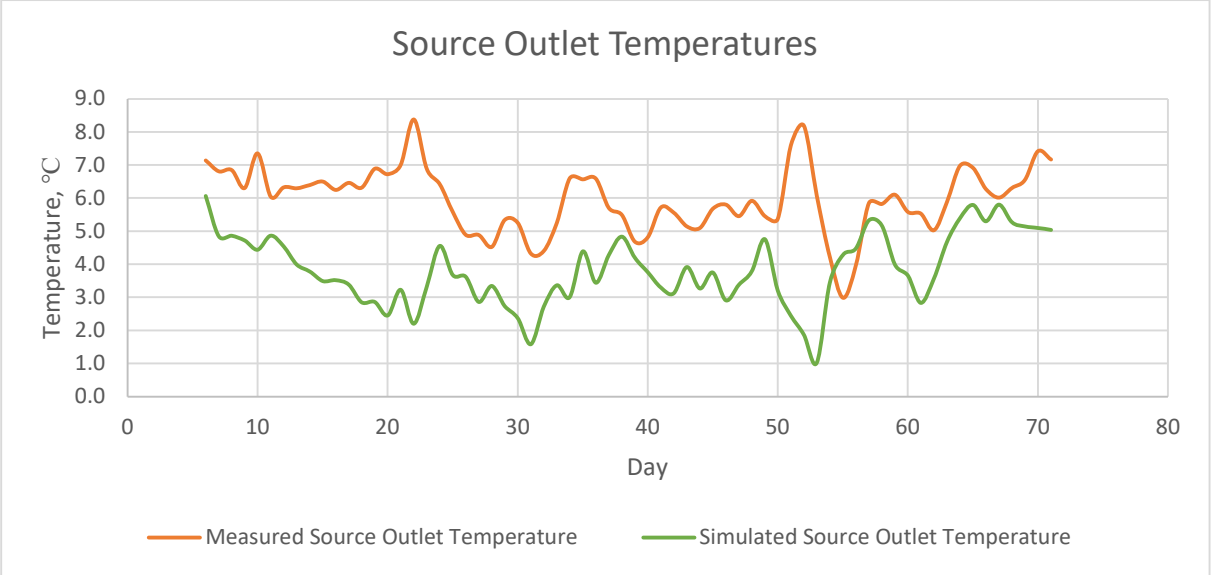

Figure 61 - Source outlet temperatures comparison

The first difference can be seen in the temperatures of the water leaving the heat exchanger of the heat pump's heat source. The temperatures obtained in the simulation are significantly lower than the temperatures measured in reality. The average daily temperature in the simulation was 3.8°C, whereas the actual temperature was 6.0°C. The average difference between individual days in the simulation and the actual installation was 2.1°C. These differences may be due to different heat pump loads for the simulation and the actual installation, as will be revealed by further analysis.

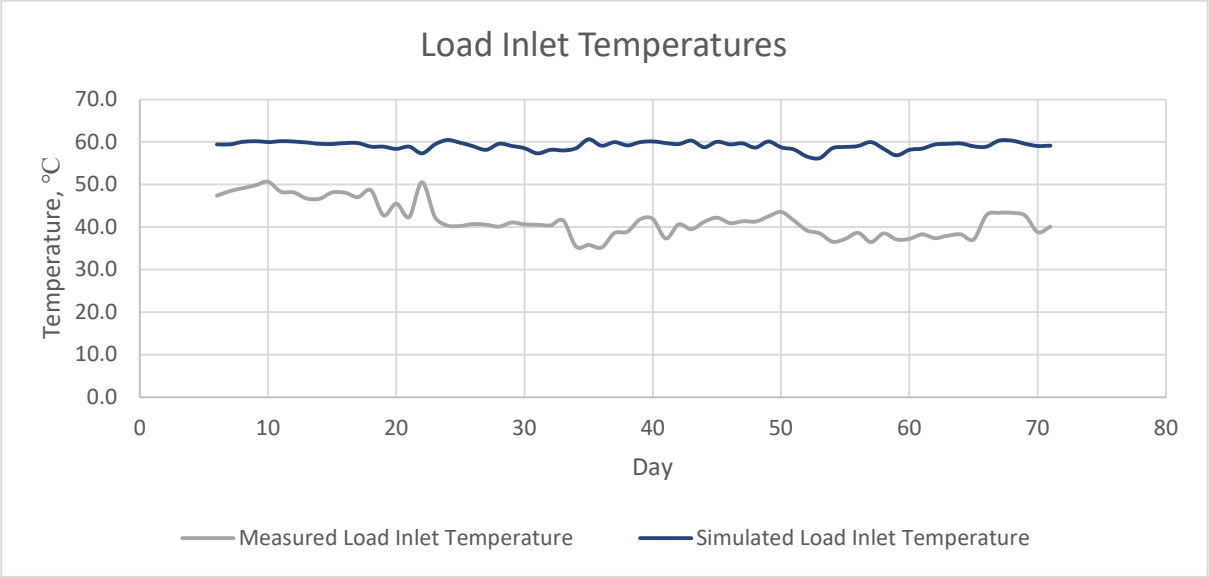

Figure 62 - Load inlet temperatures comparison

The most noticeable difference that can impact the coefficient of the heat pump's efficiency is the inlet temperature and the outlet setpoint temperature of the heat load. As can be seen in the graph above, there is a significant difference between the simulation and the actual measurements. The average inlet temperature of the load in the simulation was 59.2°C, whereas the actual measurement was 41.8°C. The average difference for individual days was 17.4°C at the inlet and 20.3°C at the outlet of the heat pump load.

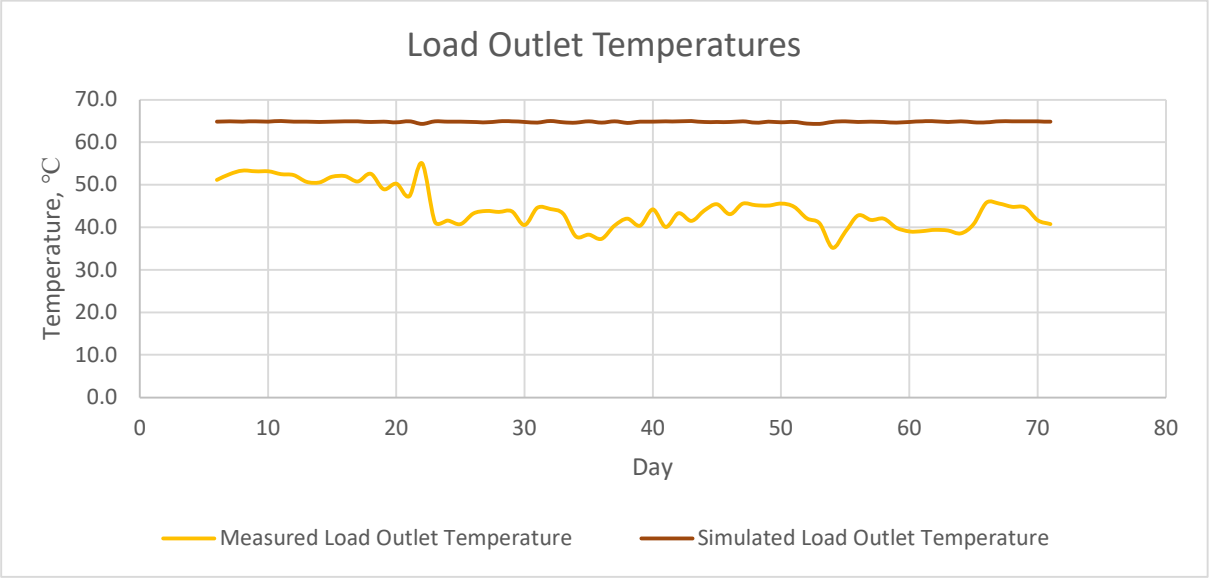

Figure 63 - Load outlet temperatures comparison

As can be seen, the temperature difference in the case of the heat load is significant, and it is clear that this has had a considerable effect on the difference between the average annual COP in the simulation results and the actual measurements.

Table 14 - COP, inlet and outlet temperatures matrix table

	Load Outlet, °C	**65**	**58.4**	**49.7**	**34.5**
	Load Inlet, °C	**55**	**50.2**	**43.8**	**29.2**
Source Outlet, °C	**Source Inlet, °C**	**COP/Heating Capacity, kW**			
20	25	3.80 / 126.60	4.70 / 126.00	6.00 / 125.60	9.60 / 124.50
15	20	3.40 / 115.50	4.20 / 114.30	5.30 / 114.00	8.10 / 112.60
10	15	3.20 / 104.80	3.80 / 104.00	4.80 / 103.30	6.90 / 101.20
5	10	2.90 / 95.00	3.50 / 93.90	4.30 / 92.70	6.00 / 90.60
0	5	2.60 / 85.80	3.20 / 84.30	3.80 / 83.20	5.30 / 80.70
-5	0	2.40 / 77.30	2.80 / 75.50	3.40 / 73.80	4.60 / 71.50

For the data presented here for the first 71 days of the year, the temperatures for the simulation would suggest that the resulting COP should be around 2.6, while for the temperatures measured in reality, the COP should be 3.8. For comparison, the average COP for the simulation and actual measurements for the same period were also calculated. For a given period of time, the COP in the actual installation was 3.3, which is significantly lower than in the laboratory data provided by the heat pump manufacturer. In the simulation, it was 2.7, which is practically identical to the laboratory data. This difference also shows the likely cause of the discrepancies between the simulation and reality. The laboratory data on the efficiency of the heat pump used in the simulation are very optimistic compared to the actual performance of the heat pump, as shown by the results obtained.

Another aspect to compare is the amount of electricity produced by the system. As mentioned earlier, the programme requirement was to cover at least 70% of the electricity demand with renewable energy – own production.

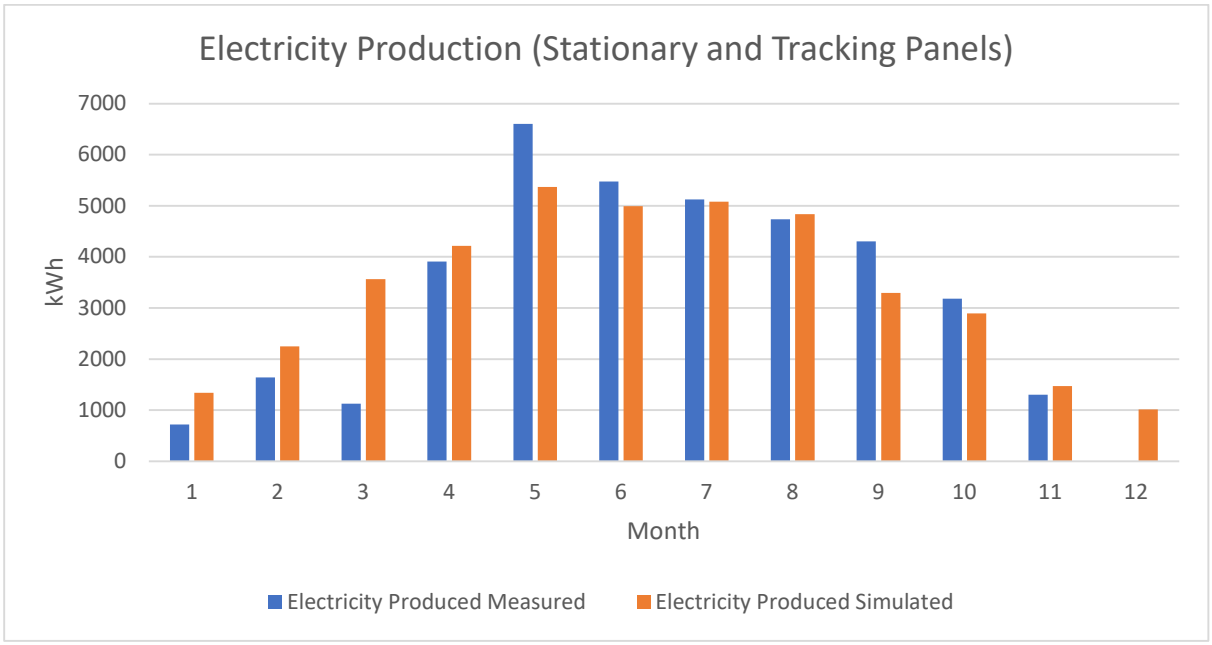

Figure 64 - Electricity production comparison

The above chart compares the energy produced by stationary photovoltaic panels and photovoltaic panels on trackers with data obtained from simulation. For comparison, the total amount of energy for 11 months (excluding December) was obtained. Initially, March and May appear to be measurement errors, as March displays lower production than would be anticipated based on the trend, and May exhibits higher energy production than in the previous and subsequent months. In order to verify this, the amount of energy produced was compared with the monthly total of solar radiation.

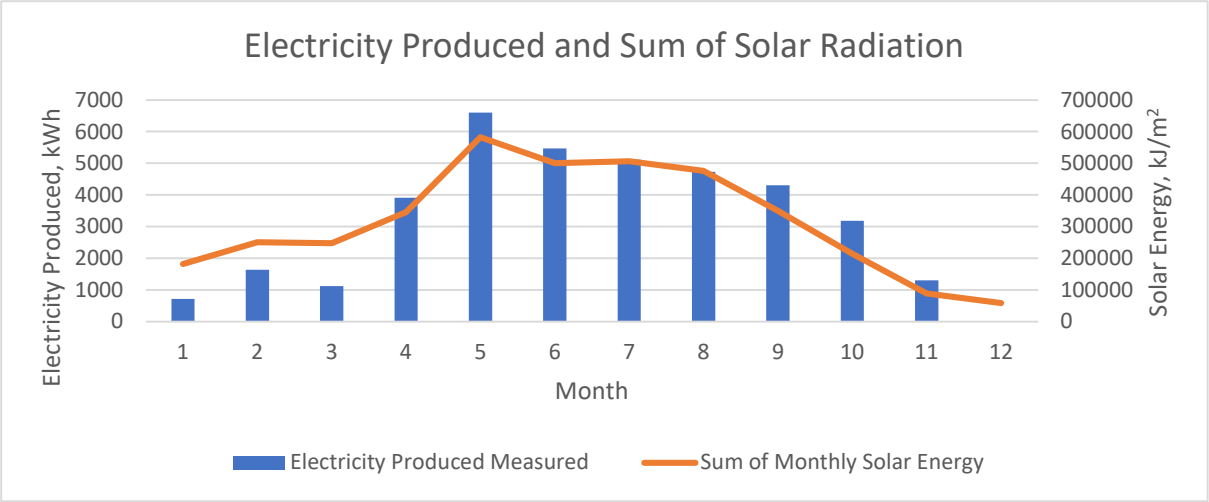

Figure 65 - Electricity produced compared to sum of solar radiation

Contrary to expectations, the amount of energy produced in March and May was confirmed and was consistent with measurements of total monthly solar radiation. In March, we observed a decrease in solar radiation, which translated into a decrease in the amount of electricity produced. Contrary to March, May saw the highest monthly total solar radiation of the year.

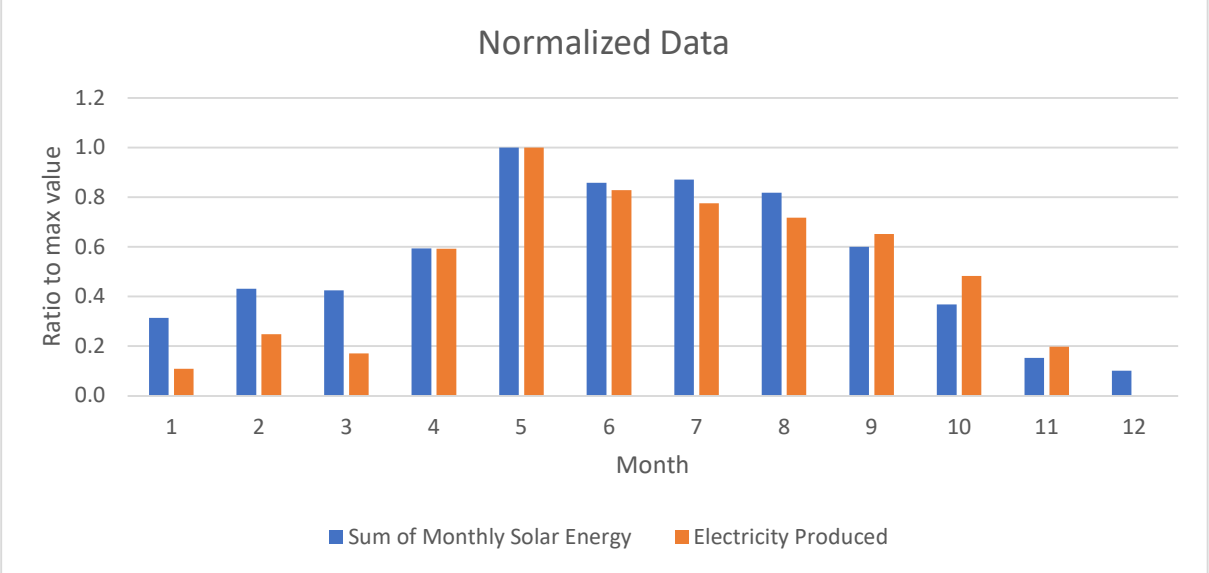

Figure 66 - Electricity and radiation normalized

When comparing normalised data (relative to the respective maximum values), it can be seen that in winter the amount of energy produced is disproportionate to the amount of solar radiation. In spring and summer, the amount of energy produced is proportional to the amount of solar radiation. The decrease in the efficiency of photovoltaic panels during winter may be caused by snow lying on them, which significantly reduces the amount of energy absorbed.

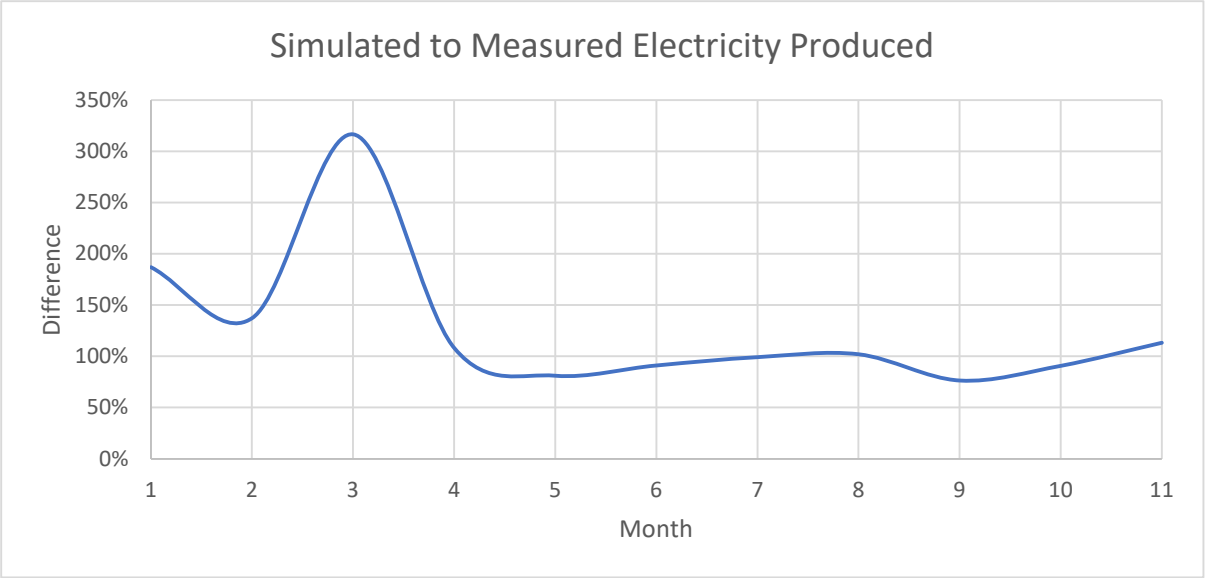

Figure 67 - Percentage difference of simulated and measured electricity produced

In general, the simulation predicts well the amount of energy produced, as for most of the month the ratio is very close to 100%. As already mentioned, the installed system noticed a drop in energy production in the winter months and this can be seen on the comparison as the difference ratio increases in these months. The simulation did not show any impact of the problems such as the snow covering the solar panels, so the amount of energy produced in the winter months is not affected as it is in real life situation.

An important aspect of photovoltaic panels is their efficiency. The typical efficiency of panels for domestic use is around 20%, with more modern ones achieving 22-24% efficiency. The main factors affecting efficiency are the angle of incidence of solar radiation on the panel and the temperature of the panels, as an increase in temperature causes a drastic drop in efficiency. The RESHeat system uses water-cooled PVT panels mounted on a tracker, both of which should significantly increase the efficiency of the panels. In the RESHeat system, 12 PVT panels were installed on a tracker and 68 stationary panels were installed on ZBK building.

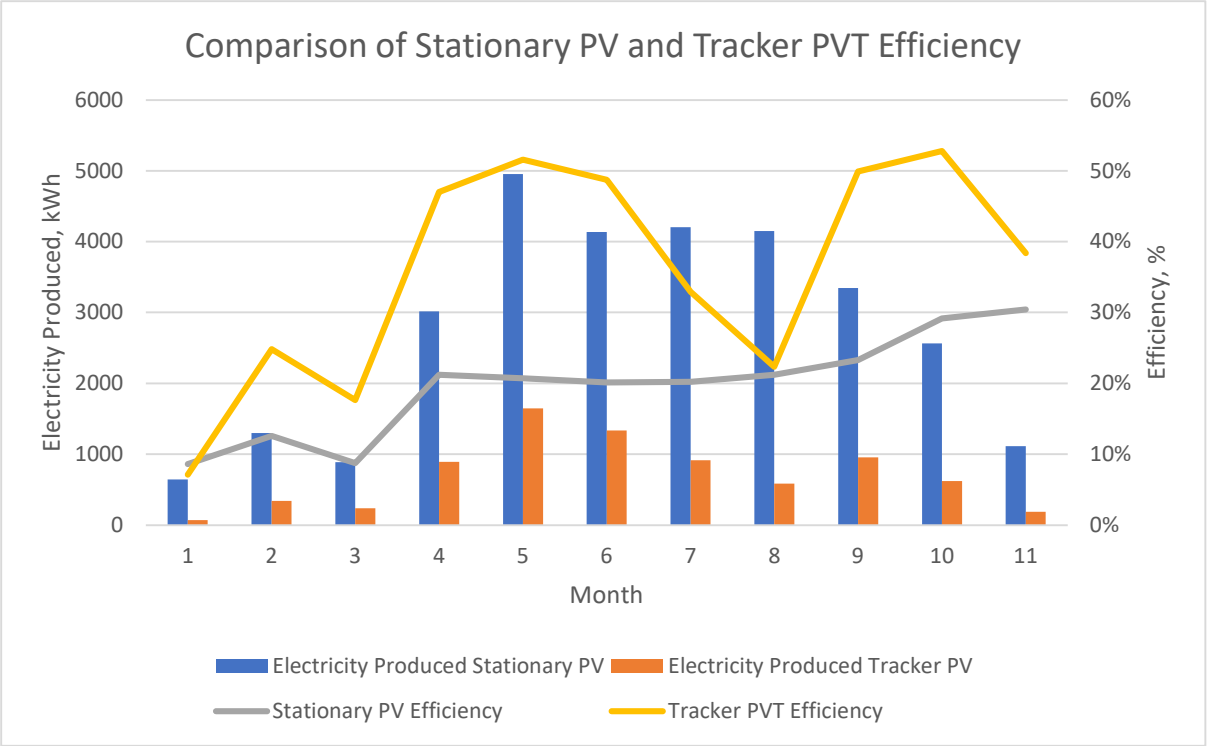

Figure 68 - Comparison of PV and PVT performance

As can be seen in the graph above, the efficiency of the PVT system on the tracker significantly exceeds that of stationary PV systems. The efficiency of the PV system ranges from 10% in winter (the drop below 20% is probably caused by snow cover) to 20-30% during the rest of the year, while the efficiency of the PVT system on the tracker shows high variability and ranges from around 20% in winter, rising to around 50% in spring, with a temporary drop in July and August, and returning to high efficiency levels by the end of the year. The solar radiation intensity readings from the weather station are most likely subject to some errors that cause variability in the readings, but despite this, it can be seen that the PVT system shows much higher efficiency than the solar PV system. This indicates the effectiveness and justifies the use of such solutions in non-commercial systems.

For reference, the efficiency of the actual system was compared with the efficiency of the simulated system (the total amount of solar radiation from Meteonorm post-processing data was used as a basis for comparison with the simulated system).

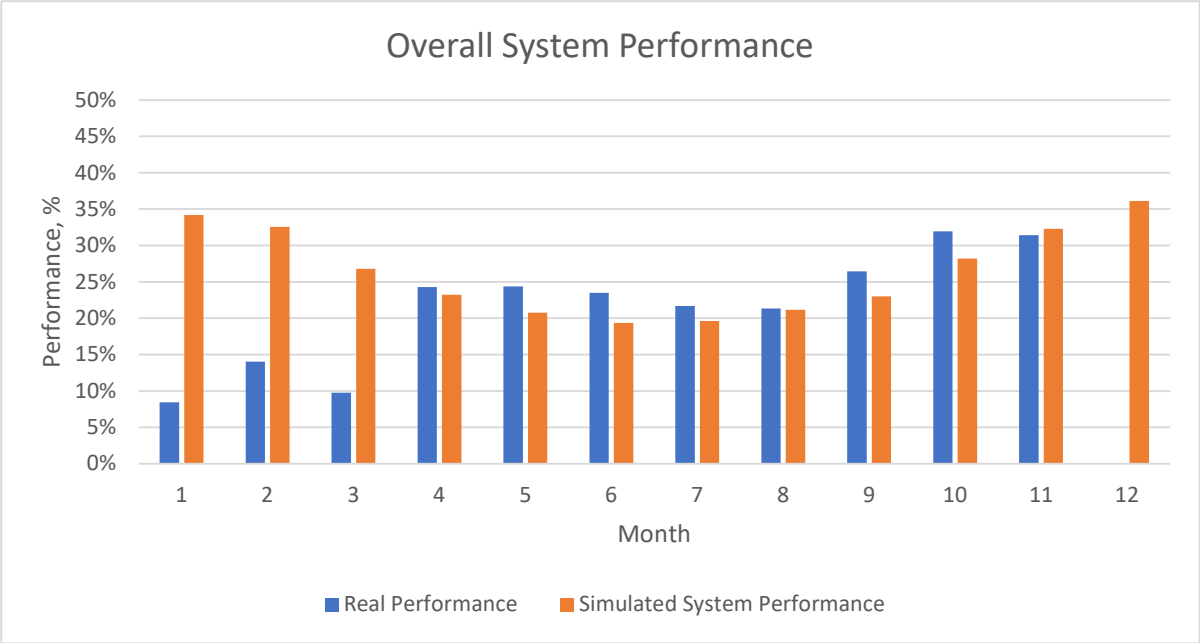

Figure 69 - Overall PV system performance comparison

Since this comparison takes into account the efficiency of the entire system (PV + PVT) and the share of energy produced by PV panels in the total amount of energy is significant, a decrease in efficiency can be observed in summer due to an increase in panel temperature. The efficiency of the system in the simulation is less volatile, and a clear trend can be observed where the efficiency of the system in winter is higher than in the warm spring and summer months. The volatility of actual measurements is much greater and depends on a number of factors not included in the simulation and difficult to predict, such as panel contamination, precipitation (snow) and others.

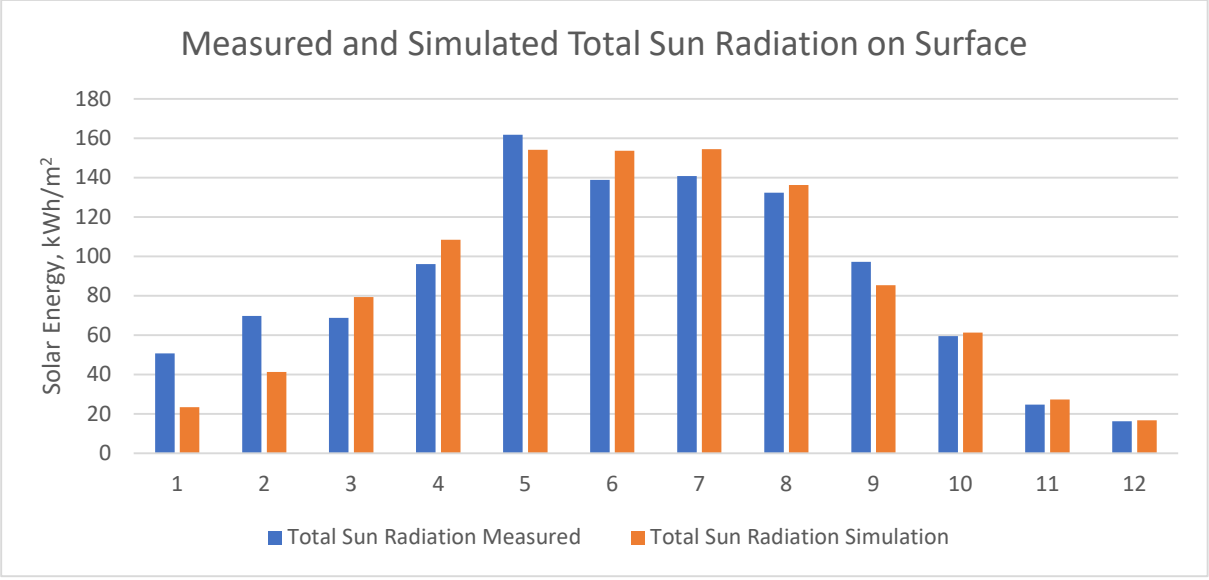

Figure 70 - Total sun radiation comparison

If we compare the input data (total solar radiation on the surface), it follows the same pattern and is generally very similar, which confirms that Meteonorm data can be used in simulation when we do not have measurements or the system is in design face and we want to predict its performance and capacity. As we can see from both Meteonorm and Measure data, May is the peak month for the amount of radiation.

Another important aspect of my work is comparing the amount of heat produced by solar collectors and PVT panels. In the following section, only the amount of heat produced by solar panels will be compared, as the recorded data for PVT panels is of very poor quality and, despite attempts at interpolation and removal of obvious errors, the data quality still left much to be desired and was not suitable for comparison with the simulation results.

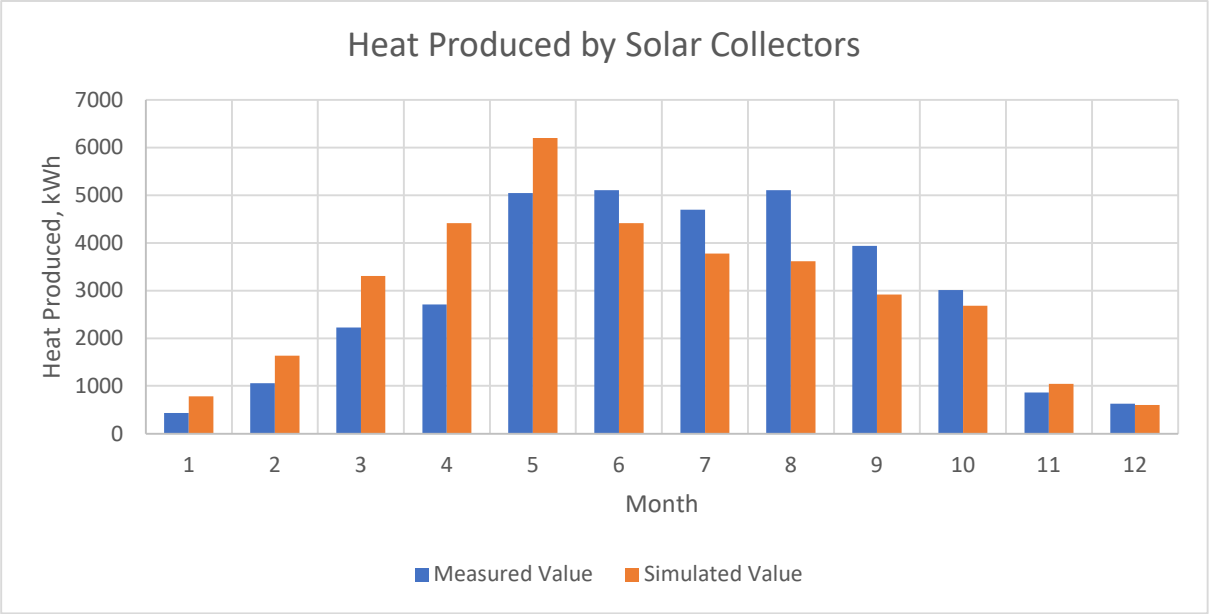

Figure 71 - Solar collectors heat production comparison

As can be seen, both values – the one measured on the actual system and the one obtained in the system simulation – follow the same trend.

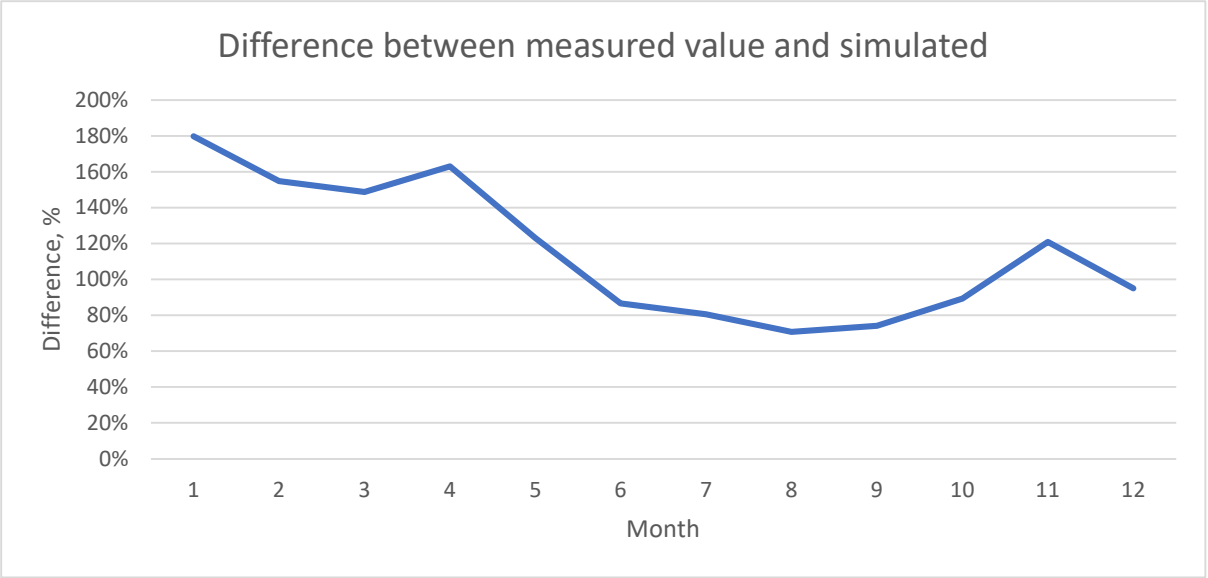

Figure 72 - Measured and simulated percentage difference

The largest percentage differences for the compared values can be seen in the winter period at the beginning of the year, however, the absolute values should be taken into account as the amount of heat produced during this period is low. When comparing the amount of heat produced throughout the year, the difference between the simulation and the actual measurements is very small and amounts to only 2%. Also for individual months in the summer period, when the amount of heat produced is highest, the difference decreases to 15-20% to the disadvantage of the simulation (the amount of heat is underestimated). The differences in the winter period can most likely be explained by weather conditions not taken into account in the simulation, such as snowfall and snow accumulation on the solar panels. In summer, the amount of heat is underestimated in the simulation. Unfortunately, this difference requires further analysis, as the amount of solar radiation, as shown earlier in my work, is very comparable for the simulation and for the actual measured values.

8. Literature research regarding simulation results and working system performance differences

The global transition towards decarbonised building energy systems is heavily reliant upon the successful large-scale deployment of high-efficiency heat pumps. Positioned as a key technology for electrification, the effectiveness of these systems is dependent on their ability to demonstrate predictable, reliable and efficient real-world performance. However, a persistent and often significant "performance gap" exists between the efficiency predicted during the design phase – based on component models and standardized laboratory ratings – and the actual

performance achieved during in-situ operation. The overestimation of operational efficiency has the potential to result in the failure to meet energy and carbon reduction targets, the imposition of unexpectedly high operational costs on consumers, and a general erosion of confidence in a technology that is of crucial importance to the energy transition.

This performance discrepancy is not a standalone issue but rather a multifaceted consequence of intertwined factors. The research articles mentioned in next part of my thesis deals with idealised assumptions at the component level, particularly in relation to the compressor, which are then amplified by system-level models that are not able to capture the dynamic, transient nature of real-world operation. At the ends issues also arise from installation quality, commissioning protocols, and control strategies, which are rarely reflected in design-stage simulations.

Brudermueller et al. [39] presented the findings of a study which constitutes the largest field analysis to date on the real-world energy efficiency of heat pumps. The study examined operational data from 1,023 residential units across Central Europe over a period of two years. The research reveals a significant performance gap among individual systems, with a two- to three-fold difference between the highest and lowest efficiency units observed in the field. A key finding is that a substantial number of heat pumps fail to meet European efficiency standards under real operating conditions, with 17% of air-source and 2% of ground-source systems falling below the required performance thresholds.

The analysis further identifies widespread issues with system sizing, a critical factor for operational efficiency. The investigation revealed that approximately 10% of the heat pumps were found to be oversized, while about 1% were undersized. This finding suggests that there are significant problems in current design and installation practices. The study also emphasises the significant impact of system settings on energy consumption. By simulating a minor adjustment – a 1°C reduction in the heating curve – the researchers demonstrated an average energy saving of 2.61%. This simple change would be sufficient for many underperforming units to meet efficiency standards, underscoring the importance of proper configuration.

In conclusion, the research highlights a significant discrepancy between the certified, laboratory-tested performance of heat pumps and their actual efficiency in residential settings. The findings indicate an urgent necessity for the implementation of standardised post-installation evaluation procedures and the development of digital tools. The implementation of such tools would facilitate the provision of crucial, actionable feedback to both users and

installers, thereby assisting in the optimisation of existing systems, the improvement of future installations, and, in turn, the enhancement of the widespread adoption and success of this critical decarbonisation technology.

A report [40] was published which presented the findings of an analysis of data from 2017-2022 for over 1,700 heat pump installations in Great Britain. The report evaluated the in-situ, real-world performance against installers' design forecasts. The findings reveal a mixed but concerning picture of heat pump efficiency. On a positive note, certain systems have demonstrated notable efficacy; one-third of the 286 Ground Source Heat Pumps (GSHPs) achieved a high Seasonal Performance Factor (SPF) of 3.5 or more, and the average GSHP performance has shown a marked improvement, reaching an SPF of 3.31 in 2022. Following the process of data cleansing, it was determined that no installation exhibited an efficiency that was less than 1.0. Nevertheless, these achievements are mitigated by substantial concerns, particularly in the context of Air Source Heat Pumps (ASHPs). A considerable discrepancy, known as a "performance gap", has been identified between the design forecast (Seasonal Coefficient of Performance, or SCOP) and the efficiency (SPF) achieved in the field. For ASHPs, this discrepancy is increasing; while average design SCOPs have risen to 3.71, the average in-situ SPF has remained stagnant at around 2.7 since 2017. The study revealed that a significant proportion of ASHPs function at low efficiency, with a higher number of systems operating between an SPF of 2.0-2.5 than between 3.0-3.5. Moreover, the correlation between the installer's forecast and the subsequent measured efficiency is found to be weak for both technologies. The report concludes that there are significant and ongoing information discrepancies within the domestic heat pump market, with a considerable proportion of design forecasts proving to be unrealistic. While certain installations demonstrate high levels of efficiency, a considerable proportion exhibit low or very low efficiency. The findings support the need for routine measurement of "real-world" performance outcomes and a comprehensive review of the industry's methods for calculating building heat loss and estimating efficiency to understand why design forecasts so often produce unrealistic estimates for consumers.

As stated in a number of research articles [41-44], there are significant discrepancies between the simulated, manufacturer-rated performance of heat pumps and their actual in-situ performance. The factors contributing to this discrepancy are numerous. A substantial body of field trial data has repeatedly demonstrated that the real-world efficiency of air-source heat pumps (ASHPs) frequently exhibits a lower value than that projected in laboratory tests or simulations. The performance ratings of heat pumps are typically determined through the

conduction of tests in ideal, steady-state conditions, which, in practice, rarely occur. It is evident that real-world factors, such as partial loads, on/off cycling, defrost cycles, and dynamic interactions with the building's envelope, are not fully captured in these ratings. For instance, the efficiency of residential air-source heat pumps (ASHPs) is significantly diminished when the compressor operates for cycles shorter than six minutes. Furthermore, the utilisation of supplementary heating in centralised systems, which is frequently not incorporated in the evaluation of system efficiency, exerts a substantial influence on the overall real-world performance. The transition to supplemental heating appears to be contingent on a conservative temperature setpoint, as opposed to being informed by the heat pump's actual capacity in relation to the home's heating demand. Finally, the methodologies employed in laboratory testing can also contribute to this discrepancy. For instance, they frequently exclude the back pressure caused by supply louvers, resulting in published volumetric flow rates for ductless units that exceed the measurements taken in the field.

In summary many article stated recurring simulation issues:

- The utilisation of non-local or legacy weather data (i.e. TMY vs site) has been observed to result in a shift in load, with a reported difference of approximately 10% in HDD. The phenomenon of sensor drift, in conjunction with technological bias (for example, that exhibited by a photovoltaic pyranometer in contrast to a thermopile), has been demonstrated to influence the model's utilisation of irradiance. [45, 46, 53]
- Simulation averages per step are often recorded, whereas loggers frequently record instantaneous values. Under conditions of rapid change (e.g. clouds, defrosting), temperatures and flows may become misaligned. The inertia of the pump and valve systems serves to amplify this effect. [46, 55]
- Controllers in the real world are subject to various limitations and imperfections. These include hysteresis, delays, override protections, and manual interventions. Absent mirroring or when the time steps are excessively large, outputs may exhibit drift. [46, 47]
- The collector effective heat capacity lumped in ISO 9806 fails to account for the effects of start-up and cool-down, and the flow regime dependence (laminar vs. turbulent) is not considered. Furthermore, the requirement for in-situ tuning of the HX UA (fouling, flow) is not taken into account. [46]

- Defrost cycles and transport delays result in energy and capacity imbalances; under the assumption of steady operation (or an erroneous timestep), power/heat predictions are inaccurate. [47, 48, 54]
- The DHW draw profiles, occupancy levels and HP operating time in relation to load timing vary on a daily basis. While daily energy consumption may be consistent, hourly consumption can exhibit significant deviation. [49, 50]
- In instances where key drivers (e.g., wind) are not measured, models are employed to calibrate loss coefficients or other parameters, resulting in a localised fit that compromises the transferability of the model. [51]
- A multitude of parameters exist yet only a limited number of outputs are observed, consequently resulting in numerous potential "fits". [47, 52]

Unlike the earlier examples, which listed reasons for discrepancies between simulations and measurements on actual systems, there are several examples in the literature where authors claim that their models largely agree with actual systems. However, such agreement only occurs under certain conditions, as cited by the authors below.

- Ruiz-Calvo et al. [48] developed a TRNSYS model for a ground-source heat pump installed at a facility in Valencia, Spain. They achieved good results by calibrating the model using a year-long set of experimental measurements from the GeoCool project installation. Following calibration, the model could accurately reproduce both short-term dynamics and long-term energy performance.
- Xuan Le et al. [58] created a simulation of a high-temperature air-source heat pump retrofitted into a terraced house in the UK. This heat pump can supply water at a temperature of 80°C, which is extremely high for a heat pump. The model was validated against the results of a field trial from an actual installation. After validation, the model was run in different climate conditions, e.g. Belfast and Camborne. The validated model was able to predict performance metrics with sufficient accuracy, demonstrating the key role that correct and precise input data, such as weather data and control strategy, play in the accuracy of the simulation output.
- Zhan et al. [59] developed a TRANSYS model of the Rødby solar district heating plant in Denmark. This model included solar collectors, an air source heat pump, and a gas boiler. The TRANSYS model was validated against long-term operational data obtained from the heating plant monitoring system. As a result, the simulation results matched

the performance of the real system at both the level of individual components and the level of the whole system. Key annual indicators (e.g. collector efficiency and heat pump COP) all remained within 5% of the actual values. This near-perfect agreement between the simulation and the real system was achieved by using manufacturer data and on-site measurements (e.g. flow rates and controller logic) as TRNSYS inputs.

- Ołtarzewska and Krawczyk [60] created a model of a PV-powered heat pump system for a small building. They modelled a small reversible heat pump powered by rooftop PV, which served as a heating and cooling source. The authors calibrated the model using real consumption data recorded from July 2021 to July 2022. They then compared the one-year heating energy use and two-year electrical use to the simulation to ensure the model's accuracy before conducting further analyses.
- Leonforte et al. [61] developed a TRNSYS model for a PVT-assisted heat pump system in a single-family home. The heat pump provided space heating, cooling and DHW. A detailed TRNSYS model was developed using high-quality manufacturer data for the PVT and heat pump components, and was then calibrated using field measurements. The simulation was validated against monitored performance, showing close alignment with the behaviour of the real system. According to the research paper, the model accurately captured seasonal performance due to the use of the actual equipment specifications and measured inputs for calibration.

Despite some research showing almost ideal convergence between the model and real-life experiments or installations, the fact remains that most of this research success is based on the model being calibrated and validated using historical data from existing installations. This causes a problem when the system does not exist and the simulation is required to predict its behaviour. Such a situation occurred with the RESHeat system when the simulation was developed before the system was built, and it was used to find the optimal system configuration. Despite this, the simulation turned out to be quite useful, with the results being similar to the measured data from the installation, albeit with some margin of error.

9. Conclusions

In recent years, especially in European Union countries, particular emphasis has been placed on the amount of energy consumed for residential purposes. This necessitates increasing the thermal efficiency of buildings, the efficiency of heating and cooling systems, and the source of energy used for these purposes – so that it comes from renewable energy sources as much as possible. The aim of the RESHeat project was to design such a system for ZBK residential buildings in Krakow.

This doctoral thesis aimed to investigate how a compressor heat pump works in such a system, and to construct simulation tools that could predict the operating parameters of the heat pump in a complex heating system consisting of renewable heat sources, such as solar and photovoltaic panels, as well as a storage system and a ground source heat pump.

For the purposes of this thesis, it was assumed that, to achieve the ResHeat project's objectives of a heat pump COP of at least 4.0 and renewable energy coverage of at least 70%, an appropriate system control algorithm must be developed to enable these objectives to be met.

The first part of the thesis describes the development of a Python program that simulates the operating parameters of a heat pump under various conditions. This program was used to determine the minimum and maximum parameters of the heat source and heat load required for the heat pump to operate with a COP of at least 4.0.

The main problem with the ResHeat system operating in ZBK buildings was that it was a retrofit installation - a new installation added to an existing, old system. This caused problems, among other things, with the efficiency of the existing parts of the system and the high parameters of the heat load, i.e. the required high temperature of the water supplying the heating and DHW systems.

Thanks to the simulation, potential weaknesses of the designed system were identified before its construction and installation, which contributed to the improvement of the system's operating parameters after its launch. Preparing similar simulations and analyses during the development of innovative systems allows problems to be predicted and eliminated at an early stage, making it possible to achieve the required operating parameters and system performance targets.

9.1. Summary of dissertation findings

In the first part of my doctoral thesis, a mathematical model of a compressor heat pump was developed and used to obtain an approximate linear equation determining the COP coefficient for the specified heat pump operating parameters. Additionally, based on climate data and measured ground temperatures at the depth at which the geothermal wells were placed, it was possible to determine the parameters of the heat source at which the heat pump will operate. As a result, it was determined that in order to meet the project requirements, the average temperature of the water leaving the heat pump (heat load temperature) must not exceed 47 degrees Celsius. This, in turn, necessitated the development of an appropriate control strategy that would allow for a gradual reduction of the heat load, e.g. when the required temperature of the water supplying the central heating system is lower.

The preceding analyses demonstrated that an increase in the heat source temperature was required for this heat pump. This objective was realised through the implementation of a heat storage tank, which functioned as an ancillary heat source or to elevate the temperature of the primary heat source.

The next stage of the research involved comparing the model and its results with laboratory data for the heat pump installed in the ZBK building, within a defined temperature range. The coefficient of performance (COP) obtained from the simulation was significantly lower than the manufacturer's specification, with discrepancies ranging from 3.4% to 25.9%. The largest discrepancies occurred when the temperatures of the heat source and heat load were closest to each other. Conversely, when these temperatures differed significantly, the simulation results were closer to the laboratory data provided by the heat pump manufacturer.

The main reasons for the discrepancies between the results obtained in the simulation and those provided by the heat pump manufacturer can be found in the following factors:

- Manufacturers conduct tests in controlled laboratory conditions, at a constant temperature
- Simulations frequently employ simplified or idealised models of compressors, heat exchangers and control systems, potentially overlooking real-world inefficiencies such as refrigerant distribution issues, pressure drops and non-ideal transient behaviour.
- The findings of field studies have repeatedly demonstrated that performance is lower in comparison to laboratory values.

In summary, manufacturers provide COP values based on the best, optimised laboratory conditions. Simulations designed to replicate actual operating conditions will therefore inherently show lower performance levels due to practical factors that are not taken into account in the manufacturer's ideal tests.

The subsequent stage of the research was to simulate the operation of the heat pump and the remaining components of the RESHeat system that had been installed in the ZBK building. The simulations were conducted utilising TRNSys software, which reproduced the system's primary components, namely the heat pump, a model of the building accounting for heat losses and gains, and additional system elements such as solar and photovoltaic panels, heat storage, and geothermal wells.

The simulation allowed us to draw the following conclusions:

The underground heat storage tank allowed for the accumulation of significant amounts of thermal energy, which meant that the heat pump did not have to operate during the warmer period of the year, from April to early October. The water in the underground tank, which is the heat storage medium in this system, had a sufficient temperature during this period to be used directly for DHW heating, so it was not necessary to start the heat pump.

The electricity demand is directly related to the operation of the heat pump in the ZBK system, and therefore in April and October it was 10 times lower than the energy demand in January, and in the months from May to September inclusive, the energy demand was minimal and related to the energy consumption of the system's circulation pumps.

The COP of the heat pump ranges from 2.7 to 3.8, with the highest COP occurring in the summer when it was possible to raise the heat source temperature using the heat stored in the underground storage tank.

The total energy demand of the heat pump during the year was 32.4 MWh, and the amount of energy produced was 40.3 MWh, thanks to which the coverage of energy demand with renewable energy was 124%, which is significantly higher than the assumed minimum ratio of 70%.

Additional simulation variants were also carried out to check the impact of individual system components on its efficiency. One of the analysed components was the impact of the number of ground heat exchangers on the inlet temperature of the heat source. As the number of exchangers decreased, the temperature dropped to -5 with 10 exchangers and -15 with 5. This

clearly shows that the designed number of exchangers is also optimal, as reducing their number would result in a significant decrease in heat load temperature as well as a decrease in the efficiency and heat capacity of the heat pump. Another element analysed was the impact of the size of the underground storage tank on the heat pump. a decrease in the storage tank capacity forced a greater demand for heat production by the heat pump - from 89.6 MWh to 91.3, while doubling the storage tank from 50 m^3 to 100 m^3 reduced the heat demand to 89.3 MWh, which is not economically justified, Therefore, the 50 m^3 option was chosen.

The last case considered was the impact of regulating the temperature of the water supplied to the CO system based on the outside temperature. Thanks to temperature regulation, the COP was increased by 18% from 3.43 to 4.06.

The final stage of the work was to compare the simulation results with the actual results from the operating system.

First, the meteorological data used in the simulation was compared with the data that actually occurred during the period of system operation from January to December 2024. In general, the data used in the simulation predicted temperatures that were on average 4.6 degrees Celsius lower than those actually measured during the period. The data followed the same seasonal trend, but this showed the need to update the statistical data due to global warming.

Another element compared was energy demand, and as with the weather data, the same trend can be observed, but the actual energy demand due to higher outdoor temperatures was lower than that obtained in the simulation.

Next, the inlet and outlet temperatures of the heat load and heat source of the heat pump were compared, and a significant difference was observed, which may explain the difference in energy demand in the simulation and in the actual system - the outlet temperature of the heat pump in the actual system was significantly lower than the design temperature - on average, it was 15 degrees lowerand was 40-45 degrees Celsius.

Another element was electricity production, but here no significant differences were observed and the results were similar for both simulations and actual measurements.

The efficiency of PV and PVT was also compared, and here the results were also similar, averaging 20 to 30%. The only discrepancy was during the winter period from January to March, when the actual measured efficiency of the devices was significantly lower than in the

simulation, which could have been caused by weather conditions not anticipated in the simulation, such as snow remaining on the panels.

The amount of solar radiation resulting from statistical data and the amount of solar radiation measured during the actual period of system operation did not differ from each other.

As the amount of solar radiation was similar in reality and in the simulation, the amount of heat produced by the solar panels was also similar, and no significant differences were observed between the simulation and the actual measurements.

Bibliography

[1] DIRECTIVE 2010/31/EU OF THE EUROPEAN PARLIAMENT AND OF THE COUNCIL of 19 May 2010 on the energy performance of buildings (recast), https://eur-lex.europa.eu/legal-content/EN/TXT/?qid=1583922805643&uri=CELEX:02010L0031-20181224

[2] COMMISSION RECOMMENDATION (EU) 2016/1318 of 29 July 2016 on guidelines for the promotion of nearly zero-energy buildings and best practices to ensure that, by 2020, all new buildings are nearly zero-energy buildings, https://eur-lex.europa.eu/legal-content/EN/TXT/?uri=CELEX:32016H1318

[3] Eurostat, https://ec.europa.eu/eurostat/databrowser/view/ten00121/default/table?lang=en

[4] https://www.ehpa.org/news-and-resources/news/port-pc-2022-was-the-year-of-heat-pumps-in-poland/

[5] https://www.ehpa.org/market-data/

[6] Girard, A., Gago, E. J., Muneer, T., & Caceres, G. (2015). Higher ground source heat pump COP in a residential building through the use of solar thermal collectors. *Renewable Energy*, *80*, 26–39. https://doi.org/10.1016/j.renene.2015.01.063

[7] Nouri, G., Noorollahi, Y., & Yousefi, H. (2019). Solar assisted ground source heat pump systems – A review. In *Applied Thermal Engineering* (Vol. 163). Elsevier Ltd. https://doi.org/10.1016/j.applthermaleng.2019.114351

[8] Zhang, S., Ocłoń, P., Klemeš, J. J., Michorczyk, P., Pielichowska, K., & Pielichowski, K. (2022). Renewable energy systems for building heating, cooling and electricity production with thermal energy storage. *Renewable and Sustainable Energy Reviews*, *165*. https://doi.org/10.1016/j.rser.2022.112560

[9] Qiu, K., & Thomas, M. (2024). Modeling and optimization of two-stage compression heat pump system for cold climate applications. *Journal of Building Engineering*, *82*, 108407. https://doi.org/10.1016/j.jobe.2023.108407

[10] Rogeau, A., Vieubled, J., Ruche, L., & Girard, R. (2024). A generic methodology for mapping the performance of various heat pumps configurations considering part-load behavior. *Energy and Buildings*, *318*, 114490. https://doi.org/10.1016/j.enbuild.2024.114490

[11] Olympios, A. v., Song, J., Ziolkowski, A., Shanmugam, V. S., & Markides, C. N. (2024). Data-driven compressor performance maps and cost correlations for small-scale heat-pumping applications. *Energy*, *291*, 130171. https://doi.org/10.1016/J.ENERGY.2023.130171

[12] Vering, C., Engelpracht, M., Göbel, S., Hoseinpoori, S., Wüllhorst, F., Schwenzer, C., Rademacher, M., Hinrichs, S., Chandra, F., Mehrfeld, P., & Müller, D. (2022). Open-Source vapor compression library (VCLib): Heat pump modeling for education and research. *Computer Applications in Engineering Education*. https://doi.org/10.1002/cae.22540

[13] Cheng, Z., Tao, L., Huang, L., & Yu, Z. (2023). Modeling and Experimental Verification of the Electrical Efficiency for Variable-Frequency Rolling Piston Compressor under Variable

Suction Conditions. *Applied Sciences (Switzerland)*, *13*(24). https://doi.org/10.3390/app132412992

[14] Ma, Y., Xi, J., Cai, J., & Gu, Z. (2023). TRNSYS simulation study of the operational energy characteristics of a hot water supply system for the integrated design of solar coupled air source heat pumps. *Chemosphere*, *338*, 139453. https://doi.org/10.1016/J.CHEMOSPHERE.2023.139453

[15] Saleem, A., & Ugalde-Loo, C. E. (2025). Thermal performance analysis of a heat pump-based energy system to meet heating and cooling demand of residential buildings. *Applied Energy*, *383*. https://doi.org/10.1016/j.apenergy.2025.125306

[16] Wang, Q., Zhang, X., Zhang, H., Ma, Y., & Zhao, S. (2022). Optimization of solar-assisted GWHP system based on the Trnsys model in cold regions. *Renewable Energy*, *196*, 1406–1417. https://doi.org/10.1016/j.renene.2022.07.072

[17] Buyukzeren, R., & Kahraman, A. (2024). A comparative study on the application of solar thermal collector and photovoltaic combinations to assist an air source heat pump. *Journal of Thermal Analysis and Calorimetry*, *149*(17), 9413–9428. https://doi.org/10.1007/s10973-024-13475-z

[18] Liu, P., Zhao, J., & Chen, J. (2023). Simulation Study of a Novel Solar Air-Source Heat Pump Heating System Based on Phase-Change Heat Storage. *Sustainability (Switzerland)*, *15*(22). https://doi.org/10.3390/su152215684

[19] Belmonte, J. F., Díaz-Heras, M., Almendros-Ibáñez, J. A., & Cabeza, L. F. (2022). Simulated performance of a solar-assisted heat pump system including a phase-change storage tank for residential heating applications: A case study in Madrid, Spain. *Journal of Energy Storage*, *47*. https://doi.org/10.1016/j.est.2021.103615

[20] Wang, W., & Zare, A. (2024). Performance simulation and analysis of a solar-assisted multifunctional heat pump system for residential buildings. *International Journal of Sustainable Energy*, *43*(1). https://doi.org/10.1080/14786451.2024.2394116

[21] Dannemand, M., Sifnaios, I., Tian, Z., & Furbo, S. (2020). Simulation and optimization of a hybrid unglazed solar photovoltaic-thermal collector and heat pump system with two storage tanks. *Energy Conversion and Management*, *206*. https://doi.org/10.1016/j.enconman.2019.112429

[22] Nouri, G., Noorollahi, Y., & Yousefi, H. (2019). Designing and optimization of solar assisted ground source heat pump system to supply heating, cooling and hot water demands. *Geothermics*, *82*, 212–231. https://doi.org/10.1016/j.geothermics.2019.06.011

[23] Pinamonti, M., & Baggio, P. (2020). Energy and economic optimization of solar-assisted heat pump systems with storage technologies for heating and cooling in residential buildings. *Renewable Energy*, *157*, 90–99. https://doi.org/10.1016/j.renene.2020.04.121

[24] Pilou, M., Kosmadakis, G., Meramveliotakis, G., & Krikas, A. (2022). Towards a 100% renewable energy share for heating and cooling in office buildings with solar and geothermal energy. *Solar Energy Advances*, *2*. https://doi.org/10.1016/j.seja.2022.100020

[25] Cohen, Jacob, Aiken, Leona S, Patricia, West, & Stephen G. (n.d.). *Applied Multiple Regression/Correlation Analysis for the Behavioral Sciences Third Edition*.

[26] Kleinbaum, David G., et al. *Applied regression analysis and other multivariable methods*. Vol. 601. Belmont, CA: Duxbury press, 1988.

[27] Pater, S., Ciesielczyk, W. (2017). Rzeczywista i teoretyczna wydajność energetyczna parowych sprężarkowych pomp ciepła. Czasopismo Techniczne, 2017, 185-194. doi: https://doi.org/10.4467/2353737XCT.17.080.6437

[28] American Society of Heating, Refrigerating and Air-Conditioning Engineers. ASHRAE Handbook - Chapter 38: Compressors. 2024.

[29] American Society of Heating, Refrigerating and Air-Conditioning Engineers. ASHRAE Handbook - Chapter 48: Unitary Air Conditioners and Heat Pumps. 2024.

[30] Mary Elizabeth Konrad, Brendan D. MacDonald, Cold climate air source heat pumps: Industry progress and thermodynamic analysis of market-available residential units, Renewable and Sustainable Energy Reviews, Volume 188, 2023, 113739, ISSN 1364-0321, https://doi.org/10.1016/j.rser.2023.113739.

[31] DEPARTMENT OF ENERGY 10 CFR Parts 429 and 430 [Docket No. EERE-2016-BT-TP-0029] RIN 1904-AD71 Energy Conservation Program: Test Procedures for Central Air Conditioners and Heat Pumps. 2016

[32] Rosenquist, G J. *Comparison of simulated and measured test data on air-source heat pumps.* Canada: N. p., 1997.

[33] Mendon V.V., K.M. Keene, S.I. Rosenberg, J.A. Rotondo, K. Nwe, J. Young, and W. Wind, et al. 2025. *Performance Results from DOE Cold Climate Heat Pump Challenge Field Validation*. PNNL-37127. Richland, WA: Pacific Northwest National Laboratory.

[34] Standard 90.1-2019, U.S. Department of Energy Building Energy Codes Program, ICC, 2019.

[35] Mikk Maivel, Jarek Kurnitski, Heating system return temperature effect on heat pump performance, Energy and Buildings, Volume 94, 2015, Pages 71-79, ISSN 0378-7788, https://doi.org/10.1016/j.enbuild.2015.02.048.

[36] M. Fatouh, E. Elgendy, Experimental investigation of a vapor compression heat pump used for cooling and heating applications, Energy, Volume 36, Issue 5, 2011, Pages 2788-2795, ISSN 0360-5442, https://doi.org/10.1016/j.energy.2011.02.019.

[37] Eneja Osterman, Uroš Stritih, Review on compression heat pump systems with thermal energy storage for heating and cooling of buildings, Journal of Energy Storage, Volume 39, 2021, 102569, ISSN 2352-152X, https://doi.org/10.1016/j.est.2021.102569.

[38] Jung, W.; Kim, D.; Kang, B.H.; Chang, Y.S. Investigation of Heat Pump Operation Strategies with Thermal Storage in Heating Conditions. Energies 2017, 10, 2020. https://doi.org/10.3390/en10122020

[39] Brudermueller, T., Potthoff, U., Fleisch, E., Wortmann, F., & Staake, T. (2025). Estimation of energy efficiency of heat pumps in residential buildings using real operation data. *Nature Communications* , *16*(1). https://doi.org/10.1038/s41467-025-58014-y

[40] *In-Situ Heat Pump Performance*. (2024). https://www.recc.org.uk/pdf/rbandm-research-project.pdf

[41] Kelly, N. J., & Cockroft, J. (2011). Analysis of retrofit air source heat pump performance: Results from detailed simulations and comparison to field trial data. *Energy and Buildings*, *43*(1), 239–245. https://doi.org/10.1016/j.enbuild.2010.09.018

[42] Byrne, P., Miriel, J., & Lénat, Y. (2012). Modelling and simulation of a heat pump for simultaneous heating and cooling. *Building Simulation*, *5*(3), 219–232. https://doi.org/10.1007/s12273-012-0089-0

[43] Chesser, M., Lyons, P., O'Reilly, P., & Carroll, P. (2021). Air source heat pump in-situ performance. *Energy and Buildings*, *251*. https://doi.org/10.1016/j.enbuild.2021.111365

[44] Marleau, C., & Sc, M. A. (2023). *In-Situ Performance of Cold Climate Air-Source Heat Pumps in British Columbia*. www.ashrae.org

[45] Kassai, M. (2020). Development and experimental validation of a trnsys model for energy design of air-to-water heat pump system. *Thermal Science*, *24*, 893–902. https://doi.org/10.2298/TSCI181206070K

[46] Bava, F., & Furbo, S. (2017). Development and validation of a detailed TRNSYS-Matlab model for large solar collector fields for district heating applications. *Energy*, *135*, 698–708. https://doi.org/10.1016/j.energy.2017.06.146

[47] St-Onge, G., Kummert, M., & Kegel, M. (2018). *Variable capacity mini-split air source heat pump model for TRNSYS*.

[48] Ruiz-Calvo, F., Montagud, C., Cazorla-Marín, A., & Corberán, J. M. (2017). Development and experimental validation of a TRNSYS dynamic tool for design and energy optimization of ground source heat pump systems. *Energies*, *10*(10). https://doi.org/10.3390/en10101510

[49] Bogatu, D.-I., Carutasiu, M.-B., Ionescu, C., & Necula, H. (2025). General rights Validation of a TRNSYS model for a complex HVAC system installed in a low-energy building VALIDATION OF A TRNSYS MODEL FOR A COMPLEX HVAC SYSTEM INSTALLED IN A LOW-ENERGY BUILDING. *U.P.B. Sci. Bull., Series C*, *81*(1).

[50] Lim, H., -Bin, Kyoung-Ho, Min-Suk, & Dong-Hyun. (2019). A Model Calibration for Residential Building Energy Simulation : A Case Study with TRNSYS and Optimization Tool GenOpt. *Journal of KIAEBS*, *13*(4), 234–245. https://doi.org/10.22696/jkiaebs.20190020

[51] Bernardo, L. R. (2013). Retrofitting conventional electric domestic hot water heaters to solar water heating systems in single-family houses-model validation and optimization. *Energies*, *6*(2), 953–972. https://doi.org/10.3390/en6020953

[52] Ayompe, L. M., Duffy, A., McCormack, S. J., & Conlon, M. (2011). Validated TRNSYS model for forced circulation solar water heating systems with flat plate and heat pipe evacuated tube collectors. *Applied Thermal Engineering*, *31*(8–9), 1536–1542. https://doi.org/10.1016/j.applthermaleng.2011.01.046

[53] Rey, A., & Zmeureanu, R. (2016). MODEL VALIDATION OF A RESIDENTIAL SOLAR THERMAL COMBISYSTEM. *Proceedings of the ESim2016 Conference*, 3–6.

[54] Hoeschele, M., & Weitzel, E. (2017). *Multifamily Heat Pump Water Heater Evaluation*. www.nrel.gov/publications.

[55] Sifnaios, I., Jensen, A. R., Dannemand, M., & Dragsted, J. (2021). Demonstration of a domestic photovoltaic-thermal (PVT)-heat pump system, performance simulation, and economic analysis for different climates. *Proceedings - ISES Solar World Congress 2021*, 588–599. https://doi.org/10.18086/swc.2021.26.03

[56] Benachir, Nouhaila, The Extensive Library of Components About TRNSYS Application (August 16, 2023). http://dx.doi.org/10.2139/ssrn.4542306

[57] Nam, Y. J., Gao, X. Y., Yoon, S. H., & Lee, K. H. (2015). Study on the performance of a ground source heat pump system assisted by solar thermal storage. *Energies*, *8*(12), 13378–13394. https://doi.org/10.3390/en81212365

[58] Xuan Le, K., Jun Huang, M., Hewitt, N. J., Xuan, K., Jun, M., Xuan, K. le, & Jun HUANG, M. (2018). Domestic High Temperature Air Source Heat Pump: Performance Analysis Using TRNSYS Simulations. https://docs.lib.purdue.edu/ihpbc/315

[59] Zhan, C., Xu, Y., Fan, J., Gao, M., Kong, W., Wu, J., Wang, D., & Tian, Z. (2025). Validation and optimization of a solar heating plant with a large-scale heat pump. *Energy*, *319*. https://doi.org/10.1016/j.energy.2025.134898

[60] Ołtarzewska, A., & Krawczyk, D. A. (2024). Simulation and Performance Analysis of an Air-Source Heat Pump and Photovoltaic Panels Integrated with Service Building in Different Climate Zones of Poland. *Energies*, *17*(5). https://doi.org/10.3390/en17051182

[61] Leonforte, F., Miglioli, A., del Pero, C., Aste, N., Cristiani, N., Croci, L., & Besagni, G. (2022). Design and performance monitoring of a novel photovoltaic-thermal solar-assisted heat pump system for residential applications. *Applied Thermal Engineering*, *210*. https://doi.org/10.1016/j.applthermaleng.2022.118304

List of Figures

List of Tables